

---

Theses and Dissertations

---

Spring 2014

## Vadose zone denitrification enhancement by poplars during dormancy

Hayden Willis Ausland  
*University of Iowa*

Follow this and additional works at: <https://ir.uiowa.edu/etd>



Part of the [Civil and Environmental Engineering Commons](#)

Copyright 2014 Hayden W. Ausland

This thesis is available at Iowa Research Online: <https://ir.uiowa.edu/etd/4566>

---

### Recommended Citation

Ausland, Hayden Willis. "Vadose zone denitrification enhancement by poplars during dormancy." MS (Master of Science) thesis, University of Iowa, 2014.  
<https://doi.org/10.17077/etd.226r0ssz>

---

Follow this and additional works at: <https://ir.uiowa.edu/etd>



Part of the [Civil and Environmental Engineering Commons](#)

VADOSE ZONE DENITRIFICATION ENHANCEMENT BY POPLARS DURING  
DORMANCY

by  
Hayden Willis Ausland

A thesis submitted in partial fulfillment  
of the requirements for the Master of  
Science degree in Civil and Environmental Engineering  
in the Graduate College of  
The University of Iowa

May 2014

Thesis Supervisor: Assistant Professor Craig L. Just

Copyright by  
HAYDEN WILLIS AUSLAND  
2014  
All Rights Reserved

Graduate College  
The University of Iowa  
Iowa City, Iowa

CERTIFICATE OF APPROVAL

---

MASTER'S THESIS

---

This is to certify that the Master's thesis of

Hayden Willis Ausland

has been approved by the Examining Committee  
for the thesis requirement for the Master of Science  
degree in Civil and Environmental Engineering  
at the May 2014 graduation.

Thesis Committee: \_\_\_\_\_  
Craig L. Just, Thesis Supervisor

\_\_\_\_\_  
Louis A. Licht

\_\_\_\_\_  
Jerald L. Schnoor

This work is dedicated to all of my family, friends, and colleagues who have helped guide me on this journey.

It is obviously impossible to decide what is good or bad, right or wrong, virtuous or evil,  
without an idea of purpose: Good for what?

E. F. Schumacher  
A Guide for the Perplexed

## ACKNOWLEDGMENTS

I wish to express my gratitude to my advisor, Dr. Craig Just, for providing guidance and insight throughout my graduate education. I would also like to thank one of my favorite mentors and people, Dr. Louis Licht, for creating this opportunity and being inspirational. Thanks to Tim Houser, Brandon Barquist, and Greg Wagner of the IIHR - Hydroscience and Engineering staff for their involvement and design expertise. Jonathan Durst, thank you for your professionalism and sense of humor. This entire project would not have been as fun without you. Lindsay Marshall, thank you for your everlasting love and moral support. Katie Langenfeld and Lee Hauser, thank you for your hard work and dependable assistance. And last, but not least, thanks to all of my friends and family for being the best group of people on the planet.

## TABLE OF CONTENTS

LIST OF TABLES .....	vii
LIST OF FIGURES .....	viii
LIST OF EQUATIONS .....	xii
LIST OF ABBREVIATIONS.....	xiii
CHAPTER 1: INTRODUCTION AND LITERATURE REVIEW .....	1
1.1 Theory.....	11
1.2 Description of Field Site.....	13
1.3 Research Objectives.....	19
CHAPTER 2: WATER FLOW AND NUTRIENT DYNAMICS.....	20
2.1 Abstract.....	20
2.2 Introduction.....	20
2.3 Materials and Methods.....	21
2.3.1 Pilot-scale Experimentation.....	21
2.3.2 Test Cell Treatment Types.....	21
2.3.3 Synthetic Wastewater.....	24
2.3.4 Temperature and Relative Humidity.....	25
2.3.5 Tracer Studies .....	25
2.3.6 Volumetric Flow Rate.....	26
2.3.7 Intermittent Dosing Experiment .....	27
2.3.8 Organic Nitrogen Hydrolysis and Denitrification Rate .....	27
2.3.9 Statistical Analysis.....	28
2.4 Results and Discussion .....	28
2.4.1 Temperature and Relative Humidity.....	28
2.4.2 Bromide Tracer Studies .....	29
2.4.3 Volumetric Flow Rate.....	32
2.4.4 Total Nitrogen.....	32
2.4.5 Nitrate .....	34
2.4.6 Ammonium .....	36
2.4.7 Nitrite.....	38
2.4.8 Organic Nitrogen Hydrolysis and Denitrification Rate Coefficients.....	39



2.4.9 Nitrogen Species by Test Cell.....	40
2.5 Conclusions.....	61
2.5.1 Summary of Findings.....	61
2.5.2 Implications on Nitrate by Treatment Type.....	62
2.5.3 Implications for Port of Morrow.....	62
2.5.4 Future Research.....	63
<b>CHAPTER 3: MODELING POPLAR VADOSE ZONE NITROGEN DURING DORMANCY.....</b>	<b>64</b>
3.1 Abstract.....	64
3.2 Introduction.....	64
3.3 Materials and Methods.....	66
3.3.1 Pilot-scale Experimentation.....	66
3.3.2 Tracer Tests.....	67
3.3.3 Intermittent Dosing Experiment.....	67
3.3.4 Numerical Modeling.....	68
3.4 Results and Discussion.....	70
3.4.1 Conservative Transport.....	70
3.4.2 Reactive Transport.....	70
3.5 Conclusions.....	82
3.5.1 Summary of Findings.....	82
3.5.2 Implications for Port of Morrow.....	82
3.5.3 Future Research.....	83
<b>APPENDIX A: WATER CHEMISTRY DATA.....</b>	<b>84</b>
<b>APPENDIX B: SOIL CHEMISTRY ANALYSIS.....</b>	<b>87</b>
<b>APPENDIX C: ORGANIC NITROGEN ANALYSIS.....</b>	<b>89</b>
<b>BIBLIOGRAPHY.....</b>	<b>92</b>

## LIST OF TABLES

Table 1: Trend line values for south side test cells.....	48
Table 2: Mass flux trend line values for north side test cells.....	48
Table 3: Mass flux trend line values for south side test cells .....	49
Table 4: Cumulative measured and predicted mass values of nitrogen for each treatment type .....	61
Table 5: Dose rate and estimated rate coefficients over the course of the experiment for all treatment types .....	61
Table 6: Optimized values for fitted soil hydraulic and solute transport parameters and associated goodness of fit measures.....	80
Table 7: Hydrus CW2D wetland module parameterization values .....	81

## LIST OF FIGURES

Figure 1: Location of food processor land application sites in the Lower Umatilla Basin Groundwater Management Area (LUBGWMA).....	15
Figure 2: Well locations and surface water bodies - Port of Morrow Farms.....	16
Figure 3: Upgradient vs downgradient nitrate comparisons - western portion of Port of Morrow Farm 1.....	17
Figure 4: Upgradient vs downgradient nitrate comparisons - eastern portion of Port of Morrow Farm 1 & western portion of Farm 3.....	18
Figure 5: 3D Schematic of the pilot-scale poplar tree vadose zone irrigation system.....	22
Figure 6: 2D Side profile of an individual test cell with trees, roots, and perforated drain tube .....	23
Figure 7: Perforations in the PVC underdrain prior to wrapping with permeable felt .....	24
Figure 8: Perforated underdrain wrapped with permeable felt and custom stand .....	24
Figure 9: Temperature and relative humidity over the course of 4 months.....	41
Figure 10: Bromide tracer study of the Calamus no tree north test cell using conductivity probe and ion chromatography .....	42
Figure 11: Bromide tracer studies of the Cal no tree north and south test cells using a 5 g KBr spike with a continuous 30 mL min <sup>-1</sup> DI flow rate .....	42
Figure 12: Bromide tracer studies of the Cal with tree north and south test cells using a 5 g KBr spike with a continuous 30 mL min <sup>-1</sup> DI flow rate.....	43
Figure 13: Bromide tracer studies of the Cal PAM no tree north and south test cells using a 5 g KBr spike with a continuous 30 mL min <sup>-1</sup> DI flow rate.....	43
Figure 14: Bromide tracer studies of the Cal PAM with tree north and south test cells using a 5 g KBr spike with a continuous 30 mL min <sup>-1</sup> DI flow rate .....	44
Figure 15: Bromide tracer studies of the POM no tree and POM with tree test cells using a 5 g KBr spike with a continuous 30 mL min <sup>-1</sup> DI flow rate.....	44
Figure 16: Mean daily synthetic wastewater application for each test cell with error bars representing ± one standard deviation.....	45
Figure 17: Total nitrogen concentration in the head tank and effluents of the north side test cells .....	46
Figure 18: Increasing total nitrogen trend lines for the Cal with tree and Cal no tree test cells.....	46
Figure 19: Decreasing total nitrogen trend lines for the Cal PAM no tree test cell.....	47

Figure 20: Total nitrogen concentration in the head tank and effluents for the south side test cells .....	47
Figure 21: Total nitrogen mass flux in the effluent of the north side test cells .....	48
Figure 22: Total nitrogen mass flux in the effluent of the south side test cells .....	49
Figure 23: Average total nitrogen mass flux comparison with error bars representing $\pm$ one standard deviation .....	50
Figure 24: Average nitrate mass flux comparison with error bars representing $\pm$ one standard deviation .....	51
Figure 25: Nitrate mass flux comparison for the north and south Cal PAM with tree test cells.....	51
Figure 26: Nitrate mass flux for all test cell treatment types over a 2 week sampling period .....	52
Figure 27: Nitrate mass flux comparison of Cal PAM with tree north vs. head tank north.....	52
Figure 28: Average ammonium mass flux comparison with error bars representing $\pm$ one standard deviation .....	53
Figure 29: Ammonium mass flux for all test cell treatment types over a 2 week sampling period.....	53
Figure 30: Ammonium mass flux comparison for the north and south Cal PAM with tree test cells .....	54
Figure 31: Average nitrite mass flux comparison with error bars representing $\pm$ one standard deviation .....	54
Figure 32: Nitrite mass flux comparison for the north and south Cal no tree test cells .....	55
Figure 33: Nitrite mass flux for all test cell treatment types over a 2 week sampling period .....	55
Figure 34: Measured and predicted nitrogen dynamics for the POM no tree test cell .....	56
Figure 35: Measured and predicted nitrogen dynamics for the POM with tree test cell.....	56
Figure 36: Measured and predicted nitrogen dynamics for the Cal no tree north test cell.....	57
Figure 37: Measured and predicted nitrogen dynamics for the Cal no tree south test cell.....	57
Figure 38: Measured and predicted nitrogen dynamics for the Cal with tree north test cell.....	58

Figure 39: Measured and predicted nitrogen dynamics for the Cal with tree south test cell.....	58
Figure 40: Measured and predicted N dynamics for the Cal PAM no tree north test cell.....	59
Figure 41: Measured and predicted N dynamics for the Cal PAM no tree south test cell.....	59
Figure 42: Measured and predicted N dynamics for the Cal PAM with tree north test cell.....	60
Figure 43: Measured and predicted N dynamics for the Cal PAM with tree south test cell.....	60
Figure 44: The with-root and no-root testing cell apparatus with influent tank, dosing valves, and under-drain equipped testing cells .....	72
Figure 45: Hydrus domain properties and boundary conditions showing the 2D mesh discretization, five observation points and the atmospheric and free drainage boundaries. All outer nodes were no flux boundaries.....	73
Figure 46: Bromide tracer study results for duplicate trials of the no-roots and with-roots test cells. Average results for each treatment were utilized as the soil hydraulic and solute transport fitting exercises in Hydrus .....	74
Figure 47: Comparisons of the Hydrus model output for a simulated bromide tracer to actual bromide tracer results for the no-root (panel A) and with-root (panel B) testing cells .....	74
Figure 48: Measured influent and effluent concentrations of ammonium (NH <sub>4</sub> ) and nitrate (NO <sub>3</sub> ) for the no-root and with-root testing cells after three weeks of intermittent dosing.....	75
Figure 49: Simulated pressure head and water content data (final 24 hours shown) at five observation points for the with-root and no-root Hydrus scenarios. Note the differing y-axis scales .....	76
Figure 50: Simulated fast- and slow-degrading organic matter data (final 24 hours shown) at five observation points for the with-root and no-root Hydrus scenarios.....	77
Figure 51: Simulated bacterial concentration data (final 24 hours shown) for total heterotrophs (top panels), <i>Nitrosomonas spp.</i> (middle panels), and <i>Nitrobacter spp.</i> (bottom panels) at five observation points for the with-root and no-root Hydrus scenarios .....	78
Figure 52: Simulated nitrogen concentration data (final 24 hours shown) for ammonium (top panels), nitrate (middle panels), and nitrogen gas (bottom panels) at five observation points for the with-root and no-root Hydrus scenarios. Note the differing y-axis scales.....	79
Figure A 1: Typical anion ion chromatography results for the north head tank.....	84

Figure A 2: Typical anion ion chromatography results for the north Cal PAM with tree test cell .....	85
Figure A 3: Typical anion ion chromatography results for the south Cal PAM with tree test cell .....	86
Figure B 1: Soil analysis results with sample taken from the Port of Morrow test cell.....	87
Figure B 2: Soil analysis results taken from the Calamus field site. This soil was used for all “Cal ” test cells .....	88
Figure C 1: Cumulative mass of nitrogen applied per day of experimentation .....	89
Figure C 2: Cumulative mass of organic-nitrogen applied per day of experimentation .....	90
Figure C 3: Cumulative mass of effluent nitrogen for each test cell .....	91

## LIST OF EQUATIONS

Equation 1: Volume dosed for each test cell ..... 27

## LIST OF ABBREVIATIONS

Cal	Calamus soil
CEC	Cation Exchange Capacity
IC	Ion Chromatography
LUBGMA	Lower Umatilla Basin Groundwater Management Area
mg-N day <sup>-1</sup>	Milligrams Nitrogen per day
mg NH <sub>3</sub> -N day <sup>-1</sup>	Milligrams Ammonium per day as Nitrogen
mg NO <sub>2</sub> -N day <sup>-1</sup>	Milligrams Nitrite per day as Nitrogen
mg NO <sub>3</sub> -N day <sup>-1</sup>	Milligrams Nitrate per day as Nitrogen
mg-N L <sup>-1</sup>	Milligrams Nitrogen per Liter
mg NH <sub>3</sub> -N L <sup>-1</sup>	Milligrams Ammonium per Liter as Nitrogen
mg NO <sub>2</sub> -N L <sup>-1</sup>	Milligrams Nitrite per Liter as Nitrogen
mg NO <sub>3</sub> -N L <sup>-1</sup>	Milligrams Nitrate per Liter as Nitrogen
PAM	Polyacrylamide
POM	Port of Morrow
ppm	Parts per Million
R <sup>2</sup>	Coefficient of Determination
TN	Total Nitrogen
μS cm <sup>-1</sup>	Millisiemens per Centimeter



## CHAPTER 1:

### INTRODUCTION AND LITERATURE REVIEW

In an agricultural setting, nitrogen-based fertilizers are used in combination with irrigation practices to deliver essential nutrients for optimal crop growth and product yield. Nitrogen is an essential element for all life and a required nutrient for plant growth, which makes a variety of nitrogen-rich industrial process waters and many treated domestic wastewaters valuable for crop irrigation (Isosaari, Hermanowicz, and Rubin 2010, 662-697; Parnaudeau et al. 2006, 1284-1295; Virto et al. 2006, 398-407). However, if constituents present in these waters are discharged into the surrounding environment above regulated limits, such as dissolved inorganic nitrogen (e.g. ammonia, nitrate, and nitrite) found in most wastewaters, there can be a significant impact on aquatic systems (Sun et al. 2012, 326-332). These inorganic forms of nitrogen are accessible, reactive and considered responsible for the eutrophication, hypoxia, loss of biodiversity, and habitat degradation in coastal ecosystems. This environmental concern is not limited to wastewaters and surface waters, as the use of any form of fertilizer in agricultural practices can result in non-point source pollution issues affecting groundwater quality and human health (Almasri 2007, 220-242; Suthar et al. 2009, 189-199; Du et al. 2011, 423-430; Galloway et al. 2003, 341-356). Globally, the primary anthropogenic source of reactive nitrogen in groundwater is leaching from agroecosystems (Galloway et al. 2003, 341-356). Without proper management, application of nitrogen above specific agronomic uptake rates can lead to high levels of ammonia and nitrate concentrations in freshwater systems that far exceed the federal drinking water limit of 10 mg/L  $\text{NO}_3^-$ -N (Darwish et al. 2011, 74-84; Jimenez and Chávez 2004, 269-276; Chen et al. 2010, 131-138; Oregon Department of Environmental Quality 2012; WHO (World Health Organization) 1998). Ideally, application of nitrogen-based fertilizers should be metered and timed to meet

crop needs instead of being dosed in one large quantity prior to planting in order to reduce, or even avoid, nitrogen leaching (Prunty and Greenland 1997, 1-13). Due to a variety of physical, chemical, and biological reasons, this method of fertilization would be both crop and site specific. In well-draining soils, even when fertilizer is applied at the recommended agronomic rates it has been found that nitrogen leaching from direct application of fertilizer is substantial for crops such as potato, sweet corn, and other shallow-root crop systems (Kraft and Stites 2003, 63-74). Studies have even shown that on well-irrigated agricultural land, vegetable and wheat-maize rotation crops may increase  $\text{NO}_3^-$ -N concentrations over time (Chen et al. 2010, 131-138).

Excess nitrate present in groundwater can be harmful to both infants and adults, causing methemoglobinemia (better known as blue-baby syndrome), stomach cancer, Alzheimer disease, vascular dementia, multiple sclerosis, hypertrophy, etc. (Chen et al. 2010, 131-138; Hajhamad and Almasri 2009, 1073-1087; Suthar et al. 2009, 189-199). Methemoglobinemia occurs when high levels of nitrate reduce the oxygen-carrying capacity of blood cells by binding to hemoglobin, potentially causing mortality by asphyxiation (Suthar et al. 2009, 189-199; Galloway et al. 2003, 341-356). This is a concern on a global scale, especially in areas where heavy agriculture has been shown to elevate the levels of nitrate present in the surrounding groundwater due to the conversion of nitrogen-based fertilizers into nitrate by nitrifying bacteria living in the soil (Hajhamad and Almasri 2009, 1073-1087; Almasri 2007, 220-242; Fortier et al. 2010, 276-287; Kraft and Stites 2003, 63-74). People who rely on groundwater as their primary source for drinking water are the most at risk, and aquatic ecosystems may also be affected by nitrate-polluted groundwater discharging into local surface waters, harming the eggs and young of some salmonids and amphibians (Kraft and Stites 2003, 63-74; Kincheloe, Wedemeyer, and Koch 1979, 575-578; Hecnar 1995, 2131-2137; Marco, Quilchano, and Blaustein 1999, 2836-2839).

Nitrification, denitrification, mineralization, immobilization, and plant uptake are the major soil transformation processes that greatly affect nitrate leaching (Almasri 2007, 220-242; Vymazal 2007, 48-65). Studies have shown that organic soil horizons containing roots have a denitrifying enzyme assay (DEA) activity of nearly 100 times higher (14.6 mg N per unit of soil weight (g) per day) than mineral horizons without roots (0.15 mg N per unit of soil weight (g) per day) (Maître et al. 2003, 76-93; Smith and Tiedje 1979, 261-267; Fortier et al. 2010, 276-287). Mineralized crop residue can also significantly contribute to nitrate leaching, ranging from 10 to 99 kg N ha<sup>-1</sup> for potato residue in a sandy region (Kraft and Stites 2003, 63-74; Bundy, Andraski, and Bland 1997, 53-61; Saffigna and Keeney 1977, 258-264).

Water moves more rapidly through sandy, or coarse textured, soils when compared to clay soils, creating a higher potential for soluble nitrate to leach into the groundwater (Hajhamad and Almasri 2009, 1073-1087; Marco, Quilchano, and Blaustein 1999, 2836-2839). Coarse textured, sandy soils have small water holding capacities and conventional irrigation practices exacerbate the potential for N leaching because soil moisture is kept near the optimum for plant growth (Kraft and Stites 2003, 63-74; Kavdir, Hellebrand, and Kern 2008, 175-186). Aerobic conditions are dominant for longer periods in sandy soils compared with clay soils, thereby limiting denitrification potential (Kavdir, Hellebrand, and Kern 2008, 175-186). Once soluble nitrate is present in the groundwater, it will freely migrate via advection and dispersion and may undergo denitrification depending on the dissolved oxygen concentration (Almasri 2007, 220-242). Total nitrogen (TN) removal is dependent on nitrification, the conversion of ammonia-nitrogen to nitrate, and subsequently the denitrification of NO<sub>3</sub><sup>-</sup>-N (Fan et al. 2013, 461-466). A field experiment on tillage land underlain by a sand and gravel aquifer in south-east Ireland found that using mustard as a winter cover crop decreased groundwater NO<sub>3</sub><sup>-</sup>-N concentrations compared to using no cover (Premrov et al. 2012, 144-153). Another study found that nitrate concentrations were lower in poorly-drained

than well-drained sandy soils, suggesting that dissolved organic matter decomposes aerobically before reaching the groundwater table (Ruijter et al. 2007, 155-167).

Wastewater from food-processing industries frequently contains large amounts of organic nitrogen and other materials such as protein, carbohydrates, and lipids with high biochemical and chemical oxygen demands (Tusseau-Vuillemin 2001, 143-152; Rittmann and McCarty 2001). Application of this food-processing wastewater has been shown to significantly increase soil organic carbon (Lin et al. 2008, 6190-6197), thus improving soil quality over time by providing higher buffering activity, longer retention of soil moisture, and increasing the overall soil fertility (Skjemstad, Janik, and Taylor 1998, 667-680). This is important to note because high soil-water content helps promote microbial denitrification by reducing oxygen supply through the soil pore structure and an available source of organic matter is necessary for denitrifiers' metabolic activity (Röver, Heinemeyer, and Kaiser 1998, 1859-1865). There are multiple studies that have found a positive correlation between soil moisture and denitrification rates in various soil types and climates (Aranibar et al. 2004, 359-373; Luo, Tillman, and Ball 2000, 497-509; de Klein and van Logtestijn 1996, 231-237; McKeon et al. 2005, 119-136). Research by Kavdir et al. found that optimal conditions for denitrification in soils occur around 50–90% water-filled pore space. If the soil water content is too high, soluble  $\text{NO}_3^-$ -N is more likely to be leached from the soil (Kavdir, Hellebrand, and Kern 2008, 175-186). The amount of organic matter present in the topsoil layer is also a main factor affecting soil-water permeability as more organic matter generally means a greater water holding capacity (Nadav et al. 2012, 275-283).

Methods of crop production can also influence denitrification rates and soil-nitrate concentrations. Studies have shown that agricultural practices employing no-tillage systems have higher denitrification rates than conventional tillage plots, with  $\text{NO}_3^-$ -N concentrations greater under conventional tillage at all soil depths (Mkhabela et al. 2008, 187-199; Elmi et al. 2003, 340-348). This discrepancy is understood to occur because no-

tillage systems improve soil structure, reduce erosion, sequester carbon, and promote higher soil water and organic matter content compared with conventional tillage systems (Mkhabela et al. 2008, 187-199; Elmi et al. 2003, 340-348). Additionally, Mkhabela et al. has reported increased nitrogen mineralization in conventional tillage systems, resulting in higher  $\text{NO}_3^-$ -N leaching than no-tillage systems. Tillage events are known to perturb soil microbial processes and have been shown to decrease soil quality by increasing greenhouse gas emissions and increasing the potential for nitrate leaching into groundwater (Jackson et al. 2003, 305-317). In one study where there was little difference in  $\text{NH}_4^+$ -N concentrations and moisture content between tillage and no-tillage systems, Jackson et al. found that  $\text{NO}_3^-$ -N concentrations became twice as high within two weeks after a tillage event. Denitrification rates temporarily increased in response to the higher  $\text{NO}_3^-$ -N concentrations, but an overall loss of N ( $\text{NO}_3^-$ -N leaching) from the soil occurred before the site returned to a pre-disturbance status (Jackson et al. 2003, 305-317). It is important to note that no-tillage systems may allow for the formation of continuous soil macro-pores, thereby increasing preferential flow for  $\text{NO}_3^-$ -N leaching into the groundwater (Mkhabela et al. 2008, 187-199; Elmi et al. 2003, 340-348). The argument for which agricultural process is preferred will depend on site-specific conditions and potential for macro-pore development. If using short-rotation coppice crops, the process of uprooting and replanting may cause soil disturbances that result in a flush of mineralization, increasing the amount of leached nitrate (Goodlass et al. 2007, 178-184). Poplar plantations grown for above-ground biomass production and wastewater treatment would not require conventional tillage.

Hybrid poplar trees are fast growing and have much deeper root systems than commonly irrigated crops (e.g. alfalfa, beets, etc.) making this plant a target species for engineering a deeper, more effective nitrate treatment zone for the protection of shallow groundwater and for the potential production of woody biomass (Chávez et al. 2012, 76-84; Chen et al. 2010, 131-138; Holm and Heinsoo 2013, 126-135; Kavdir, Hellebrand,

and Kern 2008, 175-186). Jordahl et al. (Jordahl et al. 1997, 1318-1321) found that microbial concentrations of denitrifiers were four times higher in soil samples from the rhizosphere of poplar trees than in adjacent agricultural soils and the poplar rhizosphere can increase the concentration of beneficial denitrifying microorganisms for natural bioremediation of nitrogen-rich wastewaters. Additionally, Ulrich et al. (Ulrich, Ulrich, and Ewald 2008, 169-180) found that the *Pseudomonas* genera were among the most abundant bacterial endophytes found in *Populus* clones. Research by Rennenberg et al. found that *Populus* has the ability to grow at both low and high concentrations of  $\text{NH}_4^+$  or  $\text{NO}_3^-$  (Rennenberg, Wildhagen, and Ehling 2010, 275-291). Although being out-competed for growth during the study, *P. deltoides* x *P. nigra* L. hybrids were found to have transpiration rates of  $3.0 \text{ mm day}^{-1}$  during the summer and are expected to have even higher rates when under more optimal growing conditions (Allen, Hall, and Rosier 1999, 493-501). Hybrid poplar buffers greatly increase carbon and nutrient sequestration with increasing site fertility when compared with herbaceous grass buffers and were also measured as more efficient for nitrate retention during winter months with N immobilization rates averaging  $37$  and  $16 \text{ kg N ha}^{-1} \text{ year}^{-1}$ , respectively (Fortier et al. 2010, 276-287). Rooted poplar trees can also provide perennial interception and be effective in long-term nitrate reduction (Paterson and Schnoor 1993, 986-993). Investigations involving the application of wastewater (approx.  $300 \text{ kg N ha}^{-1} \text{ yr}^{-1}$ ) to well-established poplar (second growing season) have shown enhanced plant growth while effectively retaining nitrogen, having a near-zero  $\text{NO}_3^-$ -N concentration in the drainage water, even during the snowmelt period (Dimitriou and Aronsson 2011, 161-170). However, it has also been shown that extensive N-leaching can be expected if poplars are not well-established (Dimitriou and Aronsson 2011, 161-170). Additionally, if poplar plantations are not harvested and become nutrient-saturated, nitrogen present in the biomass may be released back into the environment as the vegetation either drops its leaves or dies and decays (Fortier et al. 2010, 276-287; Kelly, Kovar, and Sokolowsky

2007, 239-251). For this reason, some studies recommended harvesting above-ground biomass from poplar plantations during late-summer when they still have all their leaves (Fortier et al. 2010, 276-287). Alternatively, one study focusing on phosphorus uptake argues that a growing-season harvest would limit the ability of cottonwood to regenerate vegetation, whereas harvest during dormancy would allow for several harvest cycles before the stand would need to be replanted (Kelly, Kovar, and Sokolowsky 2007, 239-251).

Plants used in short-rotation coppices (SRC), such as poplar or willow, can be grown to produce biomass for renewable energy production as an alternative to fossil fuels (Pistocchi et al. 2009, 137-146; Labrecque and Teodorescu 2003, 135-146). Although focusing on grassy buffers during the irrigation season, (Bedard-Haughn, Tate, and C van Kessel 2005, 1651-64) found that regular cutting of the vegetative buffer significantly increased overall N sequestration when compared with the uncut buffer. With this in mind, Labrecque and Teodorescu (Labrecque and Teodorescu 2003, 135-146) have shown that harvested biomass yield of *Salix* clones could be maintained or even increased over time so long as adequate nutrient requirements were satisfied. Interestingly, one study showed that *Salix spp.* will need more fertilizer for the third year of biomass harvest than needed during the first and second cycles (Labrecque and Teodorescu 2003, 135-146). Several studies have shown that established hybrid poplar plantations provide a reliable supply of biomass while sequestering carbon in the soil (Jassal et al. 2013, 323-333; Fortier et al. 2010, 276-287; Friend et al. 1991, 109-119; Hansen 1993, 431-436). One study using  $^{14}\text{C}$  labeling found that approximately 24% of carbon exported from hybrid poplar branches was translocated to the root system (Friend et al. 1991, 109-119). As hybrid poplar plantations develop, annual carbon sequestration and water use will continue to increase until a mature canopy is achieved (Jassal et al. 2013, 323-333). Poplars would create a belowground carbon-sink if fine root biomass replaced itself one or more times per year (Friend et al. 1991, 109-119). One main factor

controlling biomass growth in hybrid poplars is  $\text{NO}_3^-$  supply rate, which also related to carbon sequestration and nutrient accumulation (Fortier et al. 2010, 276-287).

Sandy soils and poplar tree dormancy represent particular design challenges toward an effective and predictable engineered vadose zone (Gemail 2012, 749-761; Nadav, Tarchitzky, and Chen 2012, 75-81; Ndour et al. 2008, 797-803). Water and non-sorbing solutes, such as nitrate, move quickly through sandy soils, which can limit the nitrate transformation potential (Saeed and Sun 2013, 438-447; Almasri 2007, 220-242; Marco, Quilchano, and Blaustein 1999, 2836-2839). Complex land use interactions, variable surficial nitrogen loading, heterogeneous soil physical and chemical characteristics, soil nitrogen dynamics, and depth of soil profile make accurate quantification of nitrate leaching difficult (Almasri 2007, 220-242). Studies investigating willow growth, and their productivity in sand compared with clay soils, have shown that willow planted on clayey soils produced more above-ground biomass than on sandy soils and growth-response to fertilization was more significant in sandy soils (Labrecque and Teodorescu 2003, 135-146). In a similar study, (Aronsson and Bergström 2001, 155-164) found that established willow roots on sandy soils have a high capacity to filter nitrate from percolating wastewater, even into late autumn after leaf fall. (Williams et al. 2010, 1680-1685) discovered that under sunny conditions, oxygen levels in the root zone of willow would fluctuate between completely anaerobic and fully aerobic during the day and night, respectively. Essentially, the change in subsurface redox conditions would allow simultaneous nitrification and denitrification processes with oxygen levels depending on photosynthetic activity and time of day (Williams et al. 2010, 1680-1685).

Due to the high evapotranspiration rate of poplar and willow species, these crops are commonly used to improve wastewater quality as they can treat high volumes of wastewater (Pistocchi et al. 2009, 137-146). Treating wastewaters containing nitrogen by using poplar vegetation filters is more cost efficient than conventional methods, as long as environmental standards are still being met (Pistocchi et al. 2009, 137-146). Since



poplar is considered a non-edible crop, the possible hygienic risks are reduced when compared with other vegetation filters (Pistocchi et al. 2009, 137-146). Despite the inactivity of plant growth and nutrient uptake during winter dormancy, Haycock and Pinay (Haycock and Pinay 1993, 273-278) found that denitrification capacity in grass and poplar-vegetated riparian strips was equivalent between winter and summer conditions, with the poplar-vegetated riparian zone more resilient to  $\text{NO}_3^-$ -N loading rates than the grass-vegetated riparian zone. *Populus* trees cease growth and set dormant buds in preparation for winter (Jansson and Douglas 2007, 435-458). *Populus spp.* store reduced nitrogen during winter dormancy in the form of bark storage proteins, allowing for immediate nutrient access at the end of the dormant season (Cooke and Weih 2005, 19-30). This phenotypic ability is thought to have developed in *Populus spp.* as an advantage for growth in environments with limited nutrient availability (Cooke and Weih 2005, 19-30). Although temperatures below zero will halt *Populus* growth and rapidly set buds, the length of day seems to be the main trigger for timing of bud set (Jansson and Douglas 2007, 435-458). During dormancy and colder-temperatures, root uptake is minimalized, leaving vadose zone bacteria solely responsible for nitrate treatment and removal (Maître et al. 2003, 76-93). Denitrification rates have been shown to be relatively stable and independent of seasonal variation in saturated layers of the soil (Maître et al. 2003, 76-93). Some studies have even observed higher nitrogen removal rates during the dormant season due to microbial activity (Nelson, Gold, and Groffman 1995, 691-699; Simmons, Gold, and Groffman 1992, 659-665). Multiple investigations (Bachand and Horne 1999, 17-32; Braker, Schwarz, and Conrad 2010, 134-148) have found that water temperatures had a greater effect on denitrification rates than DO concentration, nitrate availability, and organic carbon availability. For example, Jackson et al. (Jackson et al. 2003, 305-317) follow a pattern whereby microbial processes double in activity with every 10°C increase in temperature. Additionally, oxygen diffusion into sandy, unsaturated soils can limit denitrification by heterotrophic bacteria and intermittent irrigation and cool

temperatures can inhibit bacterial growth (Rittmann and McCarty 2001; Jackson et al. 2003, 305-317). Thus, the behavior of nitrate in a sandy, poplar tree vadose zone during dormancy represents a major design constraint for the successful, year-round operation of such an engineered system.

There are various other in-situ technologies employed to reduce nitrogen from waters and wastewaters. A few worth mentioning are vertical- and horizontal-flow wetlands and denitrification walls. In vertical flow wetlands, studies show that the physicochemical processes transforming ammonia include sorption onto substrate media (Connolly et al. 2004, 1971-1976), assimilation into bacterial biomass and nutrient uptake by plants (Lin et al. 2002, 413-420; Vymazal 2007, 48-65), and nitrification-denitrification processes (Sun et al. 2012, 326-332; Saeed and Sun 2011a, 439-447; Lin et al. 2002, 413-420). Investigations have shown that vertical-flow constructed wetlands can successfully remove ammonia-N, but have limited ability to denitrify, whereas horizontal-flow constructed wetlands promote favorable conditions for denitrification but are limited in their ability to nitrify ammonia (Vymazal 2007, 48-65). Specifically, planted wetlands have the ability to influence pH and temperature, resulting in more favorable conditions for a higher nitrate removal rate than unplanted wetlands (Lin et al. 2002, 413-420; Lu et al. 2009, 1036-1043). Denitrification walls are built by mixing a carbon source, such as sawdust, into the soil below the water table, arranged perpendicular to groundwater flow. The added carbon source is intended to stimulate microbial denitrifying activity (Schipper and Vojvodić-Vuković 2001, 3473-3477). One study investigating the impact on nitrate removal by denitrification walls found that there was sufficient available carbon from one soil mixing to support denitrification and nitrate removal for at least 5 years (Schipper and Vojvodić-Vuković 2001, 3473-3477). Another study from Long et al. (Long, Schipper, and Bruesewitz 2011, 514-520) found denitrification walls to be effective 14 years after installation, removing 92% of nitrate input, ranging from 2.2 to 3.7 mg N L<sup>-1</sup>, with up to 66 years of total available carbon.

Denitrification walls act as a site-specific filtration technique, targeting a nitrate contaminated groundwater source and would not fare well under non-point source conditions or above-ground wastewater application. Additionally, these walls would need replacement once the added carbon source became depleted by denitrifying activity.

### 1.1 Theory

Nitrification is the microbiological oxidation of ammonium to nitrate with nitrite as the intermediate step (Rittmann and McCarty 2001; Vymazal 2007, 48-65). Nitrifying bacteria are chemolithoautotrophic bacteria and considered obligate aerobes, using  $O_2$  for respiration (Rittmann and McCarty 2001). Nitrification is a two-step process involving two groups of microorganisms, producing soluble microbial products that can be consumed by heterotrophic bacteria (Rittmann and McCarty 2001; Vymazal 2007, 48-65). The first step, often considered the rate-limiting portion of nitrification, constitutes the oxidation of  $NH_4^+$  to  $NO_2^-$  and is commonly carried out by the genus *Nitrosomonas*; however, *Nitrosococcus*, *Nitrosopira*, *Nitrosovibrio*, and *Nitrosolobus* also have this ability to oxidize  $NH_4^+$  to  $NO_2^-$  (Rittmann and McCarty 2001; Vymazal 2007, 48-65). The second stage of nitrification involves the oxidation of  $NO_2^-$  to  $NO_3^-$ , most commonly carried out by the genus *Nitrobacter* (Rittmann and McCarty 2001; Vymazal 2007, 48-65). Investigations have shown that ammonia-nitrogen can have an oxygen demand of up to 4.57 g  $O_2$ /g  $NH_4^+$ -N (Rittmann and McCarty 2001), consuming roughly 8.64 mg  $HCO_3^-$  per mg  $NH_4^+$ -N in the oxidation process (Vymazal 2007, 48-65).

As a natural part of the nitrogen cycle, nitrate represents the most oxidized chemical form of nitrogen (Suthar et al. 2009, 189-199). Nitrate is also essential for proteins, genetic materials (DNA and RNA), hormones, and enzymes that are part of living organisms (Suthar et al. 2009, 189-199). Bacterial denitrification is the irreversible, dissimilatory reduction of nitrate ( $NO_3^-$ ) to dinitrogen ( $N_2$ ) and nitrous oxide ( $N_2O$ ) gases (Rittmann and McCarty 2001; Vymazal 2007, 48-65; Almasri 2007, 220-242).

Specifically, there are heterotrophic and autotrophic bacteria which assimilate nitrate via denitrification, reducing the overall presence of nitrate (Rittmann and McCarty 2001).

The gaseous and chemically inert dinitrogen ( $N_2$ ) is the desired end product of denitrification because it is not harmful to the environment (Sun et al. 2012, 326-332).

This bacterial reduction of  $NO_3^-$ -N is a metabolic process used in energy generation that consists of several successive intermediate steps, typically beginning with  $NO_3^-$  as the electron acceptor (Rittmann and McCarty 2001; Kumon et al. 2002, 2963-2968). These intermediaries, listed in succession, include nitrite ( $NO_2^-$ ), nitric oxide (NO), and nitrous oxide ( $N_2O$ ) (Kumon et al. 2002, 2963-2968). Physiologically, it is known that denitrification is most likely to occur when oxygen ( $O_2$ ) is unavailable, thereby functioning as a form of anaerobic respiration where any available  $NO_3^-$ -N may be used as the terminal electron acceptor (Kumon et al. 2002, 2963-2968; Rittmann and McCarty 2001; Fan et al. 2013, 461-466). However, this can be misleading as there is much evidence in the literature showing that denitrification can and is occurring at a significant rate in the presence of oxygen from a variety of microorganisms (Chen et al. 2012, 266-270; Zhang et al. 2011, 9866-9869; Takaya et al. 2003, 3152-3157; Miyahara et al. 2010, 4619-4625; Patureau et al. 2001, 189-197; Robertson et al. 1989, 289-299).

Understanding the potential for aerobic denitrification is of practical importance as it enables denitrification to occur either in the presence of oxygen or soon after establishing anoxic conditions, without altering the microbial population (Vymazal 2007, 48-65).

There are even studies showing that establishing intermittent aeration, alternating between aerobic and anaerobic conditions, can be favorable for both nitrification and denitrification potential (Fan et al. 2013, 461-466). Denitrification plays an important role in the global nitrogen cycle and denitrifiers are commonly found in soils, sediments, surface waters, groundwaters, and wastewater treatment plants (Rittmann and McCarty 2001). Although most denitrifiers do not typically show a strong sensitivity to pH, values outside the optimal range of 7 to 8 may lead to the accumulation of intermediates

(Rittmann and McCarty 2001) and the optimum pH for denitrification is near neutrality (Simek, Jisova, and Hopkins 2002, 1227-1234). Denitrification rates for saturated, sandy soils have been reported within the range of  $0.13 \text{ mg NO}_3^- \text{-N L}^{-1} \text{ h}^{-1}$  (Trudell, Gillham, and Cherry 1986, 251-268) and  $0.83 \text{ mg NO}_3^- \text{-N L}^{-1} \text{ h}^{-1}$  (Focht, Bowman, and Joseph 1972). A model from (Allen, Hall, and Rosier 1999, 493-501; Attard et al. 2011, 1975-1989) shows that carbon, oxygen, and nitrate availability is more important than abundance and community structure for denitrifying activity. Other studies have shown that nitrate reductase, the first enzyme in nitrate reduction, is not affected by salt exposure in either gene expression or protein activity level (Rennenberg, Wildhagen, and Ehling 2010, 275-291).

## 1.2 Description of Field Site

The Boardman Industrial Park is located on the Columbia River near Boardman, Oregon in Morrow County. It is owned, operated, and managed by the Port of Morrow (POM). The POM has jurisdiction that encompasses more than 12,000 acres of land and they are responsible for clean water, economical power, transportation, and advanced communications for a wide variety of industrial companies (Port of Morrow 2012). In 2003, the tenants of the Boardman Industrial Park were (1) food processors – Boardman Foods, Logan International, Oregon Potato Company, Distilling Unlimited, ConAgra Frozen Foods / Lamb-Weston, Morrow Cold Storage, and Columbia River Processing (2) power plants – Portland General Electric (PGE) Coyote Springs Power Plants I and II and (3) mining concerns – Coyote Springs Sand and Gravel (Kennedy/Jenks Consultants 2007). The majority of the food processing facilities are located in an area referred to as the “Food Processing Park” along with tens of thousands of potato and onion storage facilities. This park produces wastewater and Port of Morrow currently land applies approximately 1.8 billion gallons of food processing wastewater (4.9 MGD) and approximately 4.6 billion gallons of supplemental water annually to approximately 5700

acres of farmland (Figure 1) (Richerson 2011). The supplemental water used in conjunction with the wastewater consists of Columbia River water, canal water, and several groundwater wells. The wastewater stream is composed mainly of decomposing potatoes and onions and has been recently analyzed to have high levels of ammonia and other constituents such as total organic carbon (TOC) (Licht 2012; State Hygienic Laboratory 2013). Other stream sources for wastewater include cooling tower blow down, boiler blow down, cheese and corn processing water, ethanol plant water, and storm water (Richerson 2011). As a sustainable practice, this wastewater is land applied approximately 3 miles east of the City of Boardman using sprinkler irrigation system to three farms titled Farm 1, Farm 2, and Farm 3 providing essential nutrients to grow a variety of crops (Figure 2). Farm 1 is under contract for management with the Port of Morrow, while Farms 2 and 3 are privately owned, with areas of approximately 1366, 3810, and 2828 acres, respectively (Richerson 2011). The field site employed as the basis for this project is located on Farm 1, near the wastewater storage lagoon depicted in Figure 2. Upgradient wells for the western portion of Farm 1 include monitoring wells MW-3a and MW-6. Downgradient wells for the western portion of Farm 1 include MW-10 and MW-11. Depth to water beneath Farm 1 ranges from less than 6 feet at MW-6 to more than 80 feet at wells in the northeastern portion (Richerson 2011).

Previous analyses of the monitoring wells at Port of Morrow have developed a time series graph (Figure 3a) showing nitrate concentrations at the upgradient and downgradient wells for the western portion of Farm 1. This figure shows individual data points connected by a thin line and a thicker line that was determined using a data smoothing technique that describes the general pattern of the data throughout the timeframe. The upgradient monitoring wells, MW-3a and MW-6, shows nitrate concentration remaining fairly constant at approximately 1 ppm and 4 ppm, respectively, from 1987 through 1999. The downgradient monitoring wells, MW-10 and MW-11, started higher than upgradient wells and have increased over time. Figure 3b is a box and

whisker plot summarizing the average nitrate concentration from the upgradient and the downgradient wells. From this dataset, the Port of Morrow has concluded that facility operations have impacted and continue to impact groundwater quality at the western portion of Farm 1. Similar analyses of the monitoring wells for the eastern portion of Farm 1 and western portion of Farm 3 (Figure 4) have concluded that offsite activities and facility operations have and continue to impact groundwater quality at the eastern portion of Farm 1 and the western portion of Farm 3. This data helped determine that average nitrate trends for Farm 1 are increasing at least  $0.35 \text{ ppm yr}^{-1}$ , with three wells exhibiting average nitrate concentrations less than the federally regulated 10 ppm drinking water standard and nine wells exhibiting higher average nitrate concentrations. Overall, the site-wide trend has been increasing with over half of the monitoring wells showing statistically significant increasing nitrate trends (Richerson 2011).

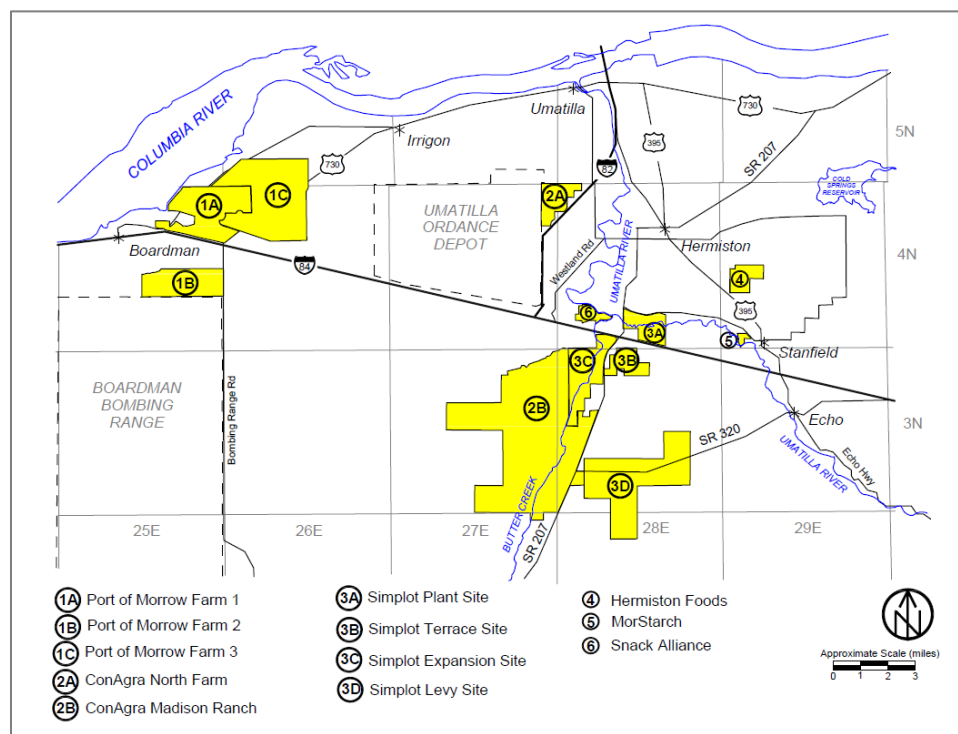


Figure 1: Location of food processor land application sites in the Lower Umatilla Basin Groundwater Management Area (LUBGWMA)

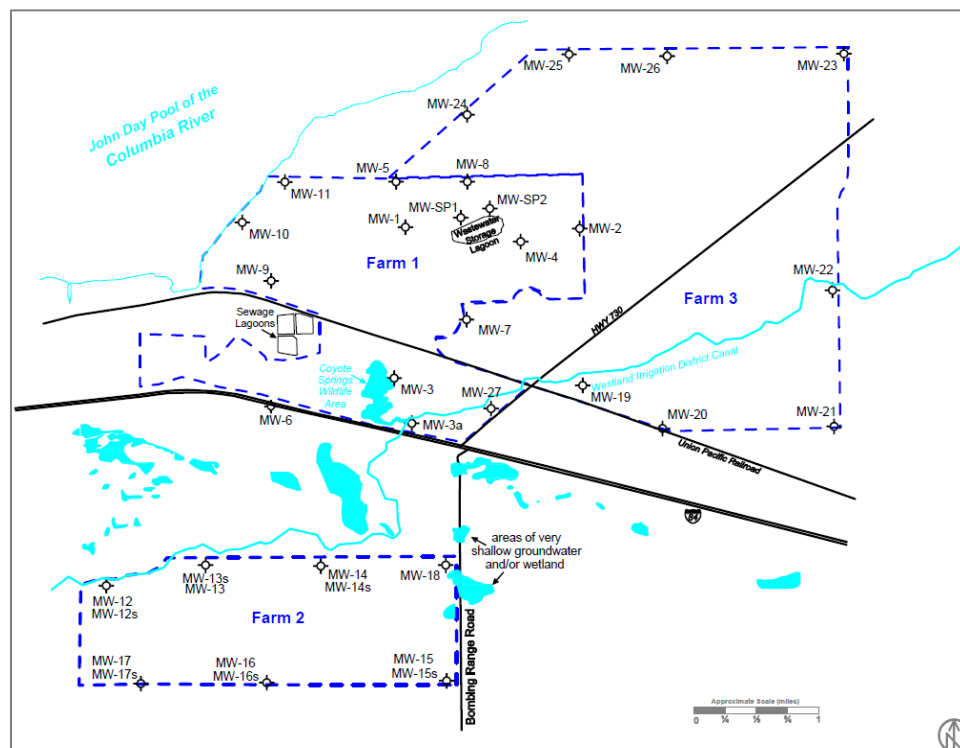


Figure 2: Well locations and surface water bodies - Port of Morrow Farms



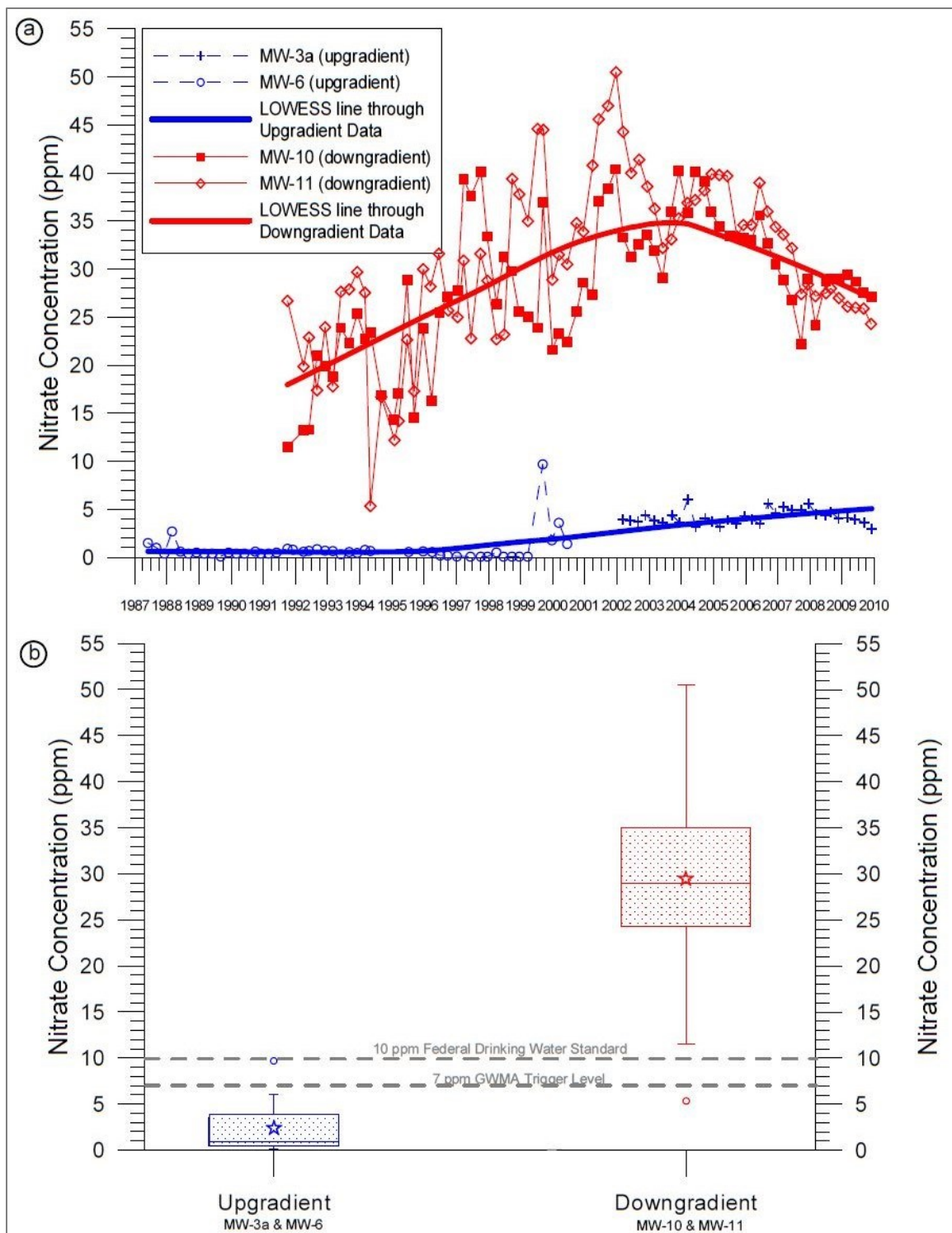


Figure 3: Upgradient vs downgradient nitrate comparisons - western portion of Port of Morrow Farm 1

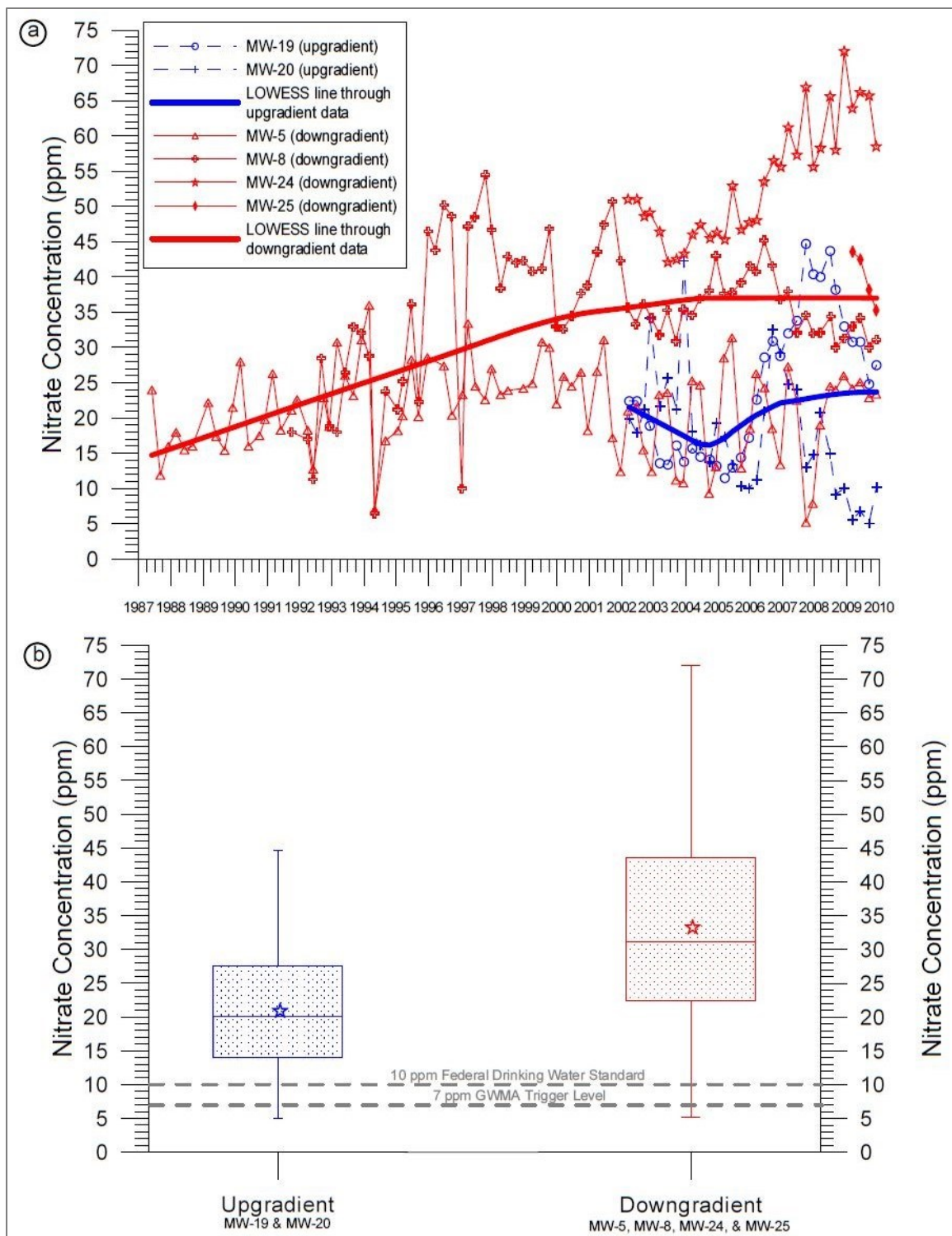


Figure 4: Upgradient vs downgradient nitrate comparisons - eastern portion of Port of Morrow Farm 1 & western portion of Farm 3

### 1.3 Research Objectives

The main objective of this research was to build, operate and model a pilot-scale, sandy soil, poplar vadose zone system to study the behavior of irrigated ammonium and nitrate-containing wastewater from industrial food processing operations during tree dormancy. The overall goal was to investigate whether or not dormant poplar-rooted vadose zones will enhance denitrification by minimizing nitrate loss to groundwater during winter in a climate with average temperatures between minus 3 and 5°C. Our central hypothesis was that sandy soils planted with poplar trees would have a higher capacity for nitrogen-containing irrigation water and therefore a greater ability to minimize nitrate loss than would unplanted soils. A central research deliverable was a model that could describe and predict the pilot-scale system behavior in two and three-dimensions with expectations of applying the model at the field-scale in the future.

Although previous studies have focused on the treatment efficiency of vegetative filters during the active growing season when evapotranspiration is a critical factor (Pistocchi et al. 2009, 137-146), few have focused on the denitrification capacity of hybrid poplar-rooted vadose zones during dormancy. During dormancy, plant uptake and evapotranspiration become extremely limited and wastewater treatment, specifically denitrification, is then controlled by the established microbial community.

## **CHAPTER 2:**

### **WATER FLOW AND NUTRIENT DYNAMICS**

#### **2.1 Abstract**

This research utilized a pilot-scale, sandy soil, poplar vadose zone system to study the behavior of irrigated ammonium and nitrate-containing wastewater during tree dormancy. After reaching steady-state conditions, the with-root and no-root treatments had statistically similar effluent ammonium concentrations representing 99% removal of the influent dose. The nitrate concentration in the with-root testing cell effluents (1.0 mg/L) was statistically different than measured in the no-root treatment (5.1 mg/L). Two-dimensional numerical modeling of the testing cells was able to describe the water movement and nitrogen transformation dynamics within the testing cells with good agreement to measured data. The study provides strong evidence that less nitrate escapes a deeply rooted vadose zone than a non-rooted, or shallow rooted, system even during dormancy (4.5°C).

#### **2.2 Introduction**

The main objective of this research was to build, operate, and model a pilot-scale, sandy soil, poplar vadose zone system to study the behavior of irrigated ammonium and nitrate-containing wastewater from industrial food processing operations during tree dormancy. The overall goal was to better understand the system conditions that allow for the maximization of irrigated wastewater and the minimization of nitrate loss to groundwater during winter in a climate with average temperatures between minus 3 and 5°C. Our central hypothesis was that sandy soils planted with poplar trees would have a higher capacity for nitrogen-containing irrigation water and a greater ability to minimize nitrate loss than would unplanted sandy soils.

## 2.3 Materials and Methods

### 2.3.1 Pilot-scale Experimentation

The pilot-scale poplar tree vadose zone system consisted of two 56.8 L (15 gallon), polypropylene tanks (A-INFD15-19, Plastic-mart.com), each connected to five testing cells via 5.1 cm (2.0 in) diameter PVC piping (Figure 5). Electronic shutoff valves (344B Series, TeeJet Technologies, Wheaton, IL) wired to a programmable microprocessor (Arduino UNO) provided customizable dosing control. Figure 6 shows a side profile of an individual test cell with trees and roots. Each polypropylene test cell (R121230B, Plastic-Mart.com), 30.5 cm x 30.5 cm x 76.2 cm (12 in x 12 in x 30 in LWH), was fitted with a 1.25 cm diameter (0.5 in) perforated underdrain (Figure 7) that was 28 cm (11 in) long and wrapped with permeable felt. Each underdrain was built with a custom stand in order to ensure free drainage from the test cell (Figure 8). The entire system was contained within a refrigerated room maintained at  $4.5^{\circ}\text{C} \pm 2^{\circ}\text{C}$ .

### 2.3.2 Test Cell Treatment Types

Port of Morrow (POM) soil was extracted from Farm 1 of the field site in Eastern Oregon and used for all POM test cells. During this research study, new test cells needed to be constructed for experimentation and a similar soil type to POM soil was available at a nearby location in Calamus, IA. Calamus soil was extracted from farmland, sieved with a #10 US standard mesh filter (2.00 mm sieve size) to remove roots, rocks, and any vegetative materials, and used for experimentation in all Cal test cells.

Experiments were carried out in ten vertical flow polypropylene testing cells with identical dimensions, 30.5 cm x 30.5 cm x 76.2 cm (12 in x 12 in x 30 in LWH). Two testing cells contained only sandy Calamus soil and served as the no root control treatments. Two other sandy Calamus soil test cells had the top 6 -8 inches amended with polyacrylamide (Hydrosorb<sup>TM</sup>, 2001F) and did not contain trees. Four testing cells were each fitted with five tightly-spaced, poplar trees (*populus deltoides x nigra*, DN-21) that

were rooted for 3 months prior to transplanting into the testing cells and filled with 74 cm of sandy Calamus soil. Two of these test cells containing trees had the top 6 -8 inches of soil amended with polyacrylamide (Hydrosorb<sup>TM</sup>, 2001F). The final two testing cells contained sandy soil from the Port of Morrow, with one cell containing five tightly-spaced poplar trees (*populus deltoides x nigra*, DN-21) that had 2 years of established growth and the other test cell containing POM sandy soil with no trees. All testing cells were placed outside and dosed manually with a synthetic wastewater for three months, until the end of the growing season. After the hybrid poplars entered dormancy, all test cells were moved inside the walk-in cooler for experimental analysis

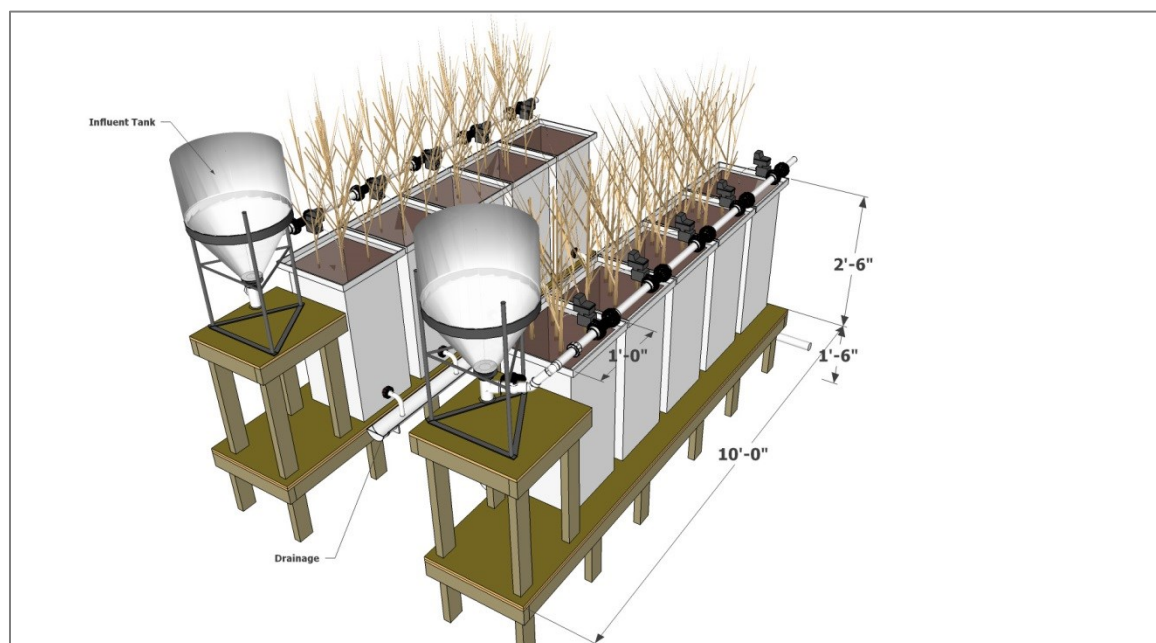


Figure 5: 3D Schematic of the pilot-scale poplar tree vadose zone irrigation system

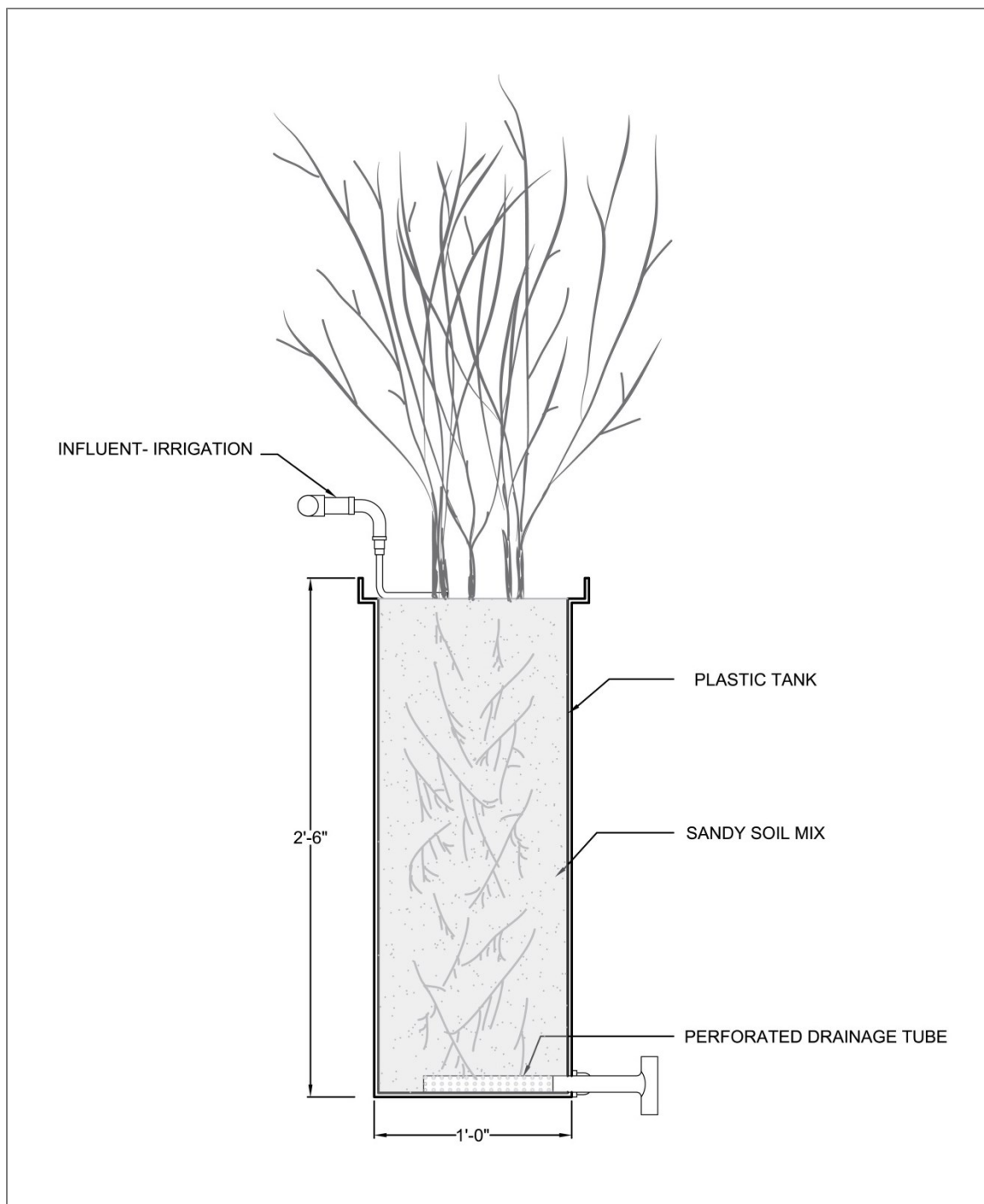


Figure 6: 2D Side profile of an individual test cell with trees, roots, and perforated drain tube



Figure 7: Perforations in the PVC underdrain prior to wrapping with permeable felt



Figure 8: Perforated underdrain wrapped with permeable felt and custom stand

### 2.3.3 Synthetic Wastewater

The synthetic wastewater was used as raw feed, for studying nitrogen removal with and without the presence of trees and polyacrylamide. The synthetic wastewater contained 1 g/L of blender pulverized, Vegetable Stew Blend (Auguson Farms), 0.29 g/L Whey Protein Powder (Six Star Pro Nutrition) and 0.17 g/L ammonium acetate (A.C.S. certified, Sigma-Aldrich). The wastewater was made in 95 L batches (in deionized water)



in a 113.5 L (30 gallon) plastic container and allowed to steep for 48 hours prior to particle removal (20  $\mu\text{m}$  fabric filter) and subsequent transfer to the dosing tanks or outdoor irrigation. See Appendix for ingredient nutrition facts and the associated calculations for making the synthetic wastewater.

#### *2.3.4 Temperature and Relative Humidity*

Temperature and Relative Humidity were recorded every 5 minutes using a HOBO<sup>®</sup> UX100 Temp/RH 2.5% Data Logger - UX100-011. Temperature inside the walk-in cooler was controlled using a customized thermostat, condenser, and fan unit set to 4.5°C. Relative humidity was not controlled throughout the experiment.

#### *2.3.5 Tracer Studies*

A series of bromide tracer tests were performed under saturated, equilibrium flow conditions. Deionized water was irrigated at 40 mL/min and then 50 mL of a 100 g/L potassium bromide (5.0 g total bromide) was added directly to the sand surface of each testing cell. The effluent conductivity was measured (IntelliCAL<sup>™</sup> CDC401, Hach Company, Loveland, CO) and recorded every 30 seconds for 20 hours. This procedure was repeated once for every testing cell studied and the two resulting breakthrough curves were averaged for modeling purposes. For the Calamus no tree north test cell, discrete samples were collected over time and analyzed for bromide concentration using an ion chromatograph (IonPac AS22 Anion-Exchange Column, IC900, Dionex, Sunnyvale, CA). This direct bromide concentration data was then used to determine a “bromide equivalent” conversion factor for the conductivity probe data. All testing cells were rinsed thoroughly with deionized water prior to subsequent experiments and microorganisms seeding.

Additional bromide tracer studies were performed under saturated, equilibrium flow conditions with DI water irrigated at 30 mL/min and spiked with a 5 gram slug of

dissolved KBr. Effluent conductivity was measured (IntelliCAL™ CDC401, Hach Company, Loveland, CO) and recorded every 1 minute for approximately 24 hours. This procedure was repeated for each test cell after grab sample analysis and synthetic wastewater application in order to determine a time-weighted average hydraulic residence time (HRT) and assess physical parameters for replicate treatment types. An average HRT under the variable flow conditions used during the pilot-scale experiment was then determined for each test cell by adjusting the measured HRT from a continuous flow rate of  $30 \text{ mL min}^{-1}$  to the measured daily volumetric flow rate for each test cell.

### 2.3.6 Volumetric Flow Rate

All volumetric dose measurements of synthetic wastewater were recorded using a 1000 mL graduated cylinder. To measure a single volumetric dose event, 1000 mL glass beakers were placed underneath each dosing valve to capture all potential influent synthetic wastewater ( $V_T$ ). In order to account for the potential overflow, or “wasted”, synthetic wastewater, the 1000 mL glass beakers were also placed underneath the overflow drain pipes to capture any potential overflow ( $V_W$ ). The wasted volume was then subtracted from the potential influent volume to give an actual volumetric dose ( $V_D$ ) for each test cell (Equation 1). This process was repeated three times over the course of the experiment for accuracy.

Equation 1: Volume dosed for each test cell

$$V_{D_i} = V_{T_i} - V_{W_i}$$

### 2.3.7 Intermittent Dosing Experiment

Prior to the start of experimental sampling, all testing cells were dosed with 300 mL day<sup>-1</sup> of primary wastewater for 4 weeks. This primary wastewater was delivered to the University of Iowa from the Port of Morrow lagoon wastewater holding facility. This inoculum was presumed to contain an assortment of microorganisms representing the field-site lagoon. This preliminary seeding of bacteria was intended to quickly establish a comparable microorganism community and population inside each individual test cell similar to that found in the field. During the inoculation period, approximately 300 mL of synthetic wastewater was dosed every 4 hours and allowed 5 weeks to reach state-state equilibrium before experimental sampling.

The influent and effluent was sampled intensively throughout the experiment. Head tank and test cell effluent samples were analyzed for ammonium (salicylate method, (CFR (Code of Federal Regulations) 2012), nitrate and dissolved oxygen. Nitrate, nitrite and ammonium were analyzed by ion chromatography using an IonPac AS22 Anion-Exchange Column, IonPac CS15 Cation-Exchange Column, or by the dimethylphenol method (CFR (Code of Federal Regulations) 2012). Dissolved oxygen was measured colorimetrically (K-7512, Chemetrics, Midland, VA).

### 2.3.8 Organic Nitrogen Hydrolysis and Denitrification Rate

A nitrogen mass balance analysis was performed to estimate the dwell-time specific first-order rate coefficients for hydrolysis and denitrification at the pilot scale. In

order to estimate the organic-N applied onto each test cell per day, the mass of all measured inorganic nitrogen species ( $\text{NH}_4^+$ ,  $\text{NO}_3^-$ , and  $\text{NO}_2^-$ ) were added together and subtracted from the total mass of nitrogen applied. In order to account for the duration of the entire experimental process and estimate a cumulative amount of applied organic-nitrogen, each specific value was multiplied by 78 days. To estimate the cumulative mass of effluent nitrogen for each test cell system, we assumed a uniform hydraulic resident time of 7 days off of the bromide tracer studies and assumed a linear relationship between day 8 and day 61 in the experimental process (Appendix C). The summation of this effluent total nitrogen represented all effluent nitrogen throughout the entire experiment. Using these results, the predicted amount of organic-N remaining in the each system was compared with the estimated amount, and any difference between these two values was assumed as loss via denitrification. A hydrolysis rate constant was then determined using this assumed denitrification loss value and a test cell specific dwell-time. Several denitrification rate values were applied until the denitrification loss value approached zero for all cases.

### 2.3.9 Statistical Analysis

The Mann-Whitney Rank Sum test and paired t-test were used to estimate the effects of roots and polyacrylamide on nitrogen dynamics (total N,  $\text{NO}_3^-$ ,  $\text{NH}_4^+$ , and  $\text{NO}_2^-$ ) as compared to control or replicate test cell influent and effluent sample data. Statistical analyses were performed using SigmaPlot software (Version 12.5, Systat Software Inc., San Jose, California).

## 2.4 Results and Discussion

### 2.4.1 Temperature and Relative Humidity

Temperature and relative humidity inside the walk-in cooler remained reasonably stable throughout the entire experimental process (Figure 9). Temperature was

maintained between 4 and 6°C prior to, and during, all experimental sampling. There were increases in temperature for short periods, representing times where either the cooler door was temporarily left open or the cooling unit was temporarily shut down.

Relative humidity (RH) inside the cooler was recorded with an average of approximately 90% RH. The recorded events show where humidity was temporarily decreased (Figure 9). Again, these events correspond with leaving the cooler door open or temporarily shutting down the cooling unit. RH inside the cooler was high due to the condenser and fan unit continuously blowing chilled air into the confined space of the walk-in cooler unit.

#### 2.4.2 Bromide Tracer Studies

Figure 10 shows the results from a 50 mL slug dose of a 100g/L KBr solution for the Calamus no tree north test cell. The average bromide flux ( $\text{mg Br}^- \text{min}^{-1}$ ) and the conductivity ( $\mu\text{S cm}^{-1}$ ) measurements were recorded simultaneously. The average  $\text{Br}^-$  flux was determined using ion chromatography (IC) and the conductivity was determined using a conductivity probe. The breakthrough for a continuous  $40 \text{ mL min}^{-1}$  application of deionized water and spiked dose of a conservative bromide tracer was determined to take approximately 4 hours for the north Cal no tree test cell, with a peak concentration occurring around 5.5 hours. Using these differing methods also confirmed that there was relatively good correlation between the two alternative measurement techniques.

The initial  $\text{Br}^-$  breakthrough curve had a noticeably abrupt slope, suggesting that advection was the dominant transport mechanism. The more gradual slope on the tail end of the breakthrough curve suggests that dispersion, tortuosity, and other soil transport mechanisms influenced the tracer as it moved through the vadose zone. It was determined from IC analysis that there was a 76% recovery of  $\text{Br}^-$ . Although the conductivity probe measurements in the effluent appear to exceed what was captured during grab sample analysis, it should be addressed that sodium ( $\text{Na}^+$ ) was highly present throughout the

vadose zone due to the application of synthetic wastewater and  $K^+$  has a lower conductivity than  $Na^+$ , with electrical conductivity values of  $1.4 \times 10^7 \text{ S m}^{-1}$  and  $2.1 \times 10^7 \text{ S m}^{-1}$ , respectively. The dissociation of  $K^+$  from  $Br^-$  and recombination of  $Na^+$  with  $Br^-$  may account for this apparent conductivity difference. Ultimately, there was good correlation between the conductivity sensor and actual bromide concentration present in the effluent, suggesting that the hydrodynamics of an individual test cell can be adequately sampled using a conductivity probe.

Bromide tracer studies comparing the south Cal with tree and Cal no tree test cells using a 5 g KBr spike with a continuous  $30 \text{ mL min}^{-1}$  DI flow rate is shown in Figure 11. Under this dosing regimen, the south Cal with tree test cell was determined to have a mean HRT of approximately 7.0 hours compared with the south Cal no tree test cell which had a mean HRT of approximately 6.1 hours. After adjusting these measured HRT values for their respective daily volumetric dose rates, it was determined that the south Cal with tree test cell had an actual HRT of 6.12 days and the south Cal no tree test cell had an actual HRT of 6.24 days. It is also important to note that the peak conductivity was significantly reduced in the with tree test cell, suggesting the occurrence of solute immobilization and ultimately a reduction of  $Br^-$  in the effluent. As the other tracer study figures also display, this phenomenon occurs with all treatment variations.

Bromide tracer studies comparing the north Cal with tree and Cal no tree test cells using a 5 g KBr spike with a continuous  $30 \text{ mL min}^{-1}$  DI flow rate is shown in Figure 12. Under this dosing regimen, the north Cal with tree test cell was determined to have a mean HRT of approximately 7.6 hours compared with the south Cal no tree test cell, which had a mean HRT of approximately 5.8 hours. After adjusting these measured HRT values for their respective daily volumetric dose rates, it was determined that the north Cal with tree test cell had an actual HRT of 8.53 days and the north Cal no tree test cell had an actual HRT of 5.90 days. Again, the peak conductivity was significantly reduced

in the with tree test cell, suggesting solute immobilization leading to reduction of  $\text{Br}^{-1}$  in the effluent.

Tracer studies comparing the POM with tree test cell against the POM no tree test cell using a 5 g KBr spike with a continuous  $30 \text{ mL min}^{-1}$  DI flow rate is shown in Figure 13. With this dosing regimen, the POM with tree test cell was determined to have a mean HRT of approximately 7.0 hours compared with the POM no tree test cell, which had a mean HRT of approximately 6.7 hours. After adjusting these measured HRT values for their respective daily volumetric dose rates, it was determined that the POM with tree test cell had an actual HRT of 7.01 days and the POM no tree test cells had an actual HRT of 5.35 days. The peak conductivity was again significantly reduced in the with-root system.

Treatments that contained polyacrylamide amendment were not successfully analyzed under the  $30 \text{ mL min}^{-1}$  continuous DI flow rate as the polymer would expand so heavily that flow through the system would be extremely reduced, creating intensive ponding and making it difficult to determine an HRT. Tracer study data was collected for the south Cal PAM with tree and Cal PAM no tree test cells (Figure 14). However, due to inconsistencies and effects from ponding, a comparable analysis between these test cells would not be reliable and was therefore not determined.

Although this study designed for replicate treatments, there remained heterogeneity between even the simplest test cells (Figure 15). Both north and south Cal no tree test cells showed strong influence from advection and displayed double concentration peaks (potentially due to varying flow paths) and also had relatively similar HRT's. However, the peak conductivities and areas under the tracer curves were significantly different. For these replicate treatments and all other treatment types, the tracer studies remained consistent with differences in effluent nitrogen concentrations, suggesting hydraulic residence time is directly related to overall nitrogen treatment.

### 2.4.3 Volumetric Flow Rate

The mean daily volume of synthetic wastewater ( $L \text{ day}^{-1}$ ) dosed on the surface of each test cell is shown in Figure 16. Due to differences in potential pressure head and distance from the head tank, there was some variation between the test cells. However, this application rate was relatively consistent at the individual test cell level. The largest mean daily dose volume was  $2.44 L \text{ day}^{-1}$  on the Cal PAM no tree north test cell, with a standard deviation of 0.10. The smallest mean daily dose volume was  $1.61 L \text{ day}^{-1}$  on the Cal with tree south test cell, with a standard deviation of 0.26. Across the system, the average volumetric dose rate of synthetic wastewater for an individual test cell was  $1.92 L \text{ day}^{-1}$ .

### 2.4.4 Total Nitrogen

For all total nitrogen (TN) measurements, the north Cal no tree, Cal with tree, and Cal PAM no tree test cells (Figure 17) had higher TN concentrations ( $\text{mg-N L}^{-1}$ ) than the head tank. The POM no tree test cell had TN concentrations consistently similar to the head tank and the Cal PAM with tree test cell was consistently lower than the head tank, with both treatment types remaining relatively stable throughout the sampling period. Alternatively, the Cal with tree and Cal no tree test cells showed an average increasing trend of 1.6x and 0.6x, respectively (Figure 18) whereas the Cal PAM no tree test cell had an average decreasing trend of -0.6x (Figure 19). Although general trends appeared to be present from this dataset, the  $R^2$  values were relatively low, ranging from 0.4 to 0.6, suggesting trend inconsistencies.

Figure 20 shows the TN concentration ( $\text{mg-N L}^{-1}$ ) of the head tank and all effluents from each south side test cell. All south test cells showed an increasing trend in TN concentration over time, while the head tank concentration remained fairly constant. The largest increasing trend occurred with the Cal no tree test cell with a slope value of



2.4x and an  $R^2$  of 0.98. The smallest increasing trend occurred with the Cal PAM no tree test cell with a slope value of 0.9x and an  $R^2$  of 0.53.

Adjusted total nitrogen mass flux ( $\text{mg N day}^{-1}$ ) values were determined in accordance with the respective volumetric doses for all north side test cells (Figure 21). Head tank data was not included in the mass flux figures as the dosed volume was different for each test cell. Even after this adjustment, the Cal with tree and Cal no tree test cells had increasing trends, while the Cal PAM no tree test cell showed a decreasing trend and the POM no tree and Cal PAM with tree test cells remained fairly consistent (Table 2).

The adjusted total nitrogen mass flux ( $\text{mg N day}^{-1}$ ) values were also determined for all south side test cells (Figure 22). Again, head tank data was not included in the mass flux figure as the dosed volume was different for each test cell. Unlike the north side, all south side test cells had an increasing trend within the fourteen-day sampling period, ranging from 2.0x to 4.2, with  $R^2$  values ranging from 0.53 to 0.98 (Table 3).

Replicate treatment types were combined to show the average total nitrogen mass flux comparison ( $\text{mg N day}^{-1}$ ) between all test cell types (Figure 23), highlighting test cells with trees against test cells without trees. Overall, the POM with tree and Cal PAM with tree test cells had statistically lower TN mass fluxes than the POM no tree and Cal PAM no tree test cells, respectively ( $P = <0.001$ ). The Cal with tree test cells also had a statistically lower TN effluent than the Cal no tree test cells were also significantly different ( $P = 0.023$ ). However, it should be noted that only the south Cal PAM with tree and north Cal no tree test cells were used for analytical comparison due to the appearance of acetate breakthrough on the north Cal PAM with tree test cell (see Appendix A) and dramatic trends in the north Cal no tree test cell. This acetate breakthrough, along with the results from nitrate and ammonium analysis, indicates a “short-circuiting” effect on only the north Cal PAM with tree test cell.

The mass flux of total nitrogen present in the effluent of most test cells appeared to increase over time, with a few exceptions. This increase in effluent total nitrogen may have happened due to the continual application of wastewater rich in organic-nitrogen (roughly 55% org-N). With continual irrigation, the soil can accumulate slowly degradable organic-N and may release large concentrations of hydrolyzed forms of nitrogen back into the system. This soil-nitrogen storage effect may also explain why there was a higher concentration of total nitrogen in the effluent than was actually being dosed at the end of the experimental process. Since there is no plant-associated nutrient uptake occurring during dormancy, all nitrogen reactions and transport can be attributed to soil-, and root-associated microorganisms.

The treatment types with the highest total nitrogen were the Cal no tree and Cal PAM no tree test cells, with average TN mass flux values of 153 and 144 mg N day<sup>-1</sup>, respectively. The treatment types with the lowest total nitrogen were the Cal PAM with tree and POM with tree test cells, with average TN mass flux values of 25 and 82 mg N day<sup>-1</sup>, respectively. From the total nitrogen data, the combination of an established root-system with polyacrylamide showed the greatest impact on reducing total nitrogen in the effluent.

When looking at the average TN mass flux across all treatment types and comparing all data for with-tree against no-tree systems, there was significantly less effluent TN in the with-root systems than no-root systems ( $P = <0.001$ ). It would be interesting to repeat this study after more than one growing season to see if further establishing a well-developed root system would further increase any significant difference between with-root and no-root treatments.

#### 2.4.5 Nitrate

The average nitrate mass flux comparison (mg NO<sub>3</sub>-N day<sup>-1</sup>) between all test cell types is shown in Figure 24. Again, replicate treatment types were combined in this

analysis, highlighting test cells with trees against test cells without trees. The POM with tree test cell had a significantly lower  $\text{NO}_3\text{-N}$  mass flux than the POM no tree test cell ( $P = <0.001$ ), with values of 94.4 and 146.3  $\text{mg NO}_3\text{-N day}^{-1}$ , respectively. The Cal PAM with tree had a significantly lower  $\text{NO}_3\text{-N}$  mass flux than the Cal PAM no tree test cells ( $P = <0.001$ ), with values of 16.9 and 106.9  $\text{mg NO}_3\text{-N day}^{-1}$ , respectively. This figure also shows the Cal with tree had a higher  $\text{NO}_3\text{-N}$  mass flux than the Cal no tree test cell ( $P = <0.001$ ), with values of 85.8 and 72.0  $\text{mg NO}_3\text{-N day}^{-1}$ , respectively.

It should be noted that only the south Cal PAM with tree and north Cal no tree test cells were used for analytical comparison. Ion chromatography results (Appendix A) revealed the presence of acetate in the effluent of only the north Cal PAM with tree test cell, which was an indicator of potential short-circuiting, and the south Cal no tree test cell had significantly increasing trends. Additionally, when comparing the average nitrate mass flux for the north and south Cal PAM with tree test cells (Figure 25), it can be seen that there was a significant difference between these replicate treatments ( $P = <0.001$ ), with values of 0.16 and 16.9  $\text{mg NO}_3\text{-N day}^{-1}$ , respectively.

Figure 26 shows the discrete nitrate mass flux samples for each test cell over a two week sampling period. From this, an increasing trend can be seen for all treatment types except the north Cal PAM with tree test cell was the only outlier, showing no signs of increasing nitrate over time. The nitrate mass flux data for the north Cal PAM with tree test cell was not different than the nitrate mass flux of the head tank ( $P = 0.675$ ), suggesting that little to no N-transformation was occurring within the north Cal PAM with tree test cell and further indicate a short-circuiting effect on only this test cell (Figure 27).

The mass flux of nitrate present in the effluent of most test cells appeared to consistently increase over time. Again, this increase may have occurred due to slowly degradable organic-N accumulating in the upper layers, deaminating into ammonium and then nitrifying into soluble nitrate before moving through the system and into the

effluent. With continual irrigation, the nitrate in the effluent would be expected to continue increasing over time, up to a point.

The treatment types with the highest nitrate were the POM no tree and Cal PAM no tree test cells, with average nitrate mass flux values of 146 and 107 mg NO<sub>3</sub>-N day<sup>-1</sup>, respectively. The treatment types with the lowest nitrate were the Cal PAM with tree and Cal no tree test cells, with values of 16.9 and 72 mg NO<sub>3</sub>-N day<sup>-1</sup>, respectively. From the nitrate data, the combination of an established root-system with polyacrylamide showed the greatest impact on reducing nitrate in the effluent.

When looking at the average nitrate mass flux across all treatment types and comparing all data for with-tree against no-tree systems, there was significantly less effluent nitrate in the with-root systems than no-root systems ( $P = <0.001$ ). It would be interesting to repeat this study after more than one growing season to see if further establishing a well-developed root system would further increase any significant difference between with-root and no-root treatments.

#### 2.4.6 Ammonium

Figure 28 shows the average ammonium mass flux comparison between all treatment types, highlighting treatment types with trees against treatment types without trees. Regardless of root presence, both POM test cells had a significantly lower NH<sub>4</sub>-N mass flux than all other treatment types ( $P = <0.001$ ). The Cal PAM with tree treatment had a significantly lower NH<sub>4</sub>-N mass flux than the Cal PAM no tree ( $P = <0.001$ ), with mean values of 11.9 and 45.1 mg NH<sub>4</sub>-N day<sup>-1</sup>, respectively. The Cal with tree treatment was also statistically less than the Cal no tree treatment ( $P = 0.002$ ), with mean values of 52.9 and 59.1 mg NH<sub>4</sub>-N day<sup>-1</sup>, respectively.

Discrete ammonium mass flux samples for each test cell treatment types over a two week sampling period showed that most treatment types remained reasonably consistent (Figure 29). However, unlike other treatment types, the south Cal PAM with

tree test cell had an initially low ammonium mass flux and had an increasing trend over time, while the north Cal PAM no tree test cell had a decreasing trend. These particular differences do not appear to follow any specific pattern related to treatment type variation. Additionally, when considering the potential short-circuiting effect of the north Cal PAM with tree test cell mentioned previously, data shows that there was a significant ammonium mass flux difference between the north and south Cal PAM with tree test cells ( $P = <0.001$ ), with values of 56.1 and 11.9 mg NH<sub>4</sub>-N day<sup>-1</sup>, respectively (Figure 30).

The treatment types with the highest average ammonium mass flux were the Cal with tree, Cal no tree, and Cal PAM no tree test cells, with average ammonium mass flux values of 52.8, 59.1, and 45.1 mg NH<sub>4</sub>-N day<sup>-1</sup>, respectively. The Cal PAM with tree test cells had a significantly lower ammonium mass flux than the Cal PAM no tree test cells, with values of 11.9 and 45.1 mg NH<sub>4</sub>-N day<sup>-1</sup>, respectively. The treatment types with the lowest ammonium were the POM with tree and POM no tree test cells, with values of 0.20 and 0.45 mg NH<sub>4</sub>-N day<sup>-1</sup>, respectively. It is interesting to discuss the two POM test cells, both with and without trees, with consistently low ammonium mass flux values of 0.2 and 0.5 mg NH<sub>4</sub>-N day<sup>-1</sup>, respectively. These two treatment types had slightly different soil types than the Calamus treatments (Appendix B) and also had three years of ammonium-rich wastewater irrigation, whereas all other treatment types had only one year. This additional time may have influenced microbial communities and densities within these test cells, enhancing ammonium treatment capabilities. Another explanation for the dissimilarity may be related to the difference in cation-exchange capacity (CEC). Although both POM and Calamus soil types were classified as sandy soils, the POM soil had a CEC of 6.7 whereas the Calamus soil had a lower CEC of 1.8. Another possibility may be that the POM soil type allows more oxygen diffusion into the upper subsurface layers, thereby promoting nitrification, an aerobically driven process, and reducing effluent ammonium concentrations.

When looking at the average ammonium mass flux across all treatment types and comparing all data for with-tree against no-tree systems, there was significantly less effluent ammonium in the with-root systems than no-root systems ( $P = 0.034$ ).

Differences in “replicate” treatment types are interesting as the containers were filled with the same sandy soil type, inoculated from the same wastewater lagoon, and allowed the same length of growing season prior to any experimental sampling. Further investigation into the hydrodynamics and microbiological composition of each test cell would need to be examined to help explain any significant variation between replicate treatments. The collected ammonium data may suggest that the soil type and amount of time allowed to establish a robust microbial community had the greatest impact on reducing effluent ammonium concentrations. It would be interesting to repeat this experiment after subsequent growing season to see if further establishing a well-developed root system or robust microbial community would further increase any ammonium treatment capabilities with the Calamus soil.

#### 2.4.7 Nitrite

The average nitrite mass flux comparison ( $\text{mg NO}_2\text{-N day}^{-1}$ ) between all test cell types is shown in Figure 31, highlighting test cells with trees against test cells without trees. The north Cal no tree test cell had a significant presence of nitrite compared with all other treatment types. The Cal with tree treatment type also showed some presence, however not nearly as significant as the north Cal no tree test cell, with values of 1.3 and 18.6  $\text{mg NO}_2\text{-N day}^{-1}$ , respectively. The standard deviation for the north Cal no tree test cell was 7.4  $\text{mg NO}_2\text{-N day}^{-1}$  and it is interesting to compare the difference between the north and south Cal no tree replicate treatments (Figure 32). The north and south Cal no tree test cells were significantly different ( $P = <0.001$ ) and had a nitrite mass flux of 18.6 and 6.5  $\text{mg NO}_2\text{-N day}^{-1}$ , respectively.

Discrete nitrite mass flux samples for each test cell over a two week sampling period showed that the Cal no tree north and south test cells were the only test cells with any significant presence of nitrite (Figure 33). There was no nitrite present in either of the head tanks throughout all sampling periods.

The mass flux of nitrite present in the effluent of most test cells is consistently low over time, with two exceptions. The Cal no tree north and south test cells both showed an increasing trend over the two-week sampling period with the north being the largest. It should be noted that the south Cal no tree nitrite data was not used for any analytical comparisons outside of comparing replicate treatments.

During nitrification, the conversion from ammonium to nitrite is usually the rate limiting step and because of this rate limitation, there is generally not a significant presence of nitrite found in environmental systems. It was unexpected to find such a large presence of nitrite in the Cal no tree test cells. The significant presence of nitrite might be an indication that there was not a strong presence of organisms capable of converting nitrite to nitrate, typically from the genus *Nitrobacter* and *Nitrospira*. This conversion is considered the second step in the nitrification process. The low presence of nitrate in the Cal no tree test cells when compared with the other no tree treatment types may also be an indication that these nitrifying organisms did not have a significant presence within these particular test cells. However, this assumption is difficult to prove as no microbial sampling was performed for any test cell or effluent samples, and all containers were inoculated from the same wastewater lagoon prior to any experimental sampling. Further investigation into the hydrodynamics and microbiological composition of each test cell would need to be examined to help explain this significant variation.

#### 2.4.8 Organic Nitrogen Hydrolysis and Denitrification Rate Coefficients

Grab sample analysis taken at the end of experimentation indicated that the mass of organic nitrogen accumulated in each test cell ranged between approximately 1350 mg

and 4788 mg org-N (Table 4). The assumed loss of nitrogen via denitrification for the Calamus test cells ranged between approximately 692 and 1315 mg N, with the greatest denitrification loss occurring in the Cal PAM with tree north test cell. For the POM test cells, the assumed cumulative nitrogen loss via denitrification was approximately 787 mg N for the POM no tree test cell and 1000 mg N for the POM with tree test cell. The hydrolysis rate coefficient ( $k_h$ ) was estimated to equal approximately 0.001 using as a dwell-time specific first-order rate relationship. Similarly, the denitrification rate coefficient ( $k_s$ ) was estimated as a dwell-time specific first-order rate coefficient of 0.0003 (Table 5). These values represent our best hydrolysis and denitrification rate coefficient estimations based on a compilation of all nitrogen analyses (Appendix C).

#### *2.4.9 Nitrogen Species by Test Cell*

Cumulative nitrogen dynamics over the course of the 78 day experiment for each individual test cell are shown in Figures 34 through Figure 43. Each figure shows the cumulative mass of applied TN and both measured and or predicted values for effluent TN, residual organic nitrogen, and  $N_2$  loss via denitrification.

These results suggest that effluent nitrate concentrations will increase over time in both a dormant, poplar-rooted sandy soil and also in a non-rooted system, even under consistent wastewater application. An increasing trend of effluent nitrogen concentration indicates that slowly-degradable organic-N accumulated in the upper layers of the vadose zone and acted as another nutrient source, increasing effluent nitrogen over time. This organic nitrogen was presumed to deaminate into ammonium, nitrify into soluble nitrate, and proceed to influence effluent TN,  $NO_3^-$ -N, and  $NH_4^+$ -N. Substrate analysis at various depths may help identify how much organic-N has accumulated throughout the soil profile.

These figures highlight how continual application of nitrogen-rich wastewater tends to accumulate slowly degradable organic-nitrogen within the vadose zone as can be



seen from the predicted organic-nitrogen residual and measured organic-N data point. This accumulated organic-nitrogen will then hydrolyze into ammonium and subsequently nitrify into soluble nitrate. Ultimately, the combination of these processes can result in nitrogen concentrations that tend to increase effluent total nitrogen over time.

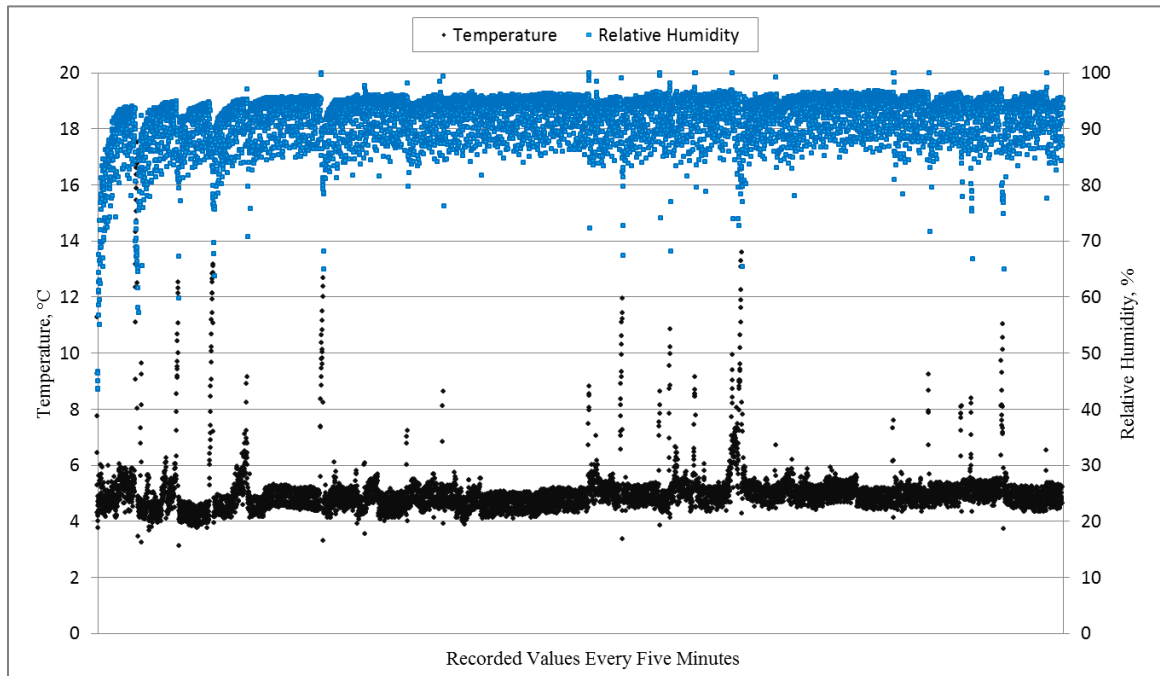


Figure 9: Temperature and relative humidity over the course of 4 months

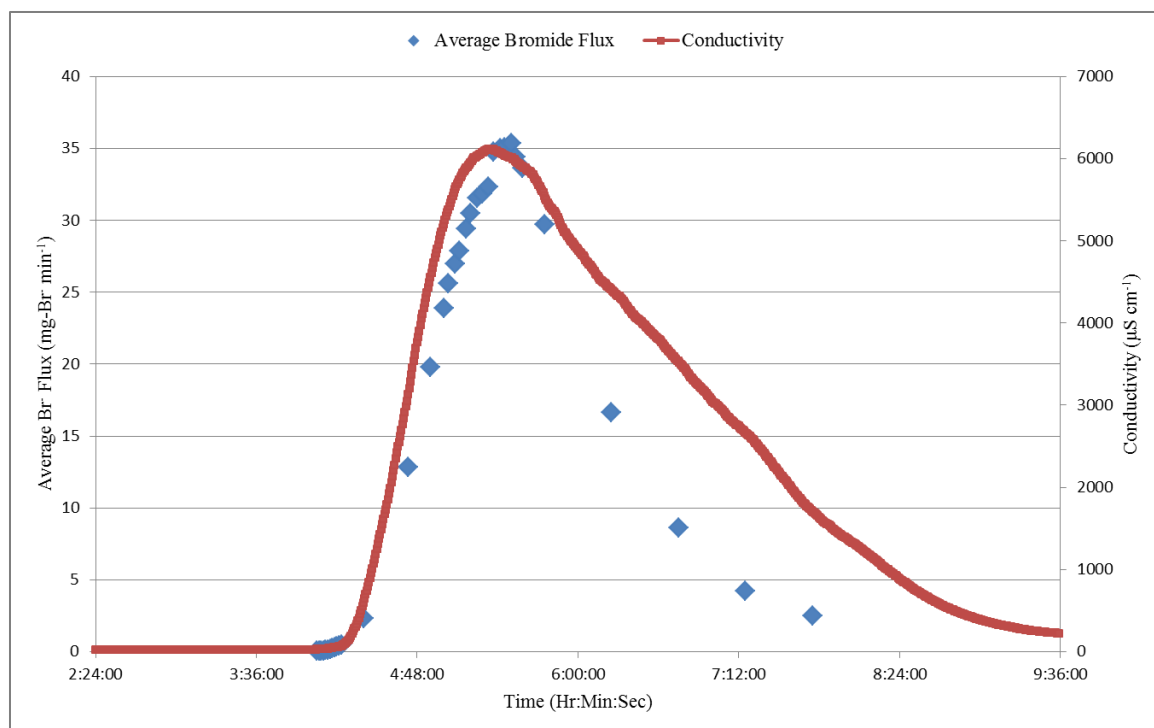


Figure 10: Bromide tracer study of the Calamus no tree north test cell using conductivity probe and ion chromatography

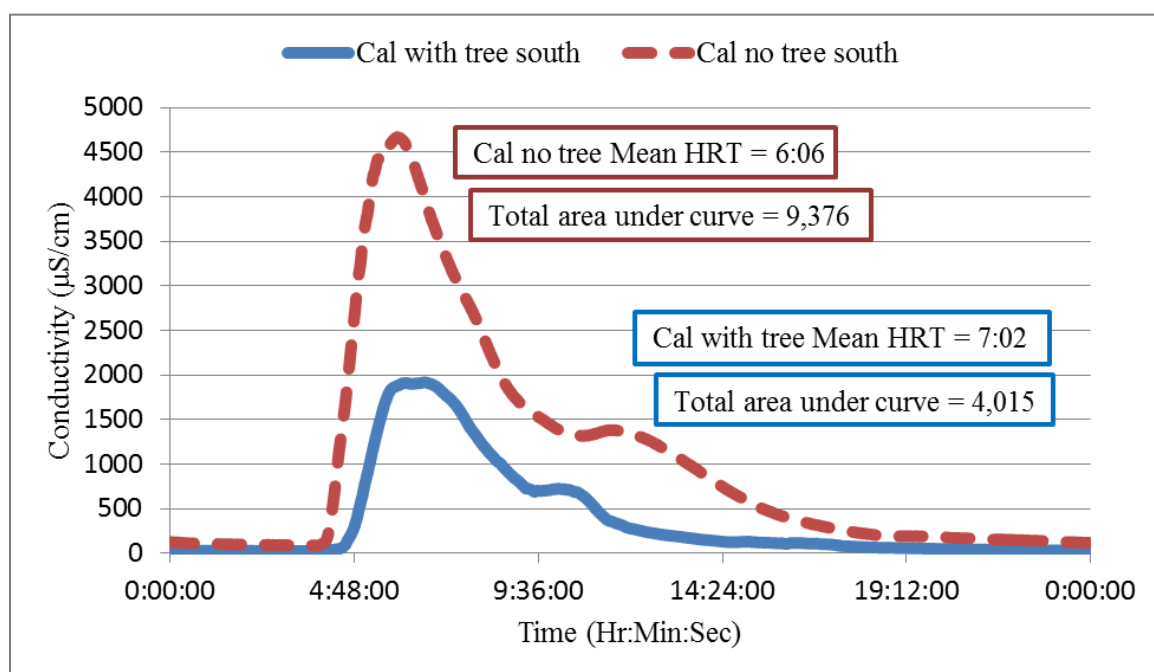


Figure 11: Bromide tracer studies comparing the south Cal with tree and Cal no tree test cells using a 5 g KBr spike with a continuous 30 mL min<sup>-1</sup> DI flow rate

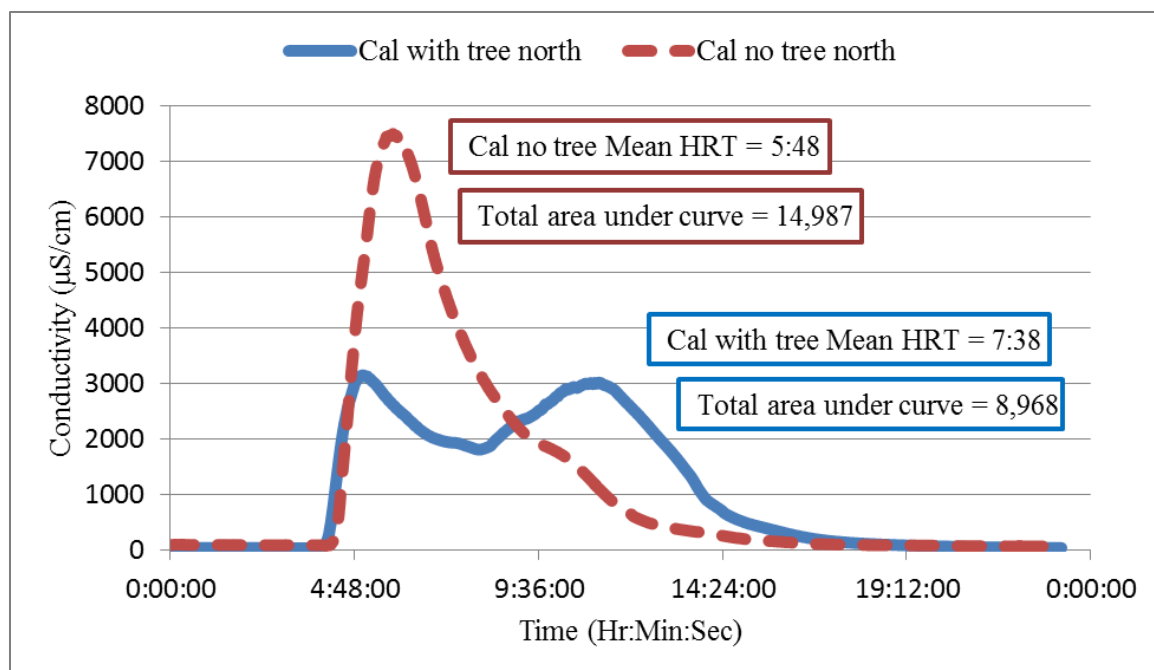


Figure 12: Bromide tracer studies comparing the north Cal with tree and Cal no tree test cells using a 5 g KBr spike with a continuous  $30 \text{ mL min}^{-1}$  DI flow rate

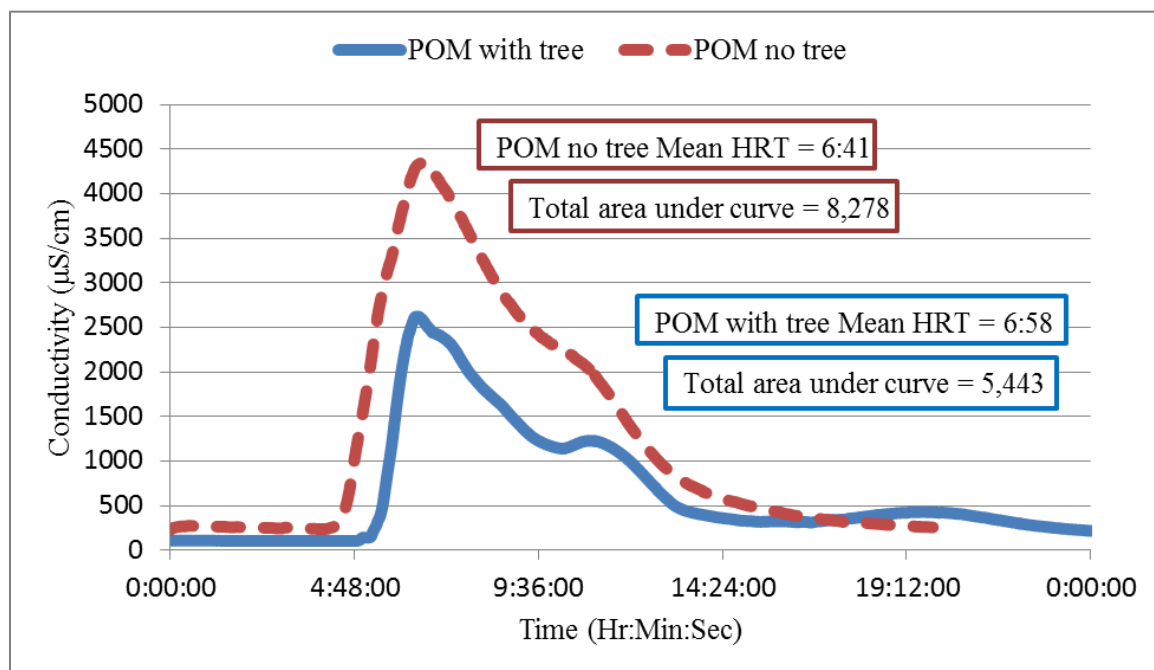


Figure 13: Bromide tracer studies comparing the POM with tree and POM no tree test cells using a 5 g KBr spike with a continuous  $30 \text{ mL min}^{-1}$  DI flow rate

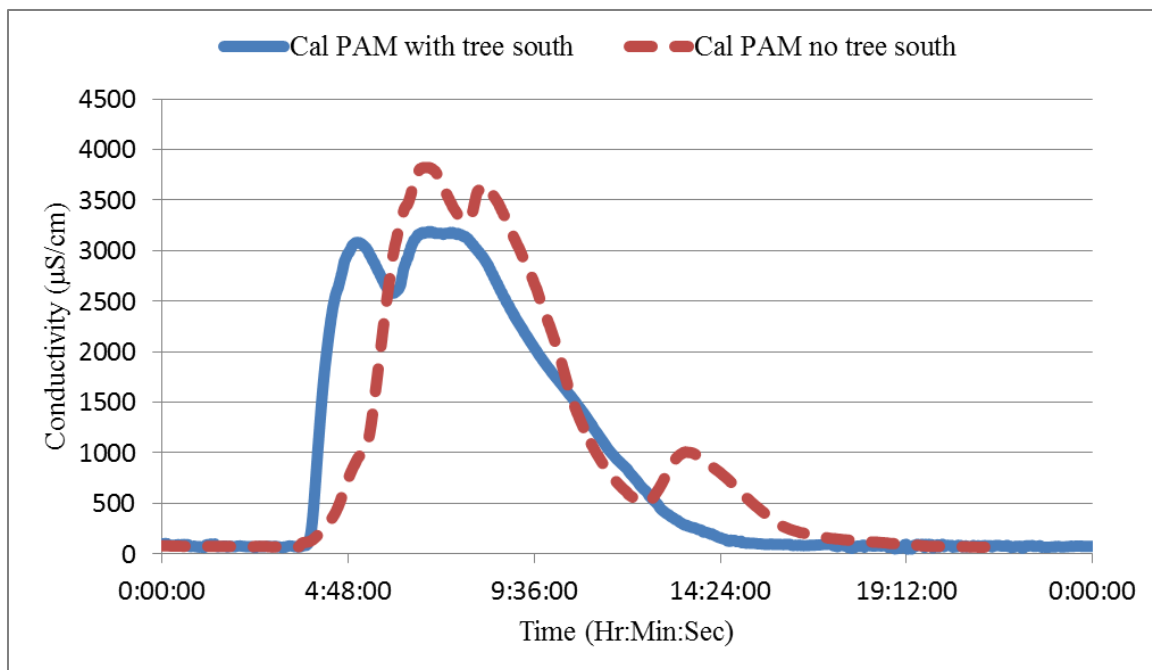


Figure 14: Bromide tracer studies of the south Cal PAM with tree and Cal PAM no tree test cells using a 5 g KBr spike with a continuous  $30 \text{ mL min}^{-1}$  DI flow rate

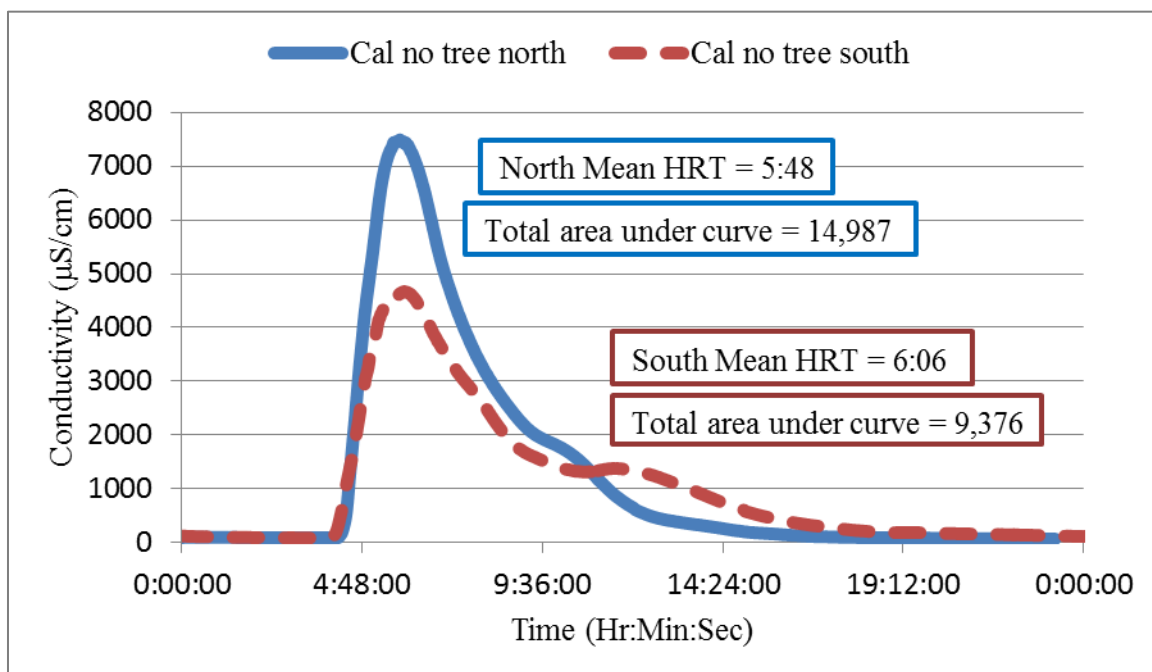


Figure 15: Bromide tracer studies of the north and south Calamus no tree “replicate” test cells using a 5 g KBr spike with a continuous  $30 \text{ mL min}^{-1}$  DI flow rate

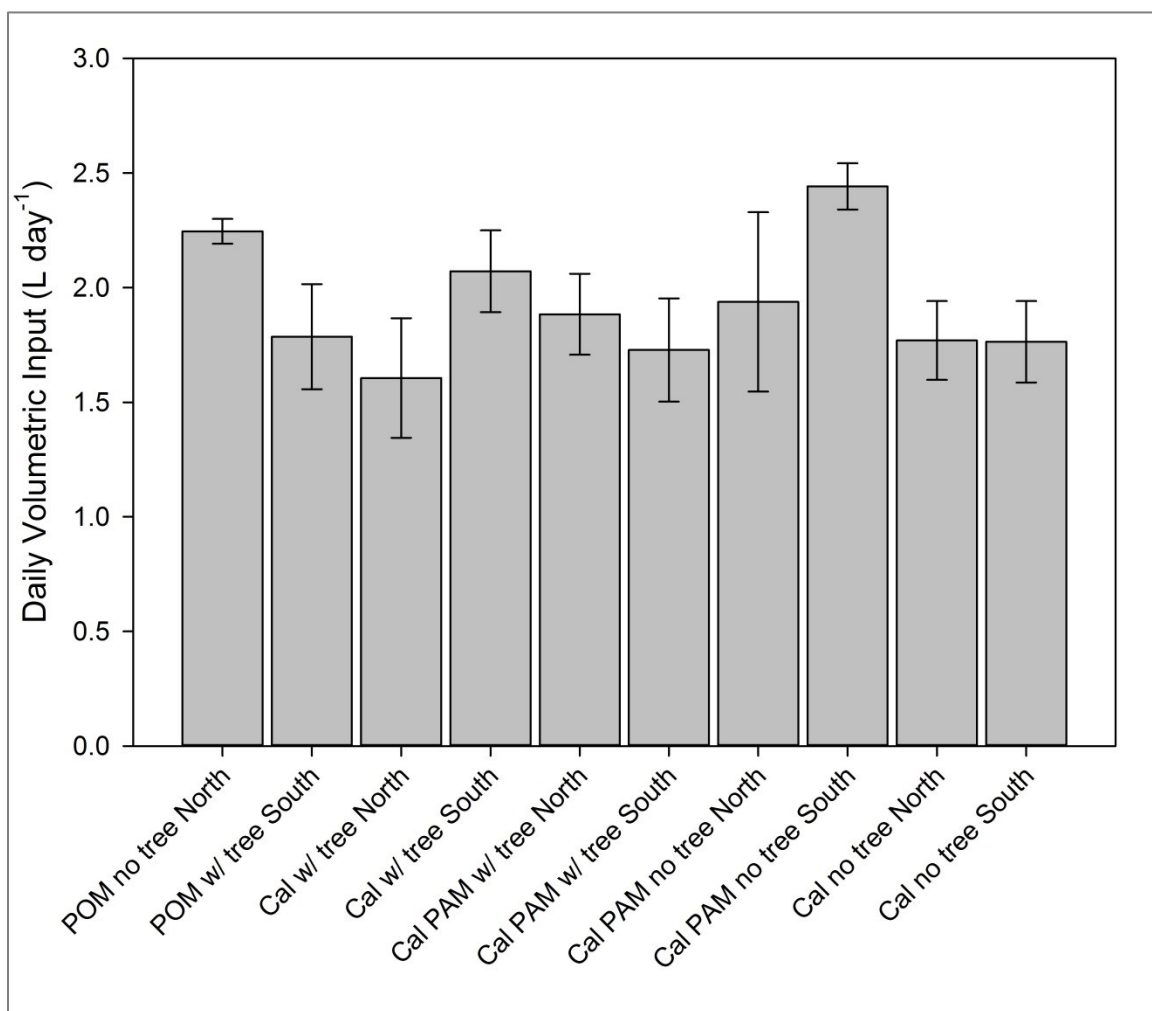


Figure 16: Mean daily synthetic wastewater application for each test cell with error bars representing  $\pm$  one standard deviation

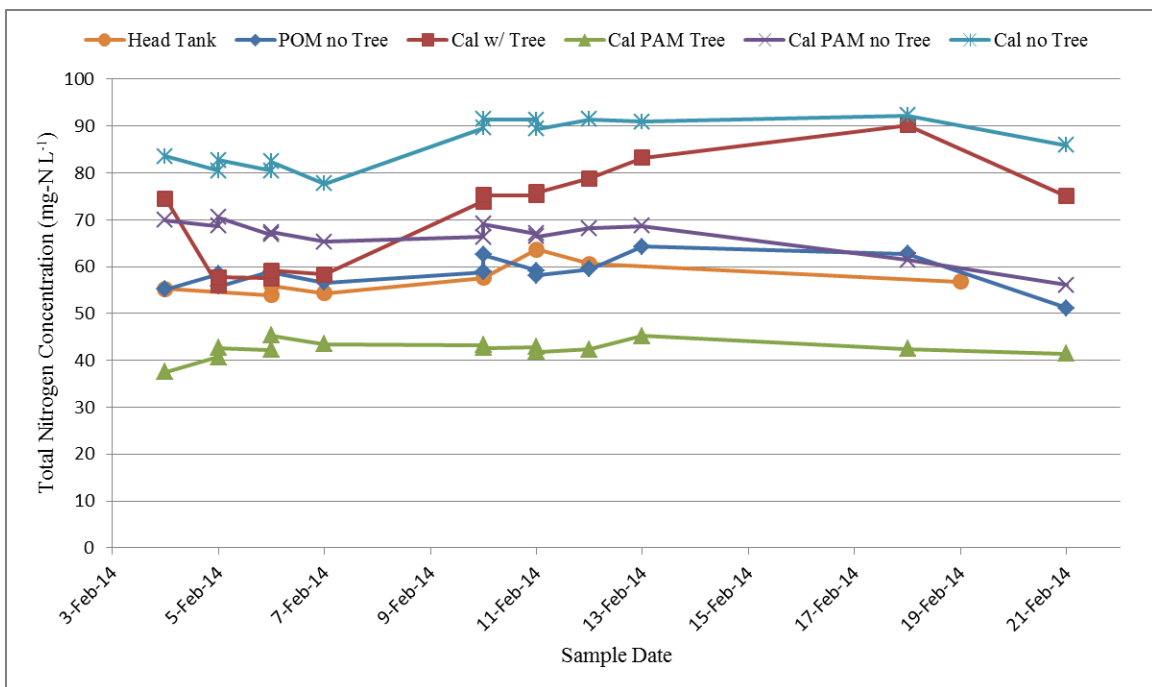


Figure 17: Total nitrogen concentration in the head tank and effluents of the north side test cells

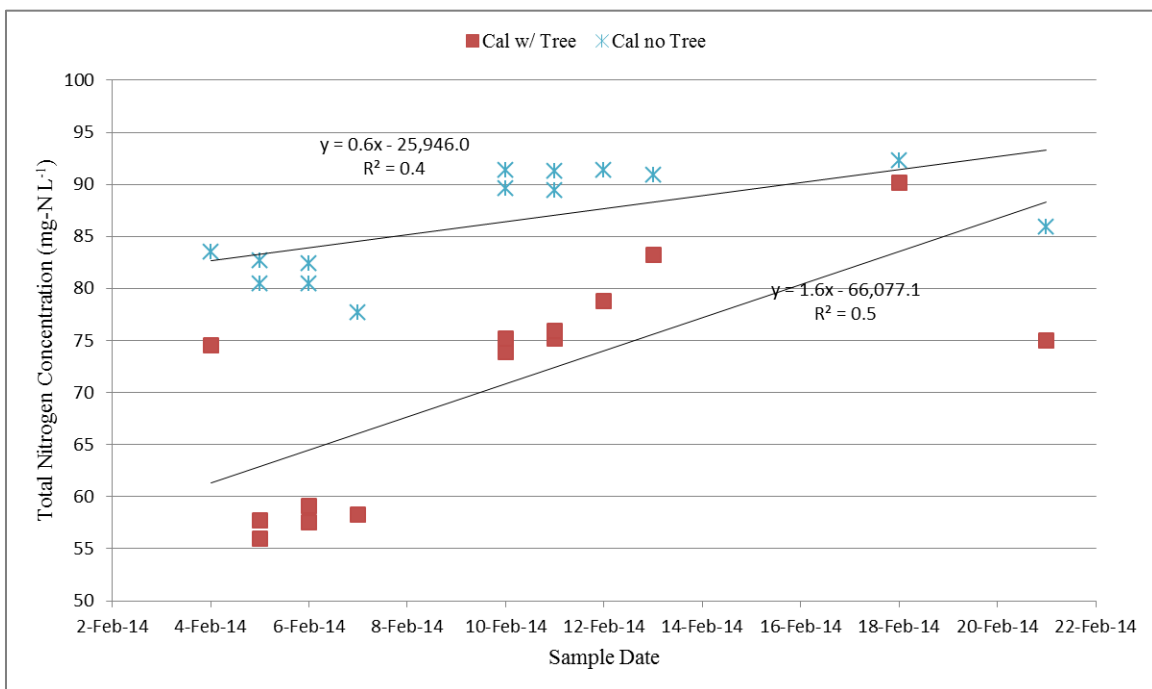


Figure 18: Increasing total nitrogen trend lines for the Cal with tree and Cal no tree test cells

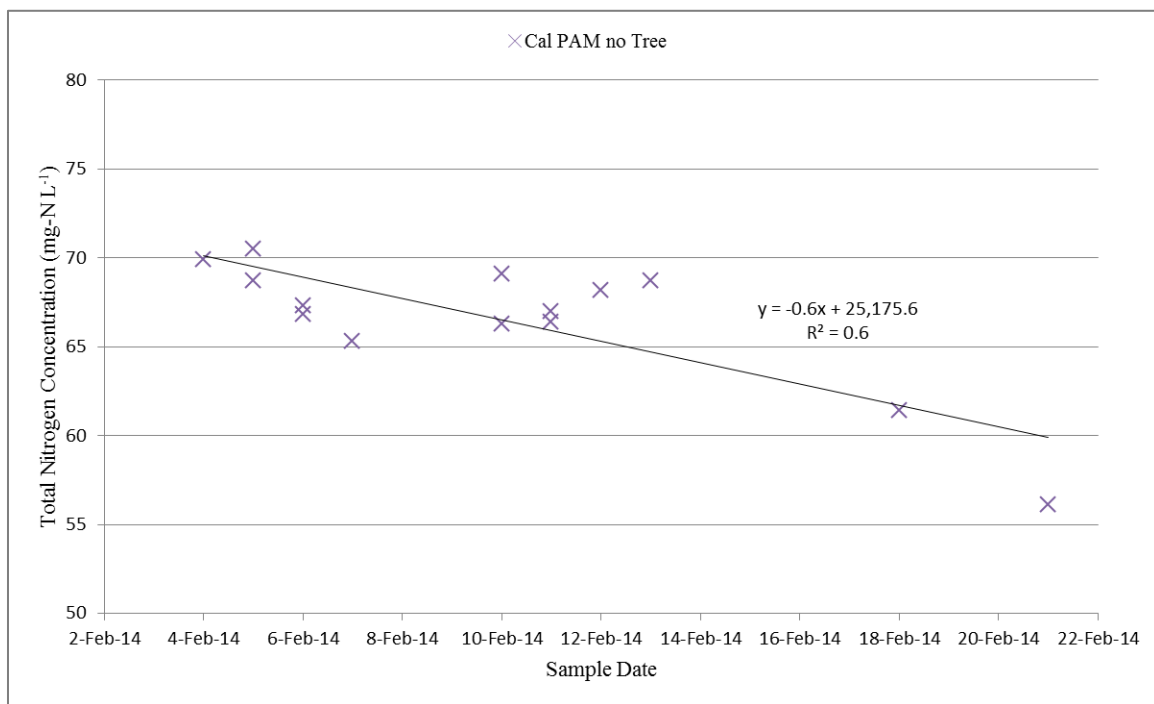


Figure 19: Decreasing total nitrogen trend lines for the Cal PAM no tree test cell

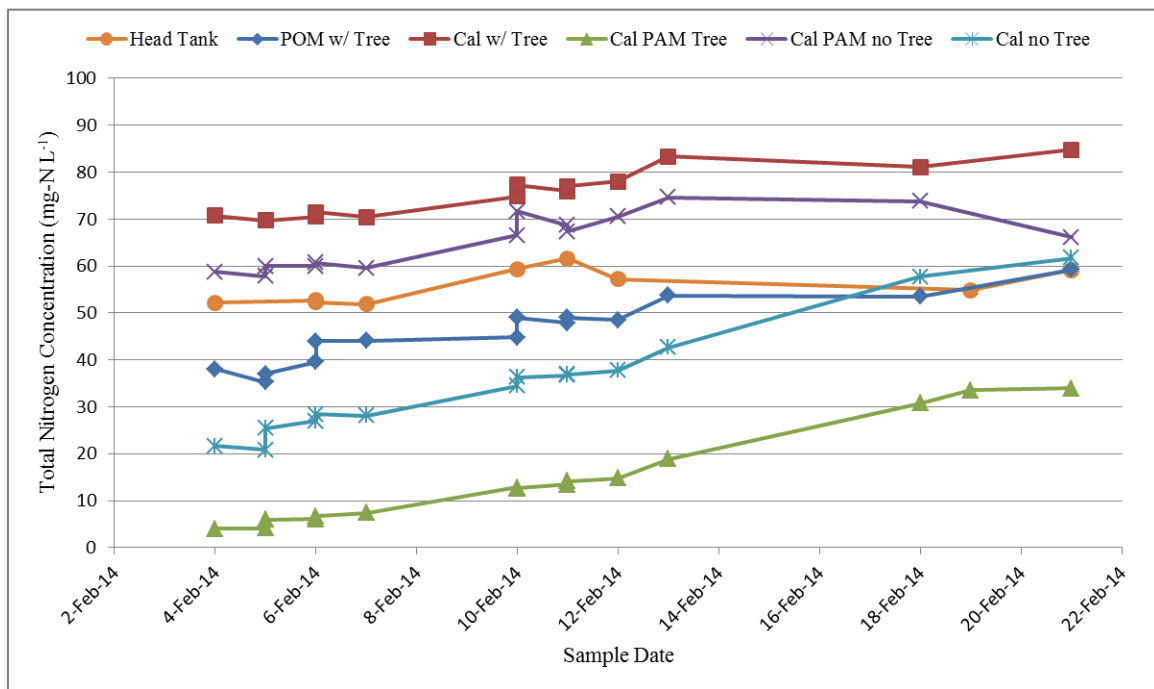


Figure 20: Total nitrogen concentration in the head tank and effluents for the south side test cells

Table 1: Trend line values for south side test cells

South Test Cell	TN Concentration Slope	R <sup>2</sup> value
POM with Tree	1.30	0.88
Cal with Tree	0.96	0.87
Cal PAM Tree	1.91	0.98
Cal PAM no Tree	0.86	0.53
Cal no Tree	2.40	0.98
Head Tank	0.35	0.30

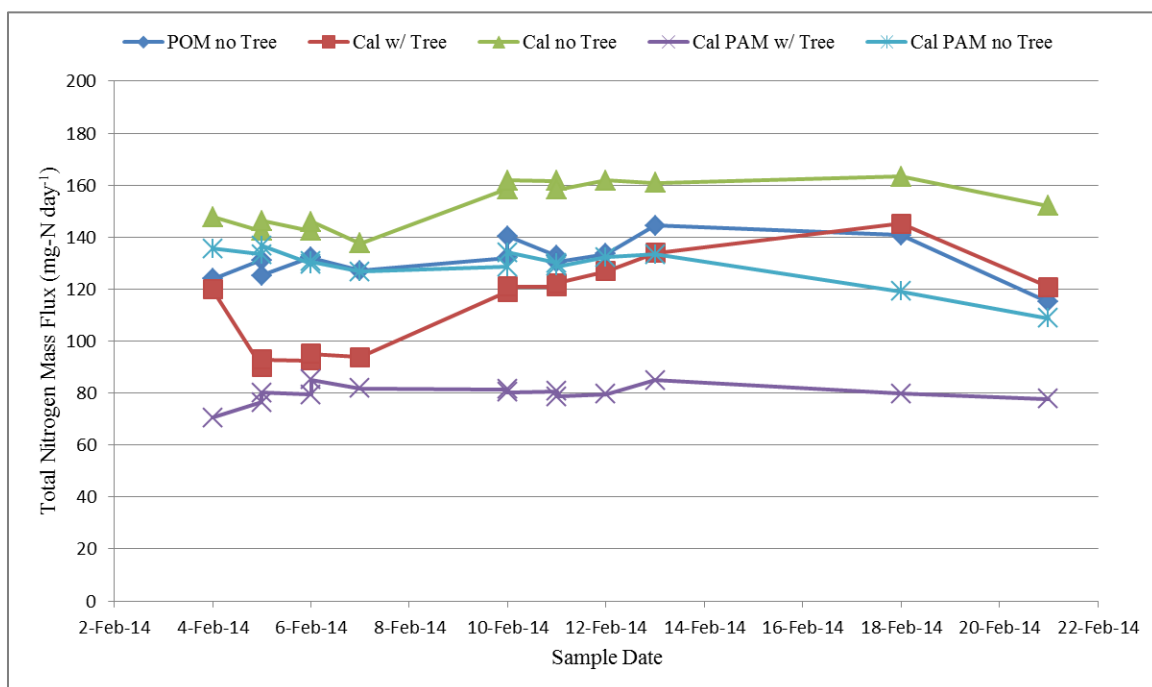


Figure 21: Total nitrogen mass flux in the effluent of the north side test cells

Table 2: Mass flux trend line values for north side test cells

North Test Cell	TN Mass Flux Slope	R <sup>2</sup> value
POM no Tree	0.07	0.01
Cal with Tree	2.56	0.53
Cal PAM with Tree	0.11	0.03
Cal PAM no Tree	-1.17	0.65
Cal no Tree	1.11	0.38



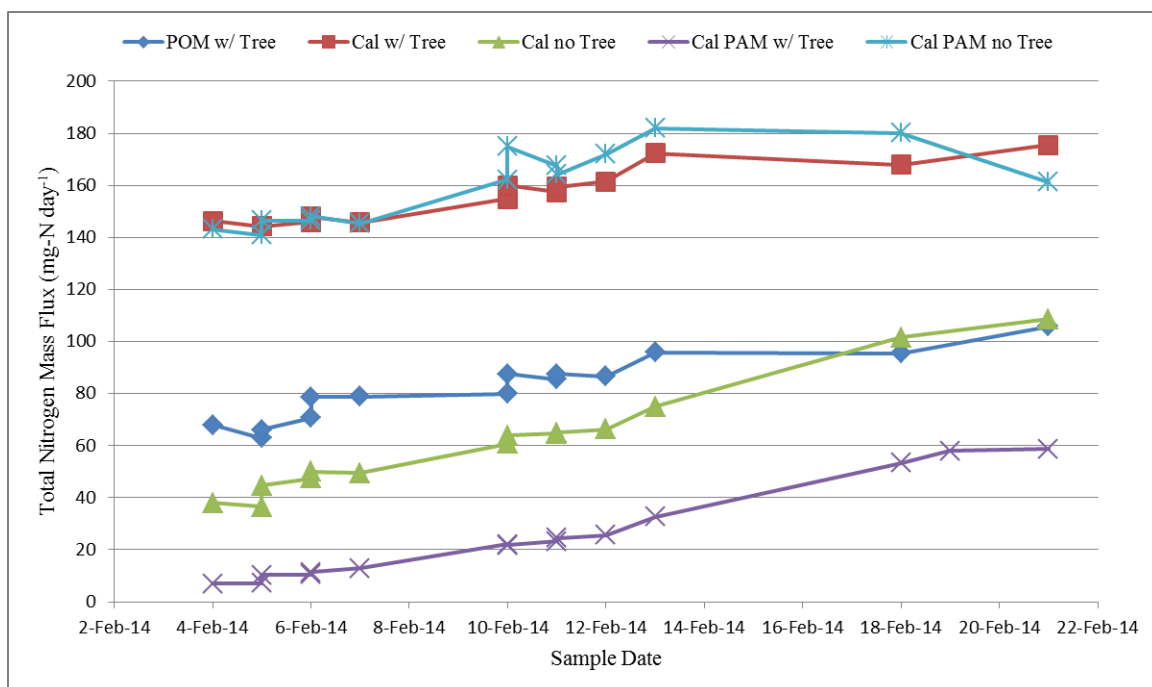


Figure 22: Total nitrogen mass flux in the effluent of the south side test cells

Table 3: Mass flux trend line values for south side test cells

South Test Cell	TN Mass Flux Slope	R <sup>2</sup> value
POM with Tree	2.32	0.88
Cal with Tree	2.00	0.87
Cal PAM with Tree	3.30	0.98
Cal PAM no Tree	2.10	0.53
Cal no Tree	4.23	0.98

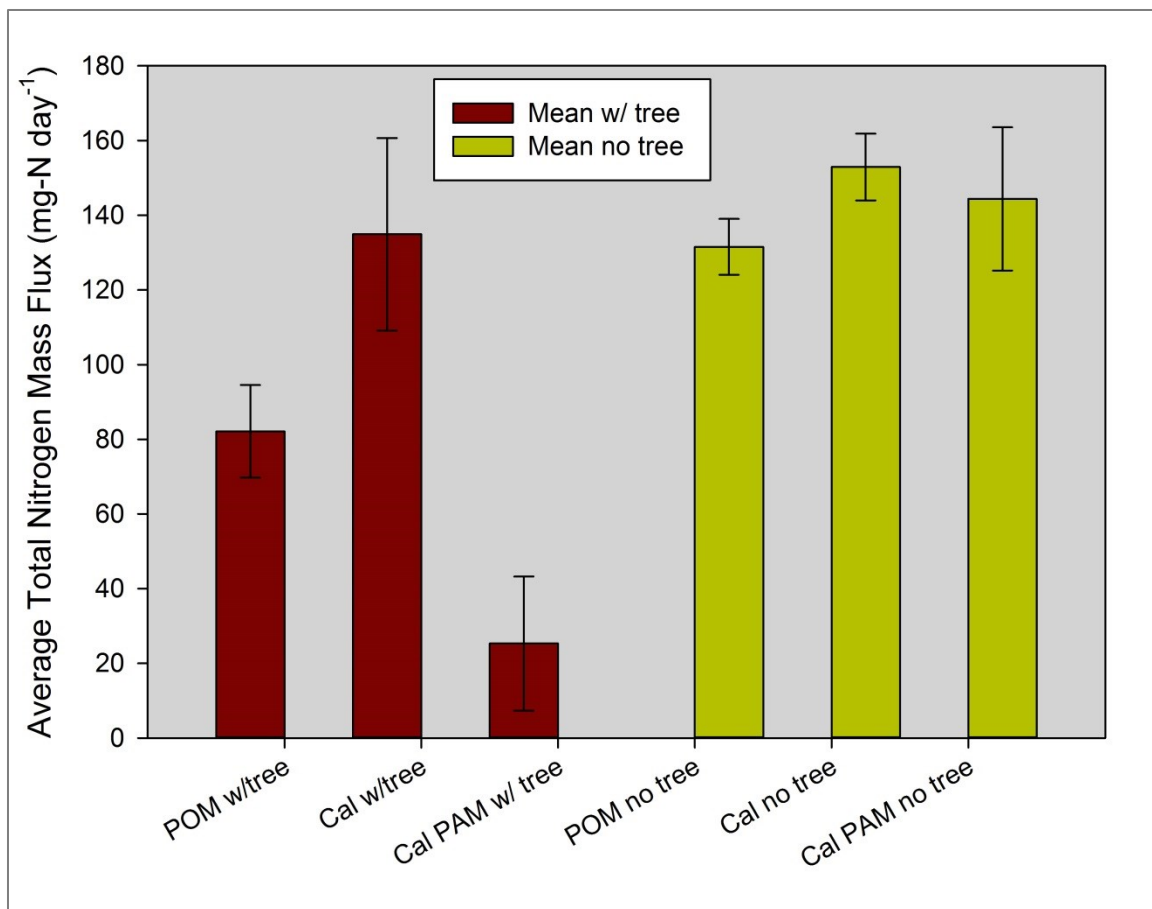


Figure 23: Average total nitrogen mass flux comparison with error bars representing  $\pm$  one standard deviation

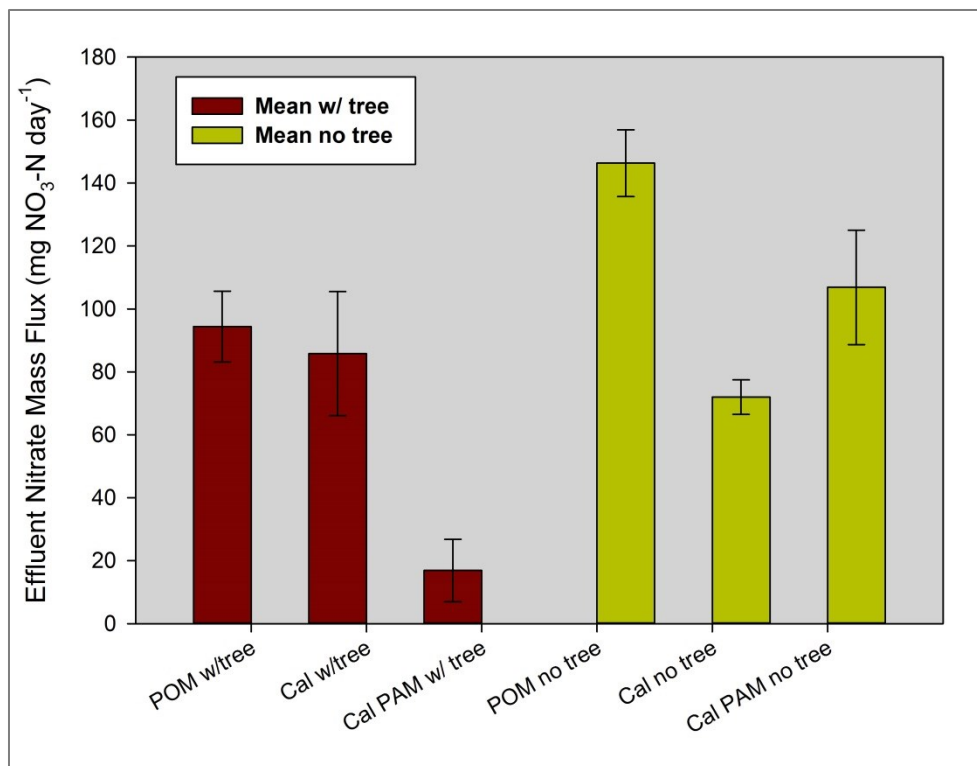


Figure 24: Average nitrate mass flux comparison with error bars representing  $\pm$  one standard deviation

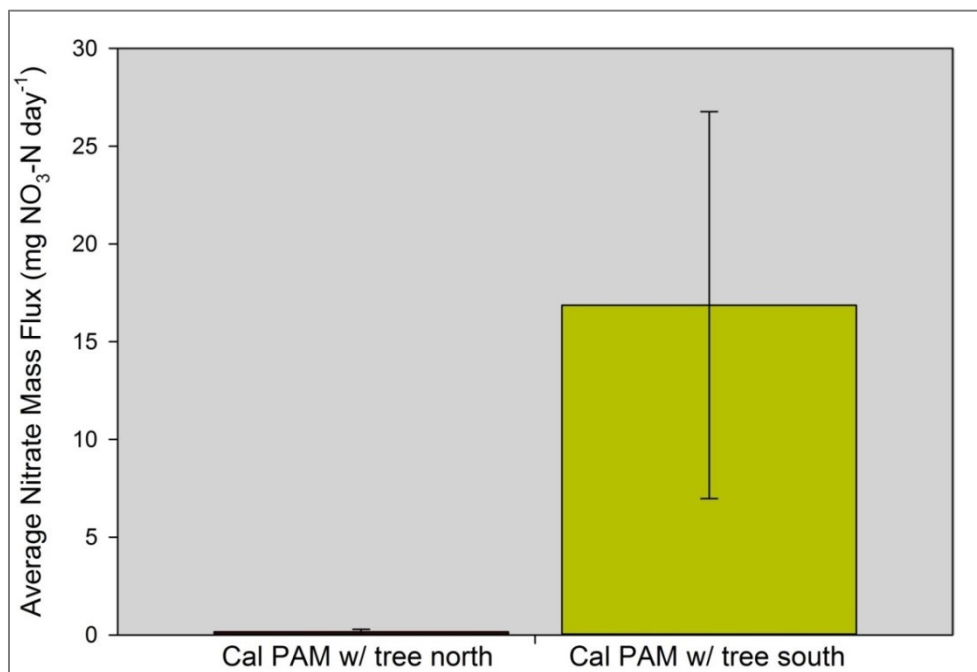


Figure 25: Nitrate mass flux comparison for the north and south Cal PAM with tree test cells

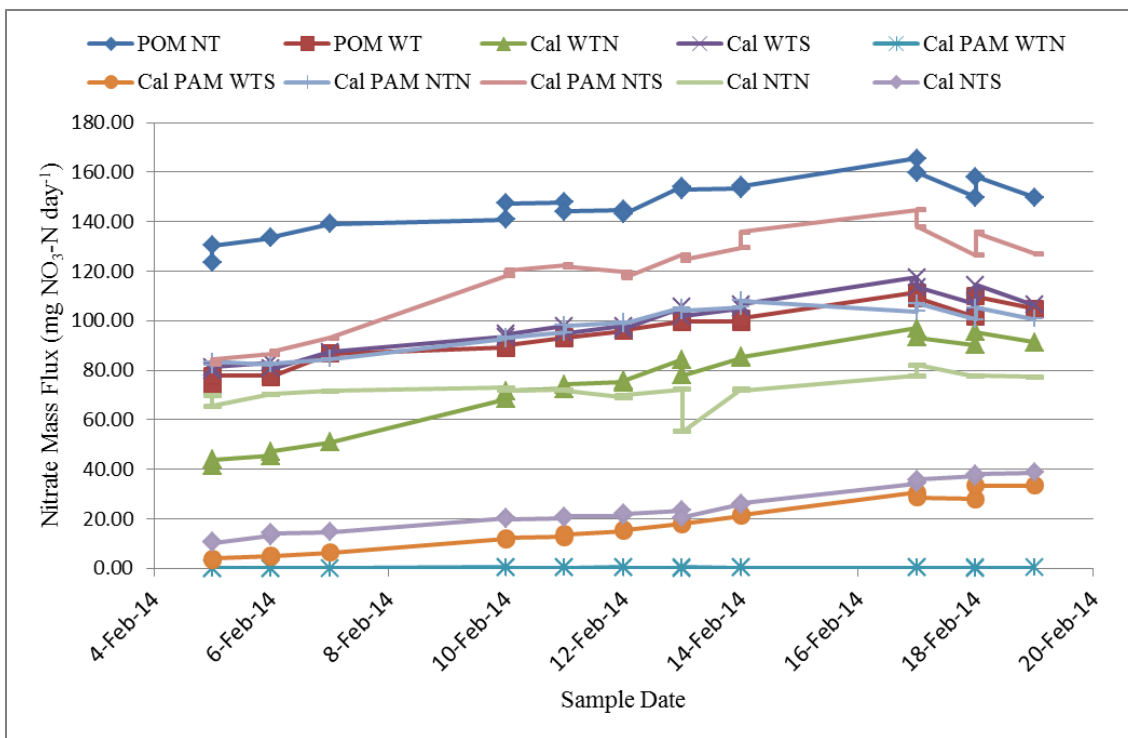


Figure 26: Nitrate mass flux for all test cell treatment types over a 2 week sampling period

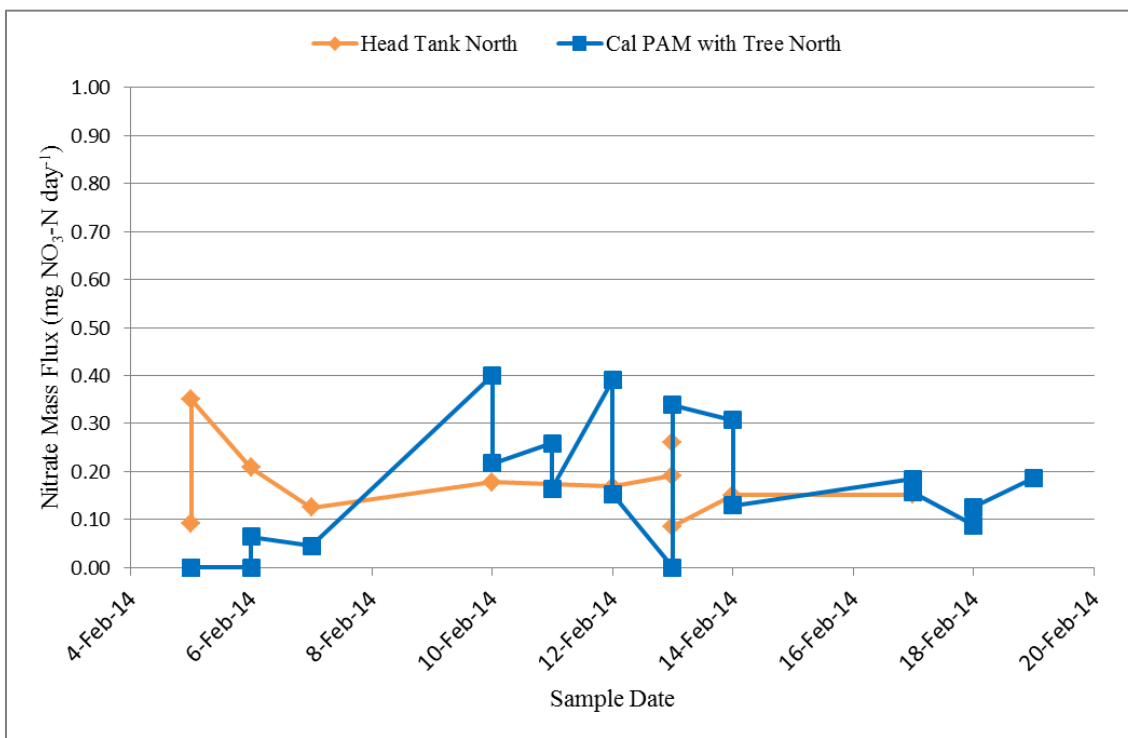


Figure 27: Nitrate mass flux comparison of Cal PAM with tree north vs. head tank north

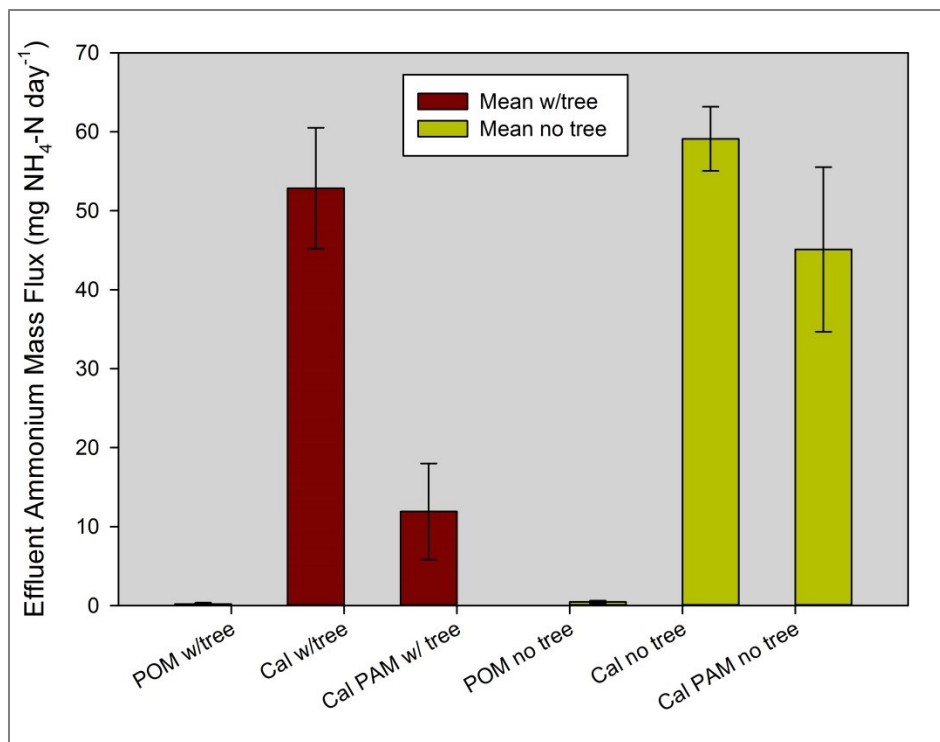


Figure 28: Average ammonium mass flux comparison with error bars representing ± one standard deviation

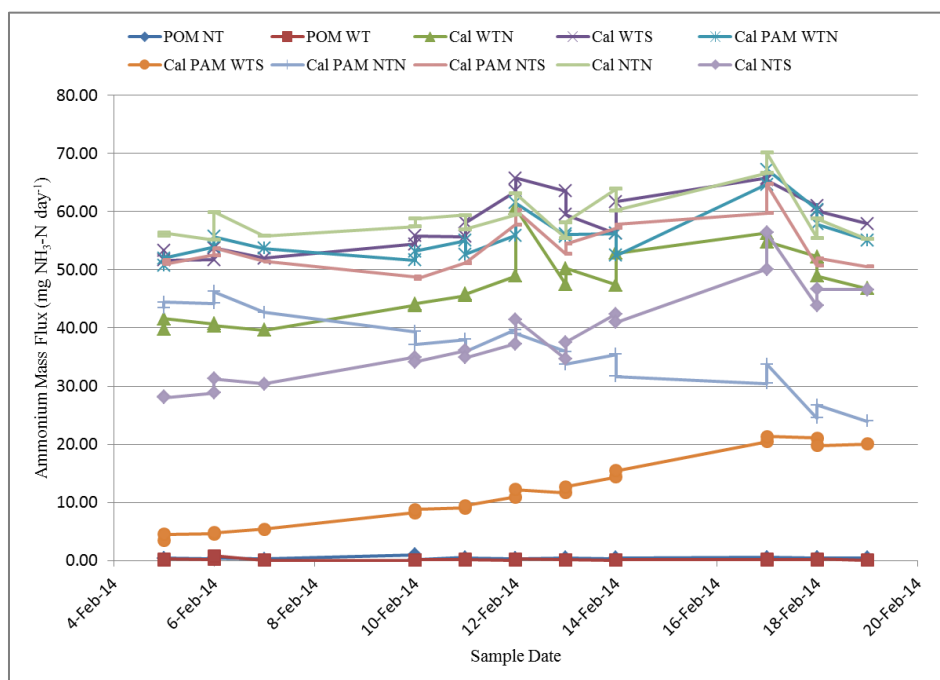


Figure 29: Ammonium mass flux for all test cell treatment types over a 2 week sampling period

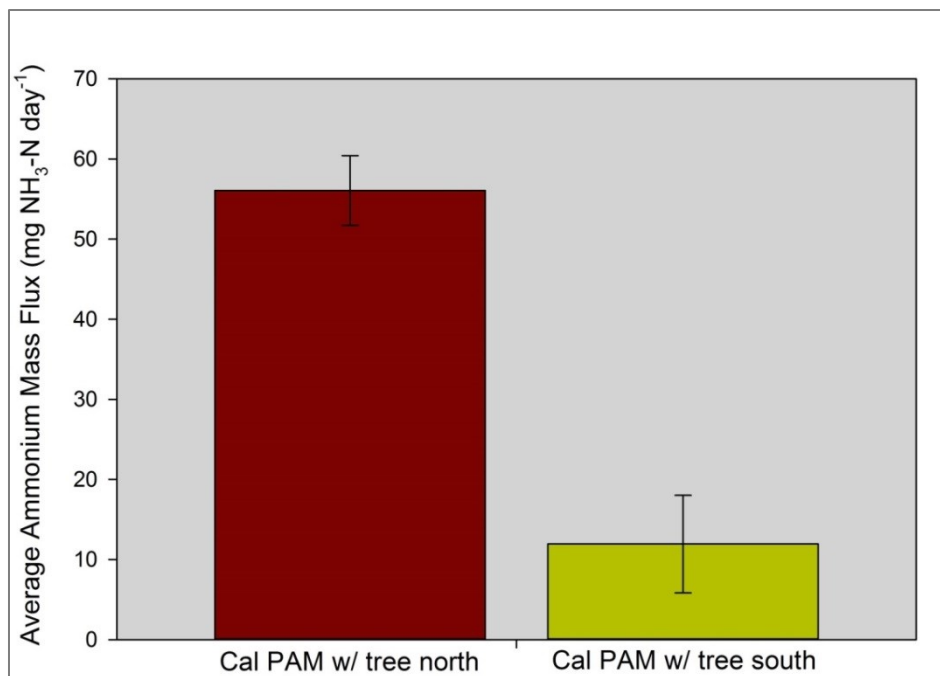


Figure 30: Ammonium mass flux comparison for the north and south Cal PAM with tree test cells

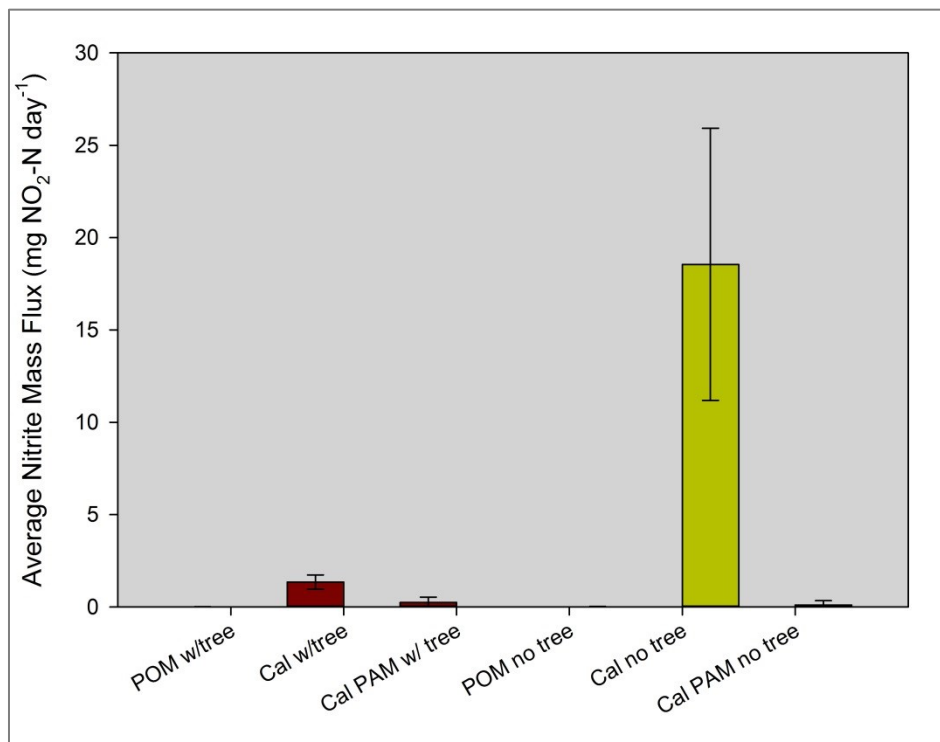


Figure 31: Average nitrite mass flux comparison with error bars representing  $\pm$  one standard deviation

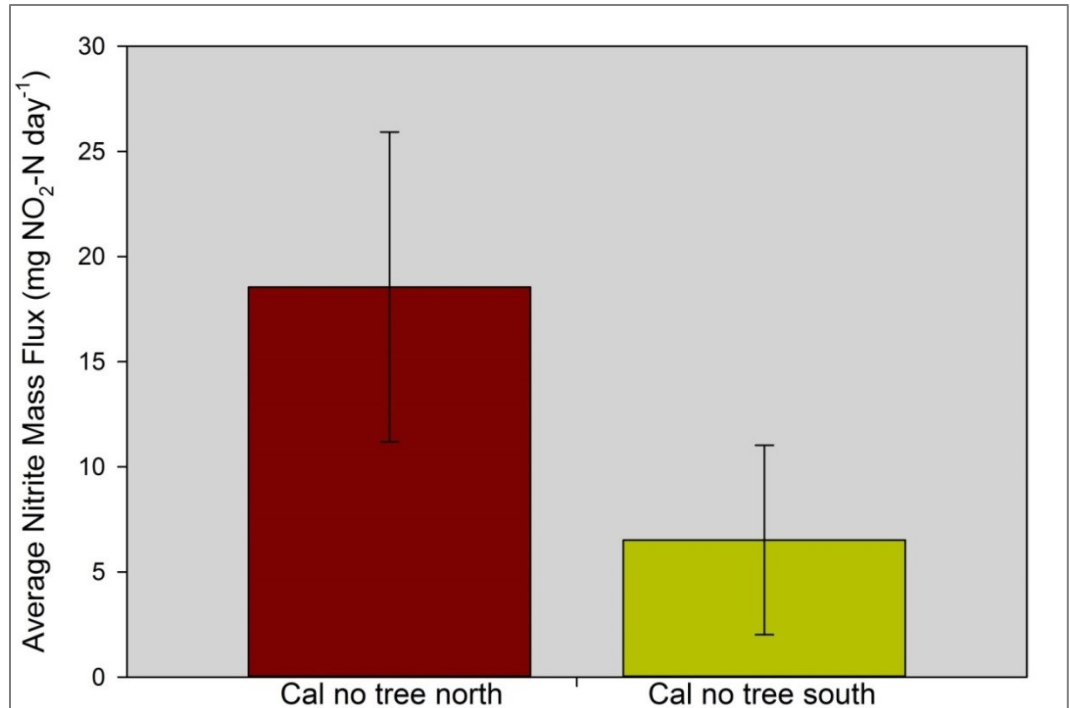


Figure 32: Nitrite mass flux comparison for the north and south Cal no tree test cells

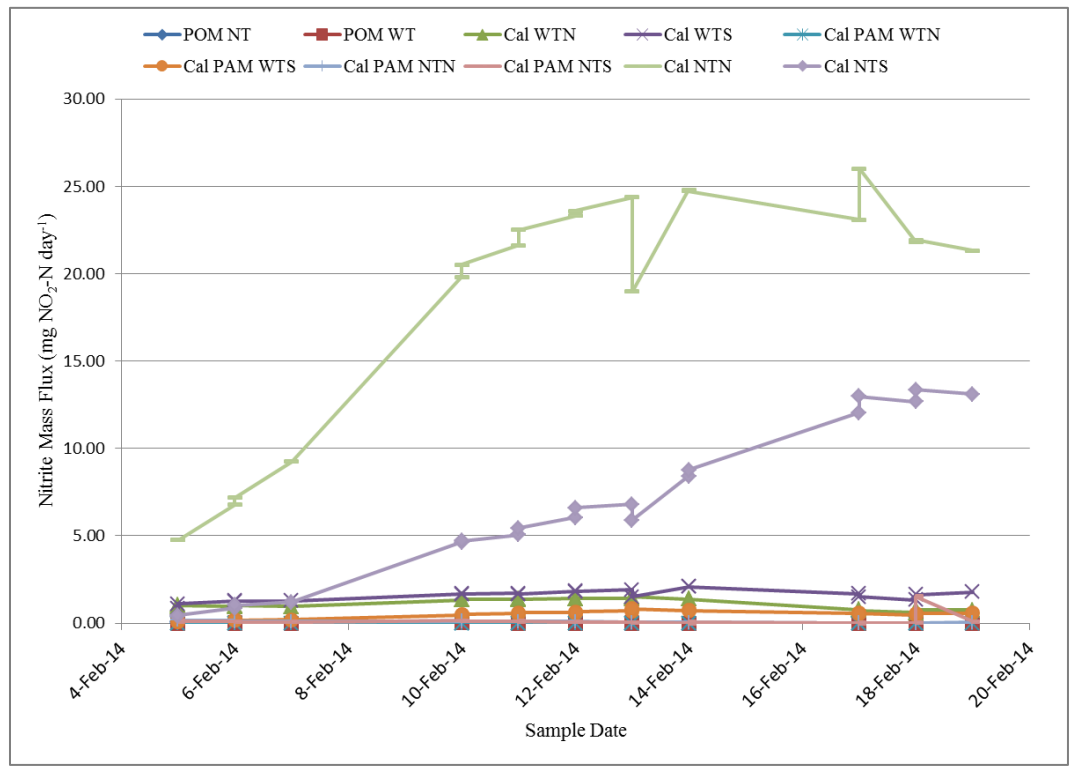


Figure 33: Nitrite mass flux for all test cell treatment types over a 2 week sampling period

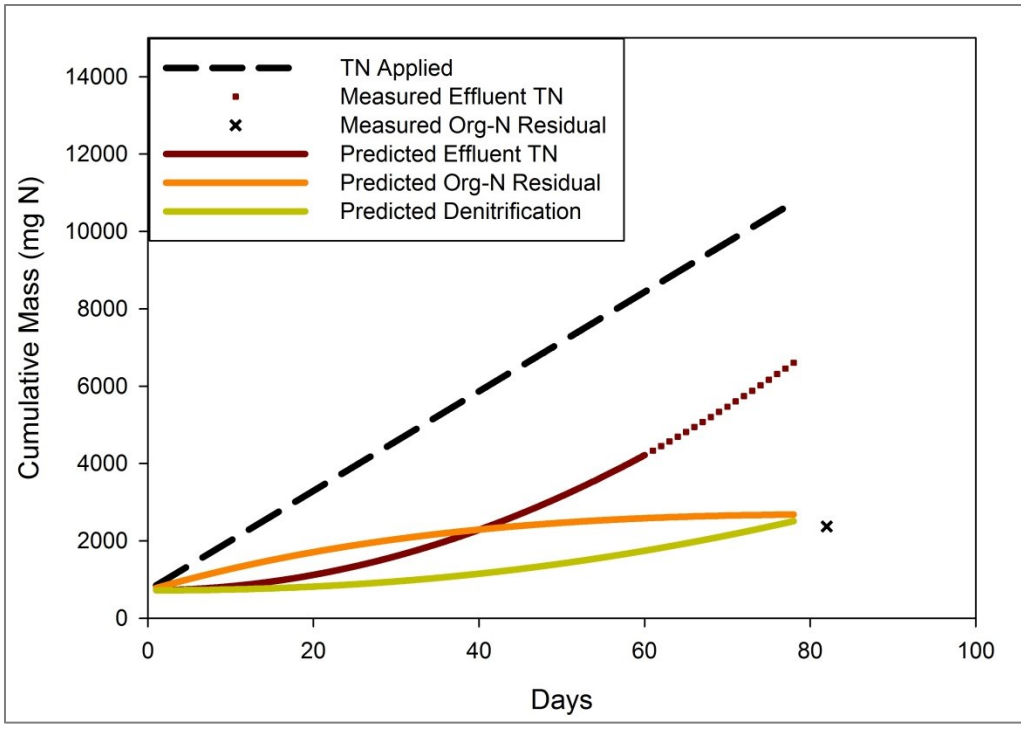


Figure 34: Measured and predicted nitrogen dynamics for the POM no tree test cell

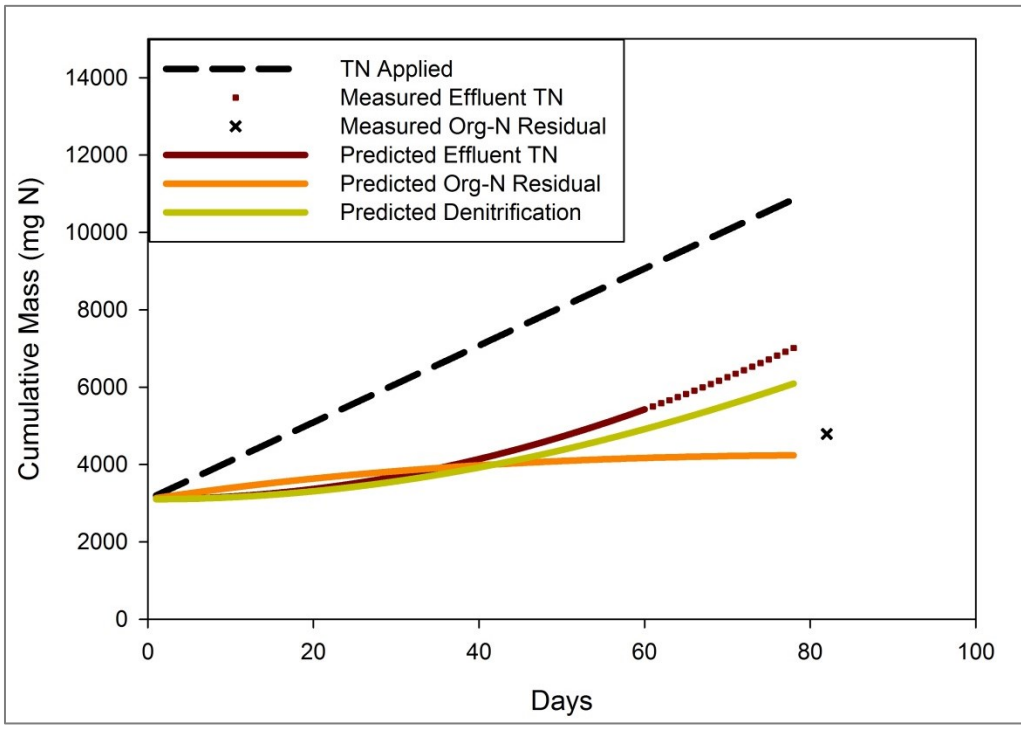


Figure 35: Measured and predicted nitrogen dynamics for the POM with tree test cell



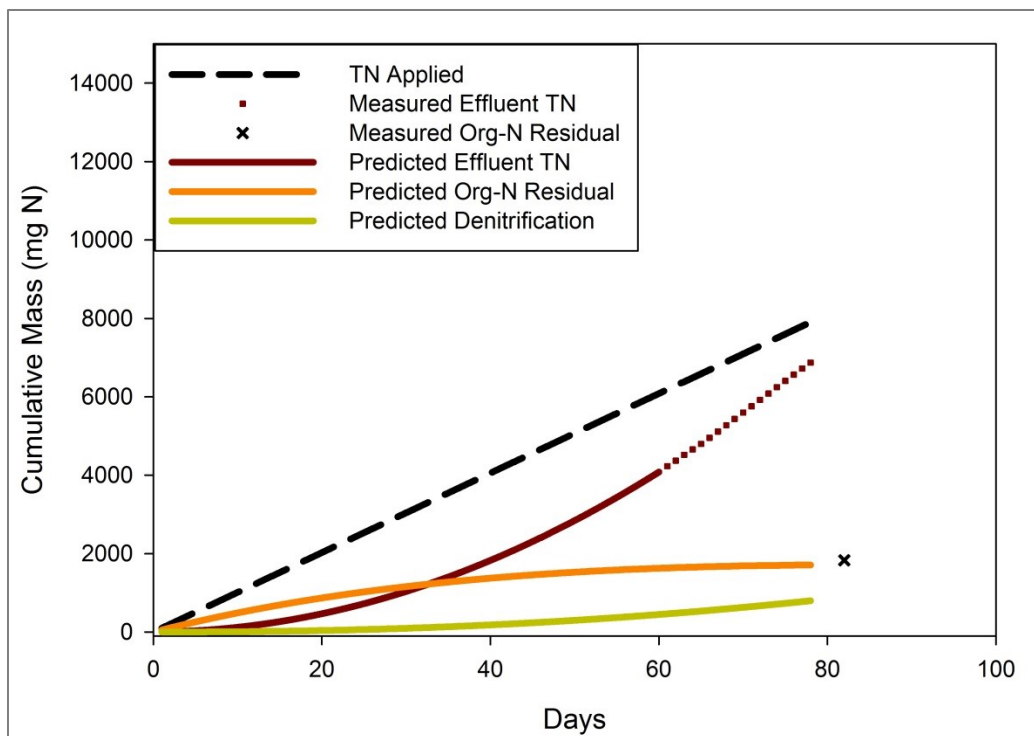


Figure 36: Measured and predicted nitrogen dynamics for the Cal no tree north test cell

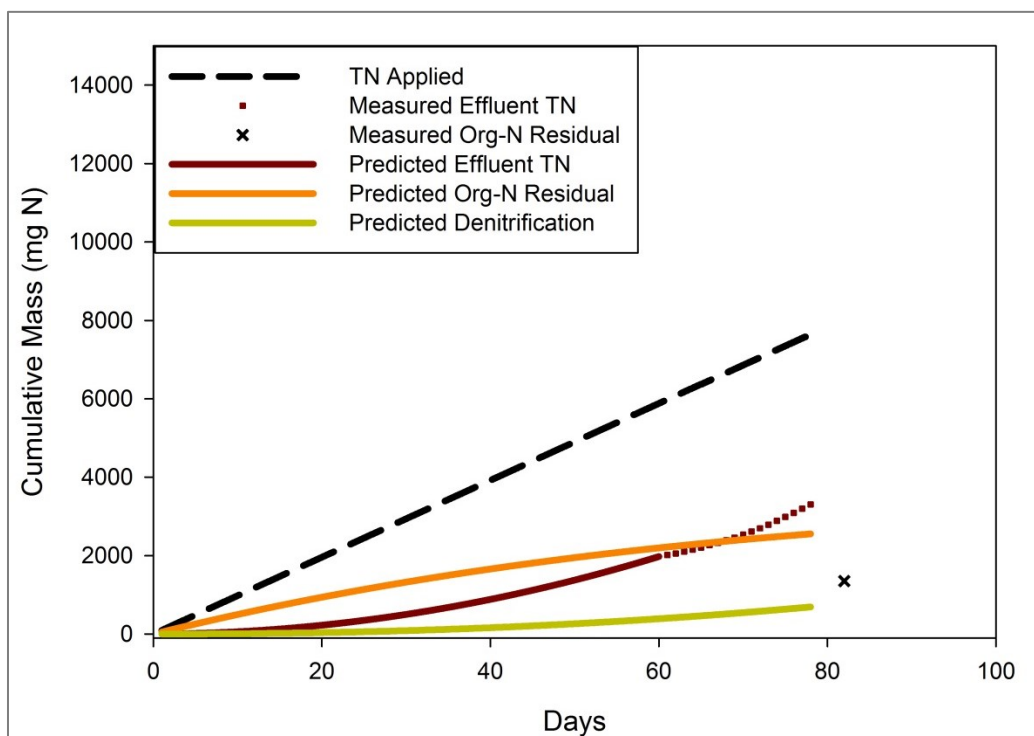


Figure 37: Measured and predicted nitrogen dynamics for the Cal no tree south test cell

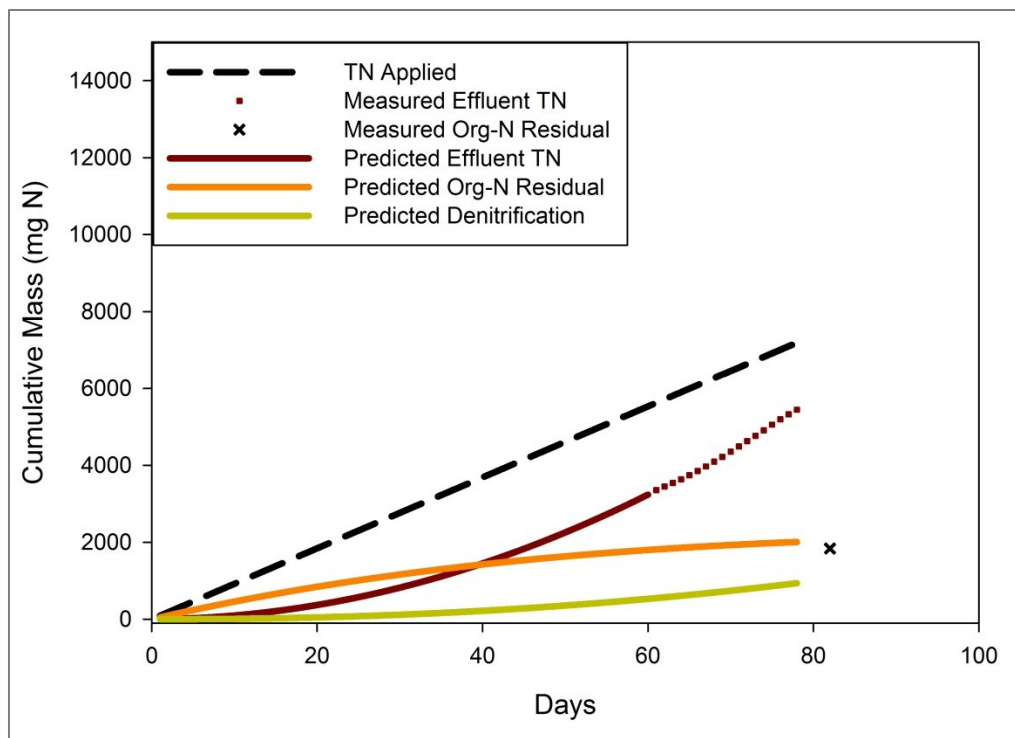


Figure 38: Measured and predicted nitrogen dynamics for the Cal with tree north test cell

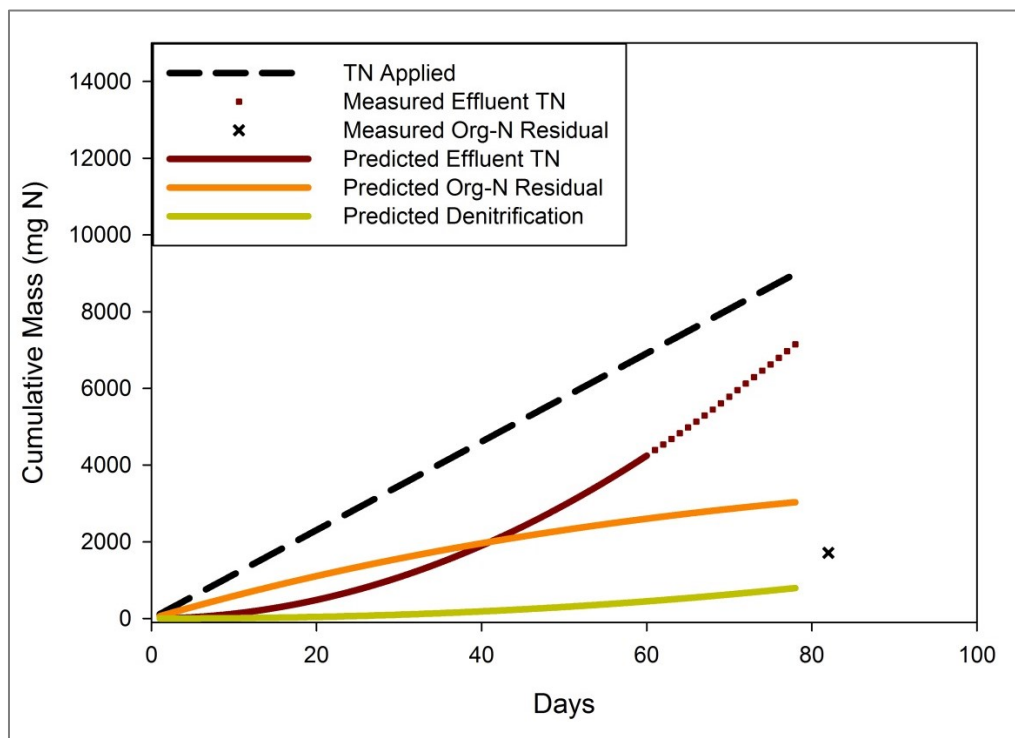


Figure 39: Measured and predicted nitrogen dynamics for the Cal with tree south test cell

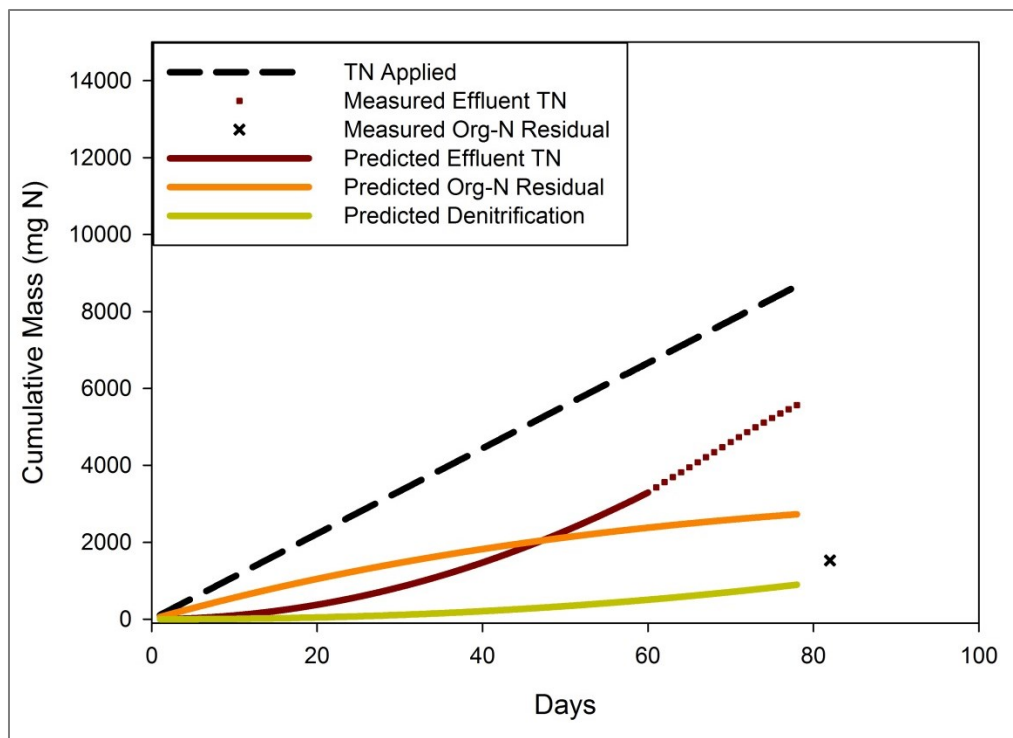


Figure 40: Measured and predicted N dynamics for the Cal PAM no tree north test cell

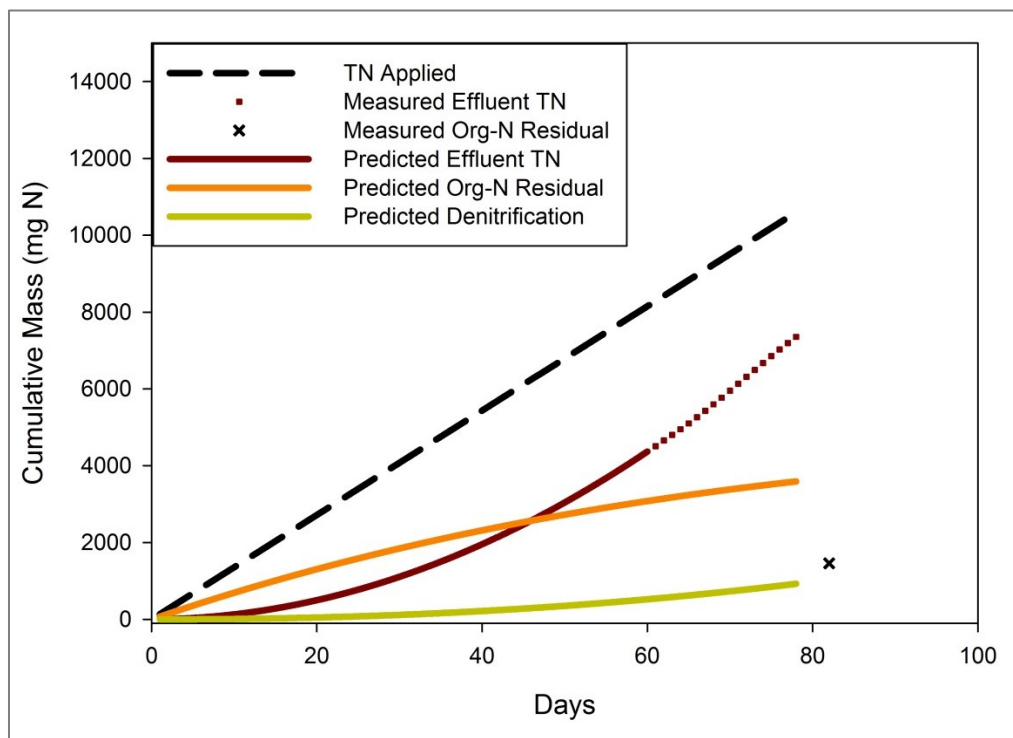


Figure 41: Measured and predicted N dynamics for the Cal PAM no tree south test cell

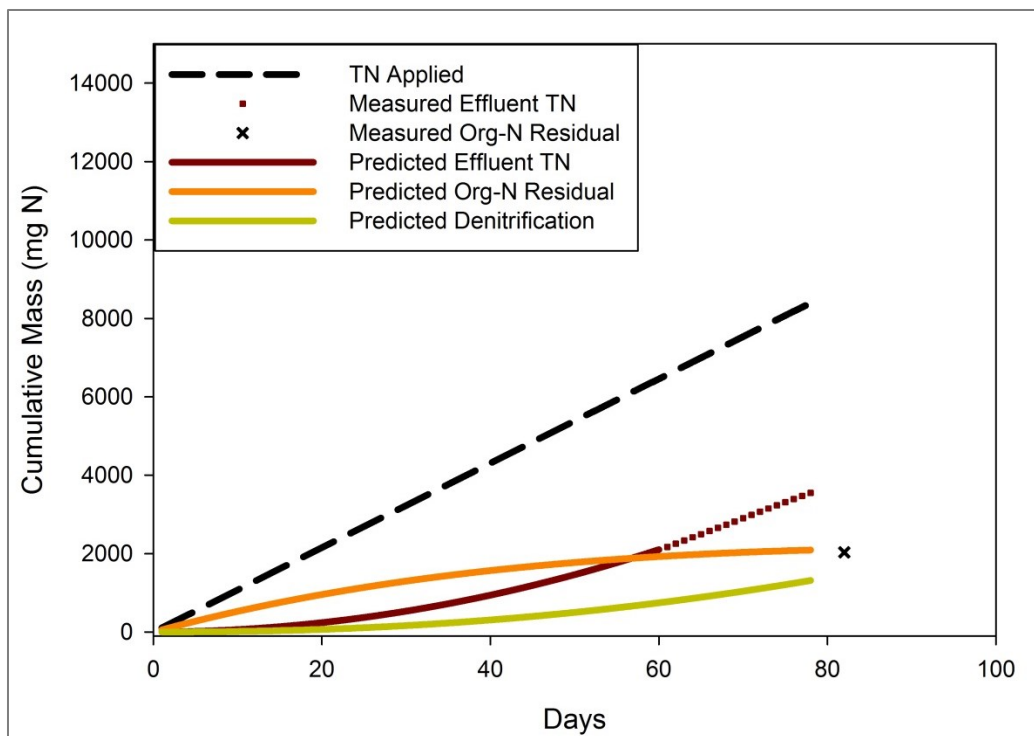


Figure 42: Measured and predicted N dynamics for the Cal PAM with tree north test cell

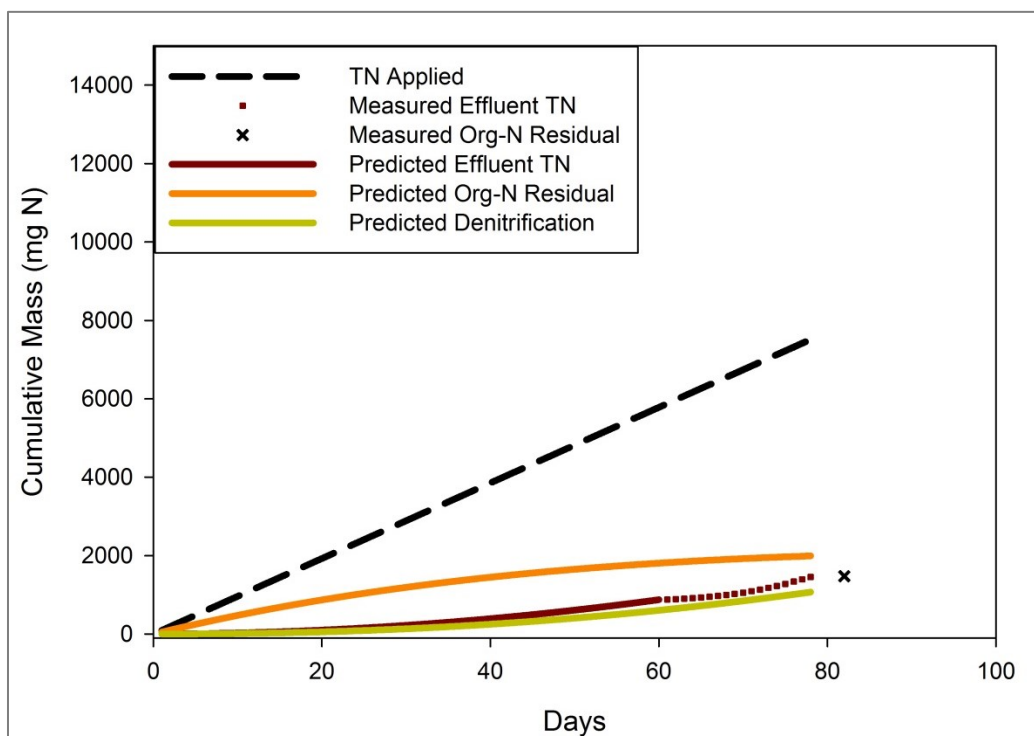


Figure 43: Measured and predicted N dynamics for the Cal PAM with tree south test cell

Table 4: Cumulative measured and predicted mass values of nitrogen for each treatment type

Treatment Type	Cumulative Mass (mg N)				
	TN Applied	TN Effluent	Pred. Org-N Residual	Pred. Denitrification	Measured Org-N Residual
POM no tree	10754	6605	2679	2509	2372
POM with tree	10859	7013	4238	6090	4788
Cal with tree north	7192	5445	2009	938	1840
Cal with tree south	8993	7149	3032	795	1714
Cal no tree north	7908	6875	1712	799	1829
Cal no tree south	7646	3307	2554	692	1350
Cal PAM with tree north	8399	3548	2092	1316	2034
Cal PAM with tree south	7516	1455	1993	1070	1476
Cal PAM no tree north	8667	5566	2728	897	1530
Cal PAM no tree south	10601	7357	3591	927	1462

Table 5: Dose rate and estimated rate coefficients over the course of the experiment for all treatment types

Treatment Type	Days	Dose Rate (L day <sup>-1</sup> )	Hydrolysis Rate Coefficient	Denitrification Rate Coefficient
	78	2	0.001	0.0003

## 2.5 Conclusions

### 2.5.1 Summary of Findings

The effects of hybrid poplar root systems on hydraulic retention time (flow), total nitrogen, nitrate, ammonium, and nitrite in the vadose zone were investigated using polypropylene test cells with an intermittent irrigation of synthetic wastewater. Highly time resolved (1 min) water chemistry data and influent and effluent grab sample measurements were collected from sandy soil test cells containing dormant hybrid poplar roots, test cells without roots, and test cells with polyacrylamide amended into the upper 6 to 8 inch surface layers. The test cell design was determined to sufficiently mimic natural conditions for temperature and groundwater sampling capabilities.

Concentration changes for total nitrogen, nitrate, ammonium, and nitrite were determined to be significantly different (Mann-Whitney Rank Sum Test,  $p = <0.001$ ) between the with-root treatments and the no-root control treatments. Results from this

study indicated that roots affected the nitrogen cycle within the test cells by slowing down the movement of synthetic wastewater through the vadose zone and ultimately increasing the time for microbial processes to occur. Polyacrylamide was also determined to increase the retention time within the vadose zone when combined with a rooted system.

### *2.5.2 Implications on Nitrate by Treatment Type*

With the Calamus soil, effluent nitrate was consistently lowest for the rooted treatment types with the addition of polyacrylamide in the upper 6 to 8 inch subsurface layer. Additionally, effluent nitrate with POM soil was consistently lower in the treatment with roots than with no roots. These findings indicate that a poplar rooted vadose zone will enhance denitrification potential when compared with a non-rooted system of the same soil type.

### *2.5.3 Implications for Port of Morrow*

This research study was able to replicate the phenomenon of nitrate leaching during the winter months at levels above applied concentrations. This finding has also been shown to occur at the Port of Morrow field site from groundwater sampling well analysis. The excess nitrate leaching can be attributed to the continual application and accumulation of slowly degrading organic-N. Nitrogen poor sandy soil can act like a water filter that over time will accumulate organic-N in the upper layers of the vadose zone. This organic-N will slowly deaminate, or hydrolyze, into ammonia and the newly formed ammonia compounds will then oxidize in the upper reaches into nitrate, increasing the nitrate load to levels above applied concentrations. Due to this process, there may become a much larger steady state nitrate leaching once the wastewater application process begins because the organic-N will continue to build up over time under these experimental conditions.

#### *2.5.4 Future Research*

The results obtained from this study provide opportunities for several future research areas. For example, soil analysis could be performed in order to determine nitrogen and other nutrient accumulation rates as well as organic carbon deposition and the presence of microbial communities throughout the soil profile. Further research could also investigate root density after subsequent growth cycles in combination with repeating the study to determine whether age and establishment of a rooted poplar system influenced nitrogen dynamics. It would be valuable to move these test cells outside, continue synthetic dosing and sampling throughout the year, and investigate how the treatment types are able to manage nitrogen application. Specifically, this study could investigate the ability of tree systems coming out of dormancy to handle the total nitrogen load and accumulated organic-N that has built up throughout the winter months the influence of organic-N and deamination rates.

Much time and research could also be spent investigating larger, field-scale studies with deeper rooted poplar systems, alternative irrigation application methods, and the direct influence from varying climatic conditions. Detailed studies at this scale could help explain site-specific leaching patterns while accounting for naturally occurring soil heterogeneity.

## CHAPTER 3:

### MODELING POPLAR VADOSE ZONE NITROGEN DURING DORMANCY

#### 3.1 Abstract

This research utilized a pilot-scale, sandy soil, poplar vadose zone system to study the behavior of irrigated ammonium and nitrate-containing wastewater during tree dormancy. After reaching steady-state conditions, the with-root and no-root treatments had statistically similar effluent ammonium concentrations representing 99% removal of the influent dose. The nitrate concentration in the with-root testing cell effluents (1.0 mg/L) was statistically different than measured in the no-root treatment (5.1 mg/L). Two-dimensional numerical modeling of the testing cells was able to describe the water movement and nitrogen transformation dynamics within the testing cells with good agreement to measured data. The study provides strong evidence that less nitrate escapes a deeply rooted vadose zone than a non-rooted, or shallow rooted, system even during dormancy (4.5°C).

#### 3.2 Introduction

Nitrogen is a required nutrient for plant growth which makes a variety of nitrogen-rich industrial process waters and many treated domestic wastewaters valuable for crop irrigation (Isosaari, Hermanowicz, and Rubin 2010, 662-697; Parnaudeau et al. 2006, 1284-1295; Virto et al. 2006, 398-407). But, the application of nitrogen above agronomic uptake rates can lead to high levels of ammonium in shallow aquifers and nitrate concentrations that far exceed the federal drinking water limit of 10 mg/L  $\text{NO}_3^-$ -N (Darwish et al. 2011, 74-84; Jimenez and Chávez 2004, 269-276; Oregon Department of Environmental Quality 2012). Hybrid poplar trees have much deeper root systems than commonly irrigated crops (e.g. alfalfa, beets, etc.) making this plant a target species for



engineering a deeper, more effective nitrate treatment zone for the production of woody biomass and for the protection of shallow groundwater (Chávez et al. 2012, 76-84).

Sandy soils and poplar tree dormancy represent particular design challenges toward an effective and predictable engineered vadose zone (Gemail 2012, 749-761; Nadav, Tarchitzky, and Chen 2012, 75-81; Ndour et al. 2008, 797-803). Water and non-sorbing solutes, such as nitrate, move quickly through sandy soils which can diminish the nitrate transformation potential (Saeed and Sun 2013, 438-447). Cold-temperature dormancy halts root uptake which leaves vadose zone bacteria solely responsible for nitrate treatment and removal. Additionally, oxygen diffusion into sandy, unsaturated soils can limit denitrification by heterotrophic bacteria and intermittent irrigation and cool temperatures can inhibit bacterial growth. Thus, the behavior of nitrate in a sandy, poplar tree vadose zone during dormancy represents a major design constraint for the successful, year-round operation of such an engineered system.

Well calibrated and validated numerical models can simulate engineered vadose zone behavior under various biogeochemical conditions and a range of temporal and spatial scales (Langergraber 2007, 210-219; Langergraber et al. 2009, 3931-3943; Saeed and Sun 2011b, 1205-1213; Sklarz et al. 2010, 2010-2020; Toscano et al. 2009, 281-289). Of particular interest for simulating vadose zone nitrate behavior is variable water flow through saturated and unsaturated media, solute transport and reactivity, root density and sorption capacity, bacterial activity and temperature. It is desirable to calibrate these models with data collected at the pilot-scale before simulating at field-scale. But, pilot-scale experimental designs often involve dosing geometries that are better represented in three-dimensions whereas most field-scale modeling problems require only two-dimensional approximations. Therefore, a tandem three-dimensional and two-dimensional modeling approach can help transcend flow and solute reactivity differences beyond the bench-scale.

The main objective of this research was to build, operate and model a pilot-scale, sandy soil, poplar vadose zone system to study the behavior of irrigated ammonium and nitrate-containing wastewater from industrial food processing operations during tree dormancy. The overall goal was to better understand the system conditions that allow for the maximization of irrigated wastewater and the minimization of nitrate loss to groundwater during winter in a climate with average temperatures between minus 3 and 5°C. Our central hypothesis was that sandy soils planted with poplar trees would have a higher capacity for nitrogen-containing irrigation water and a greater ability to minimize nitrate loss than would unplanted soils. A central research deliverable was a model that could describe and predict the pilot-scale system behavior in two and three-dimensions with expectations of applying the model at the field-scale in the future.

### 3.3 Materials and Methods

#### 3.3.1 Pilot-scale Experimentation

The pilot-scale poplar tree vadose zone system consisted of a 56.8 L (15 gallon), polypropylene tank (A-INFD15-19, Plastic-mart.com) connected to four testing cells via 3.8 cm (1.5 in) diameter PVC piping (Figure 44). Electric shutoff valves (344B Series, TeeJet Technologies, Wheaton, IL) equipped with adjustable needle valves (4995K13, McMaster-Carr) wired to a programmable microprocessor (Arduino UNO) provided customizable dosing control. Each polypropylene test cell (R121230B, Plastic-Mart.com), 30.5 cm x 30.5 cm x 76.2 cm (12 in x 12 in x 30 in LWH), was fitted with a 1.25 cm diameter (0.5 in) perforated underdrain that was 28 cm (11 in) long and wrapped with permeable felt. The entire system was contained within a refrigerated room maintained at 4.5°C ± 2°C.

Two testing cells contained sand alone and served as the no root control treatments. Two other cells were each fitted with five tightly-spaced, poplar trees (*populus deltoides x nigra*, DN-21) that were rooted for 3 months prior to transplanting

into the testing cells and filled with 74 cm of sand. The testing cells were placed outside and were dosed manually with a synthetic wastewater until the end of the growing season (an additional 3 months). The synthetic wastewater contained 1 g/L of blender pulverized, Vegetable Stew Blend (Auguson Farms), 0.29 g/L Whey Protein Powder (Six Star Pro Nutrition) and 0.17 g/L ammonium acetate (A.C.S. certified, Sigma-Aldrich). The wastewater was made in 95 L batches (in deionized water) in a 113.5 L (30 gallon) contain and was allowed to steep for 48 hours prior to particle removal (20  $\mu$ m fabric filter) and subsequent transfer to the dosing tanks.

### 3.3.2 Tracer Tests

A series of bromide tracer tests were performed under saturated, equilibrium flow conditions. Deionized water was irrigated at 40 mL/min and then 50 mL of a 100 g/L potassium bromide (3.4 g total bromide) was added directly to the sand surface of each testing cell. The effluent conductivity was measured (IntelliCAL™ CDC401, Hach Company, Loveland, CO) and recorded every 30 seconds for 20 hours. This procedure was repeated once for each testing cell and the two resulting breakthrough curves were averaged for modeling purposes. For one test cell, discrete samples were collected over time and analyzed for bromide concentration using an ion chromatograph (IonPac AS22 Anion-Exchange Column, IC900, Dionex, Sunnyvale, CA). This direct bromide concentration data was then used to determine a “bromide equivalent” conversion factor for the conductivity probe data. The testing cells were rinsed thoroughly with deionized water prior to subsequent experiments.

### 3.3.3 Intermittent Dosing Experiment

Synthetic wastewater was dosed every two hours for 4 minutes at 40 mL/min over the course of 3 weeks. Prior to the experiment, the testing cells were inoculated with 4 L of effluent collected from the trickling filter of a municipal wastewater treatment plant.

This inoculum was presumed to contain anaerobic denitrifying bacteria as well as aerobic nitrifying bacteria. The influent and effluent was sampled intensively at the beginning and end of the experiment with additional samples collected on occasion throughout. Head tank and effluent samples were analyzed for ammonium (salicylate method, CFR 2012), nitrate and dissolved oxygen. Nitrate was analyzed by ion chromatograph or by the dimethylphenol method (CFR 2012). Dissolved oxygen was measured electronically (IntelliCAL™ LDO101, Hach Company) and colorimetrically (K-7512, Chemetrics, Midland, VA).

### 3.3.4 Numerical Modeling

The Hydrus 2D/3D (version 2.03.0520) software package was selected for the ability to describe variably saturated flow using the Richards equation (Šimůnek, Sejna, and van Genuchten 1999, Colorado School of Mines, Golden, Colorado). The van Genuchten-Mualem soil hydraulic model with no hysteresis was used. The material property variables included residual and saturated water contents ( $\theta_r$  and  $\theta_s$ ), the van Genuchten shape parameters ( $\alpha$  and  $n$ ), the saturated hydraulic conductivity ( $K_s$ ), and Mualem's pore connectivity parameter,  $l$ . The solute transport parameters utilized the Crank-Nicholson time weighting scheme and the Galerkin finite elements space weighting scheme. The Millington & Quirk tortuosity function was utilized. Values were selected or determined for the soil specific solute transport parameters of bulk density, dispersion (longitudinal and transverse), fraction of type-1 adsorption sites, and for immobile water content. The soil hydraulic parameters of  $\alpha$ ,  $n$  and  $K_s$  along with the solute transport parameters for dispersion (Disp.L. and Disp.T.) and immobile water content (ThImob.) were iteratively optimized using the average bromide tracer data (2401 points) for the no-root and with-root treatments. These parameters were estimated using the Hydrus inverse solution function with comparison to outflow concentration of

bromide with weighting by standard deviation. The maximum number of iterations was set to 5.

The solute specific aqueous and gaseous diffusion coefficients were inputted and time-variable boundary conditions were parameterized to simulate continuous or variable flow conditions, bromide and nitrate spikes, and to parameterize for synthetic wastewater solute concentrations. The 2D model geometry was 30cm x 30cm x 74 cm (LWH) with an 11 unit x-axis and 20 unit z-axis discretizations. A no-flux boundary condition was selected for all outer nodes except for those at coordinates (12, 74); (15, 74) and (18, 74) which were defined as the atmospheric boundary and node (15, 0) that was defined as a free drainage boundary (Figure 45). Observation points were positioned at 70.1 cm, 62.3 cm, 50.6 cm, 31.2 cm and at the virtual drain (0 cm).

Biochemistry was modeled with the Constructed Wetlands 2D (CW2D) Hydrus software extension. The biochemical parameters considered were dissolved oxygen (DO), organic matter (OM, readily and slowly degradable and inert), ammonium, nitrite, nitrate, nitrogen gas, inorganic phosphorus, and heterotrophic and autotrophic organisms. The CW2D extension uses temperature dependent, Monod-type rate expressions. Heterotrophic bacteria were assumed responsible for hydrolysis, OM mineralization, and denitrification. Autotrophic bacteria were assumed responsible for a two-step nitrification process ( $\text{NH}_4^+$  to  $\text{NO}_2^-$  and  $\text{NO}_2^-$  to  $\text{NO}_3^-$ ). Initial values for these parameters were obtained from (Langergraber and Šimůnek 2005, 924-938) and over 50 model iterations were performed to determine optimal values. Once optimized, simulations of 720 hours were run for both the no-root and with-root scenarios to allow the system to reach equilibrium, particularly with respect to sorbed bacteria concentrations. After reaching equilibrium, a 24 hour simulation was completed and the output files were plotted and analyzed.

### 3.4 Results and Discussion

#### 3.4.1 Conservative Transport

The bromide breakthrough curves (BTC) for the no-roots and with-roots treatments (Figure 46) showed markedly different solute transport characteristics. The BTCs for the no-root treatment tests were much sharper compared to the broader and flatter shape of the BTCs resulting from the with-roots treatment. The sharp front and the slight tail of the no-root BTCs are indicative of mobile-immobile, non-equilibrium transport which was considered as a soil specific parameter in the Hydrus model. The optimal values for soil hydraulics and for solute transport (Table 6), determined from the inverse solution function, resulted in simulated BTCs in close agreement with the observed BTCs (Figure 47A and Figure 47B).

#### 3.4.2 Reactive Transport

Ammonium and concentration data (Figure 48A) collected at the conclusion of the 3 week intermittent dosing experiment showed significant transformation by both the no-root and with-root treatments. Effluent concentrations were statistically the same at 0.23 and 0.12 mg/L for the no-root and with-root treatments, respectively. This represents over 99% removal of the influent ammonium concentration that was measured at 30.5 mg/L. The effluent nitrate concentration (Figure 48B) was significantly higher in the no-root treatment (5.1 mg/L) compared to the with-root treatment (1.0 mg/L). The influent nitrate concentration was measured at 1.2 mg/L.

The hydrolysis rate constant,  $K_h$ , was the only CW2D solute transport parameter (Table 7) that was optimized for our system. Relatively low amounts of the ammonium were measured in the effluent of all testing cells which indicated a hydrolysis rate lower than utilized by Langergraber & Šimunek was warranted. Additionally, the test cells were not force-aerated so the re-aeration rate was set to a low value of 2.

At the conclusion of a 24 hour, equilibrium simulation, the pressure heads for the with-root and no-root scenarios (Figure 49, top panels) were significantly different. The with-root system showed greater pressure at all observation points which coincided with a greater water content (Figure 49, bottom panels). This result implies that rooted systems “perch” water within sandy soils by retaining water longer than no-root systems. This difference in water retention has implications for fast-degrading organic material (Figure 50, top panels) within the synthetic wastewater in that the increased dwell time in the with-root system gives bacteria more time to utilize the carbon for metabolic activity. As a result, the maximum fast-degrading organic carbon at observation point 1 was approximately 325 mg/L in the with-root system compared to nearly 600 mg/L in the no-root system. Conversely, slow-degrading organics (Figure 50, bottom panels) is retained at higher concentrations and at deeper depth in the with-root system compared to the no-root system. The with-root system supports a higher concentration of heterotrophic bacteria (Figure 51, top panels) and slightly lower concentrations of *Nitrosomonas spp.* and *Nitrobacter spp.* (Figure 51, middle and bottom panels).

The ammonium concentration at the effluent (observation point 5) of the with-root system (Figure 52, top panels) was 3.6 mg/L compared to 2.1 mg/L for no-root system. The relatively low effluent concentrations predicted by the model are consistent with the measured testing cell results (Figure 48). The with-root system was predicted to convert more ammonium in the upper reaches (observation point 1) than the no-root system which is facilitated by the greater number of associated heterotrophic bacteria. The effluent nitrate concentration in the with-root system was 6.4 mg/L in the with-root system and 12.0 mg/L in the no-root system (Figure 52, middle panels). This was consistent with the effluent nitrate concentrations measured in the testing cells with-roots (1.0 mg/L) and without roots (5.1 mg/L). This is the most significant result of the research in that the goal of the project was to determine if a poplar tree vadose zone could better protect groundwater from nitrate contamination than could a no root scenario. The

measured and simulated data show the rooted system allowed less nitrate to escape to groundwater – even during root dormancy. This appears to a result of greater conversion of nitrate to nitrogen gas at shallow depths (Figure 52, bottom panels) within the rooted system.

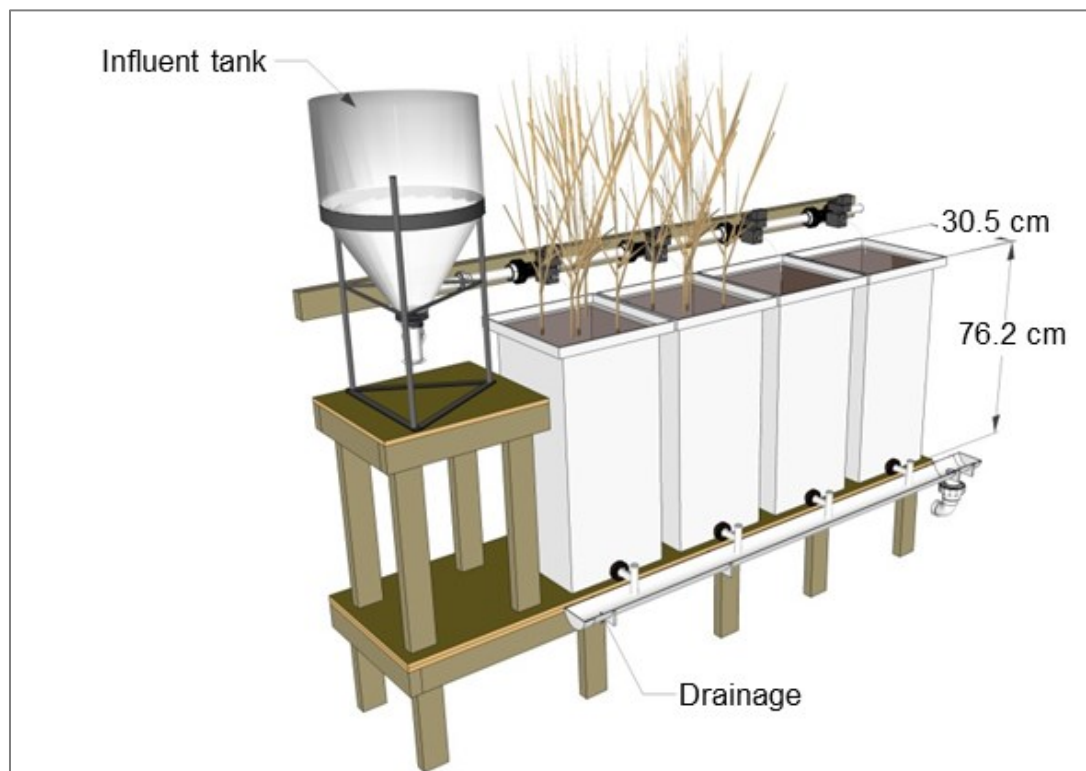


Figure 44: The with-root and no-root testing cell apparatus with influent tank, dosing valves, and under-drain equipped testing cells



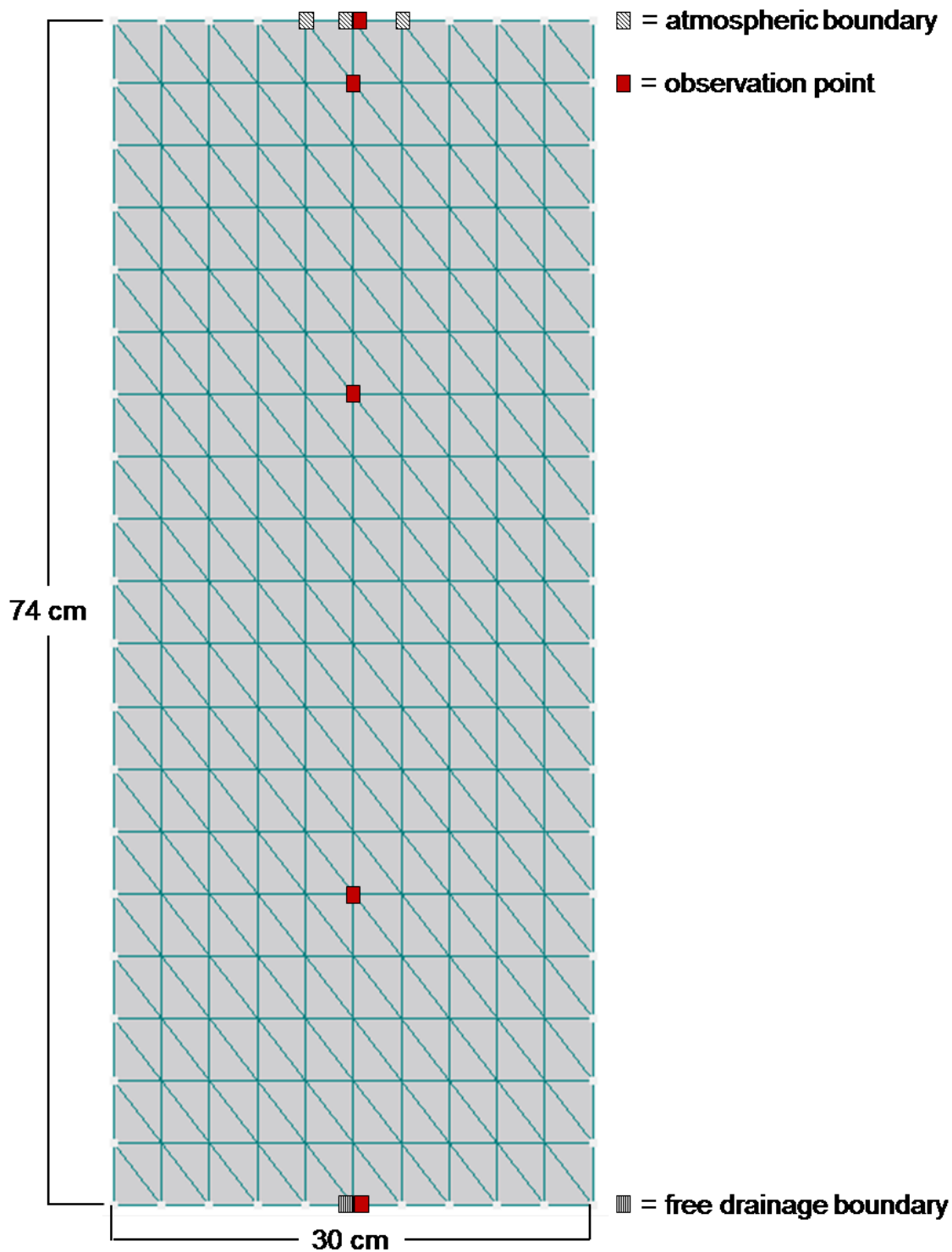


Figure 45: Hydrus domain properties and boundary conditions showing the 2D mesh discretization, five observation points and the atmospheric and free drainage boundaries. All outer nodes were no flux boundaries

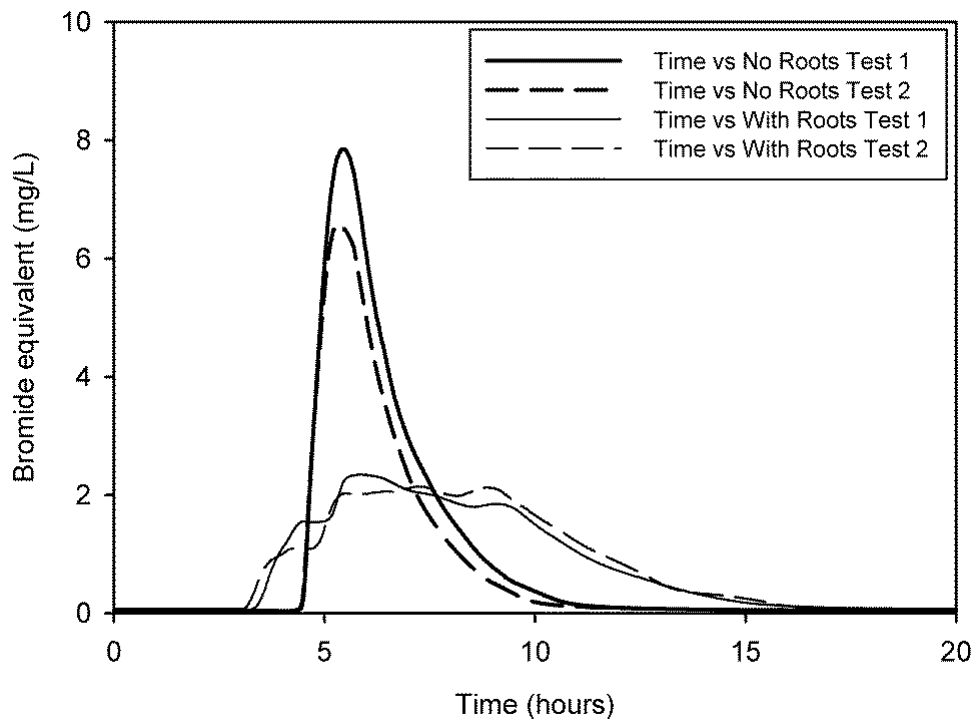


Figure 46: Bromide tracer study results for duplicate trials of the no-roots and with-roots test cells. Average results for each treatment were utilized as the soil hydraulic and solute transport fitting exercises in Hydrus

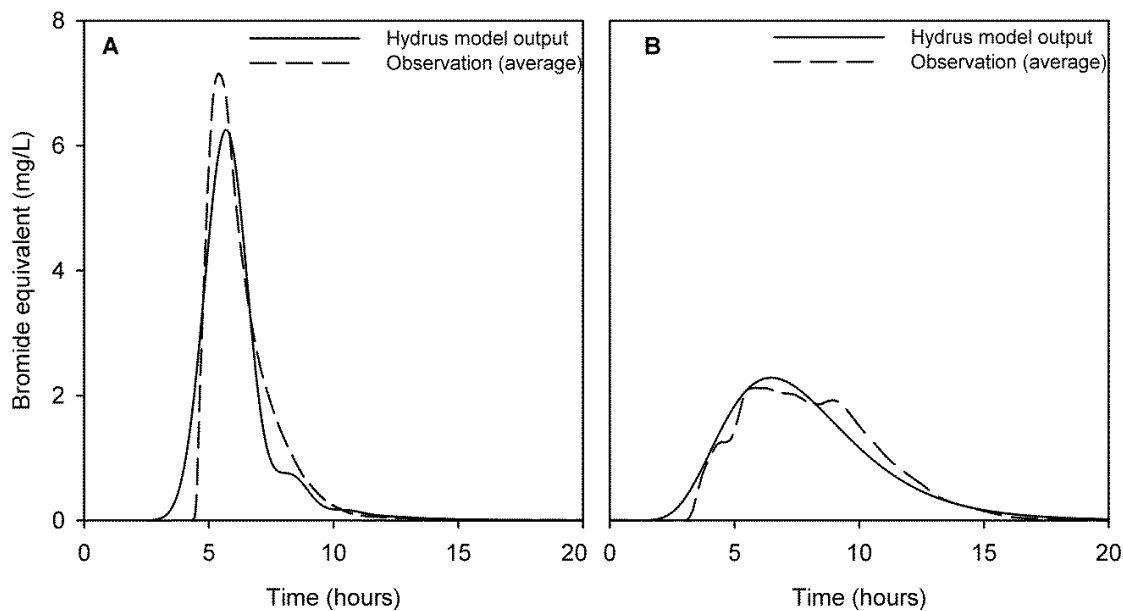


Figure 47: Comparisons of the Hydrus model output for a simulated bromide tracer to actual bromide tracer results for the no-root (panel A) and with-root (panel B) testing cells

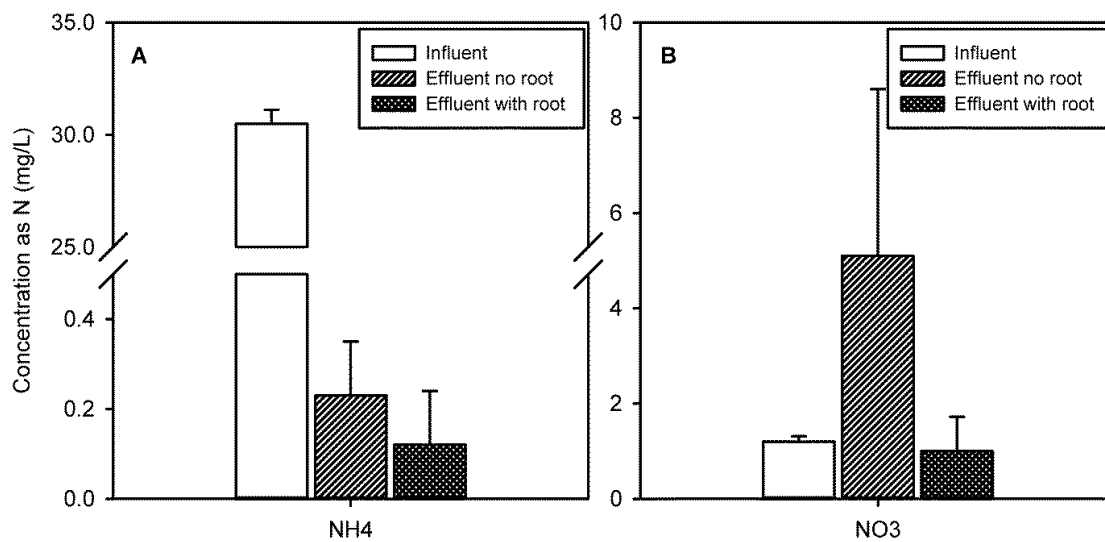


Figure 48: Measured influent and effluent concentrations of ammonium (NH<sub>4</sub>) and nitrate (NO<sub>3</sub>) for the no-root and with-root testing cells after three weeks of intermittent dosing

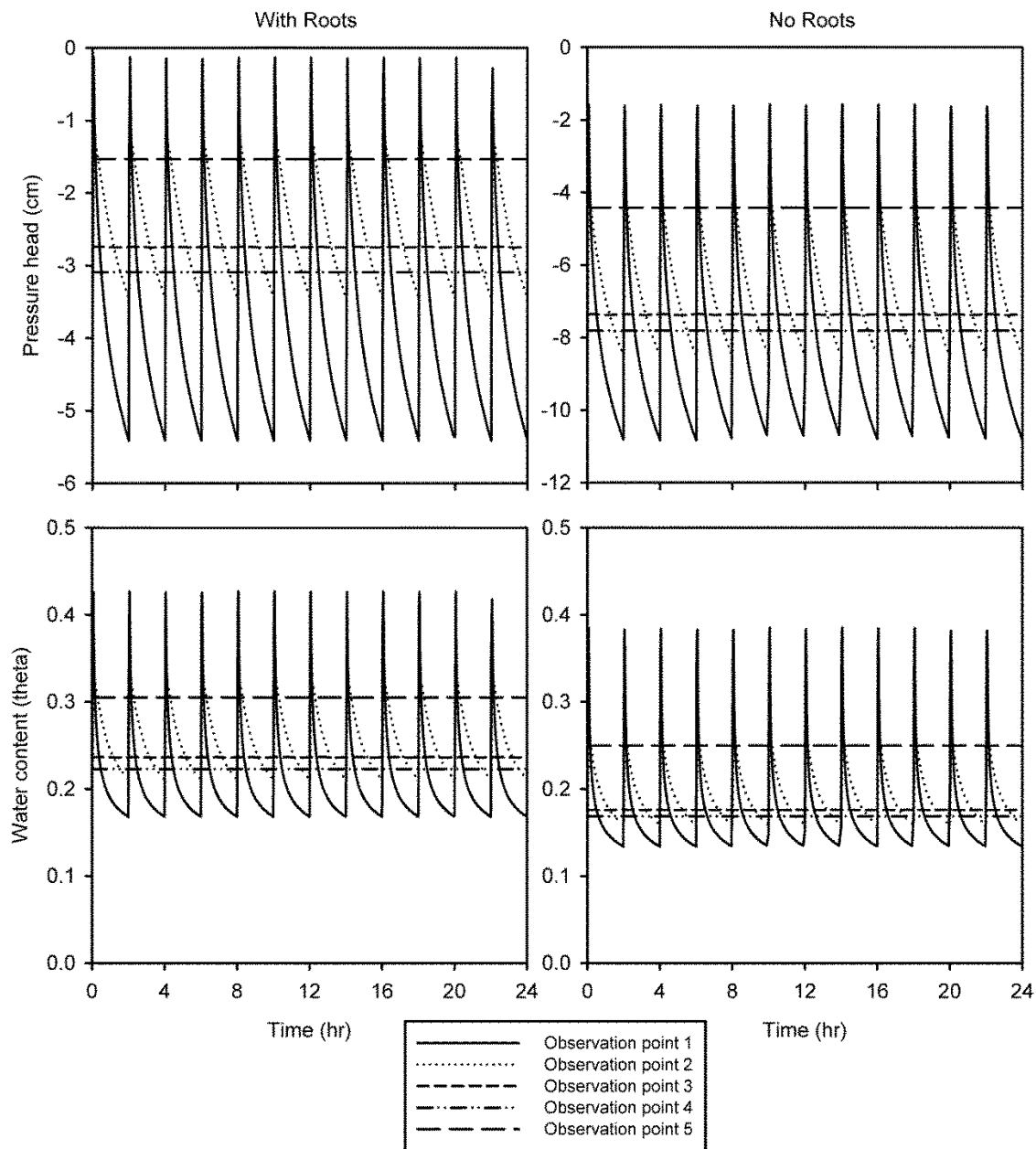


Figure 49: Simulated pressure head and water content data (final 24 hours shown) at five observation points for the with-root and no-root Hydrus scenarios. Note the differing y-axis scales

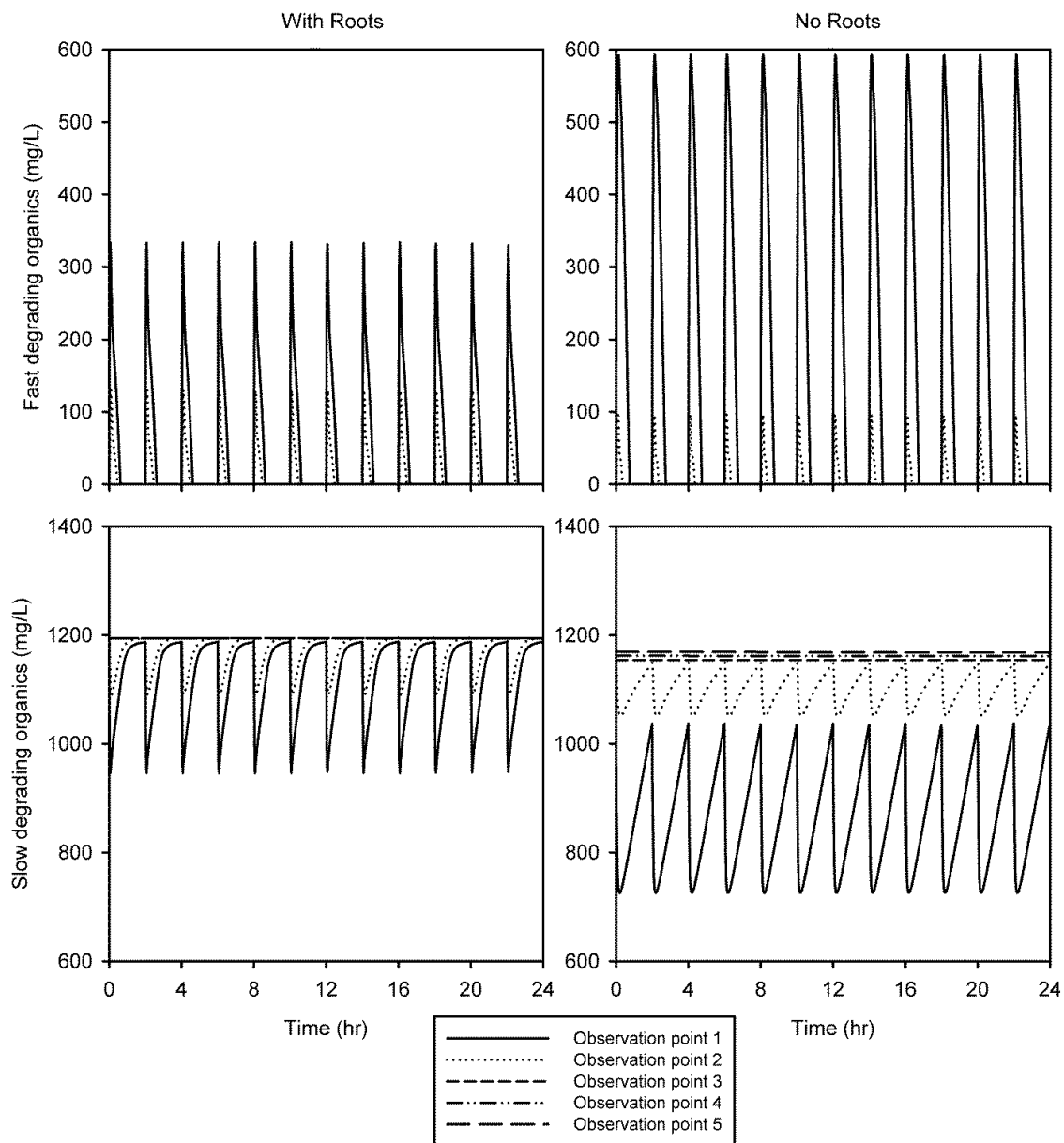


Figure 50: Simulated fast- and slow-degrading organic matter data (final 24 hours shown) at five observation points for the with-root and no-root Hydrus scenarios

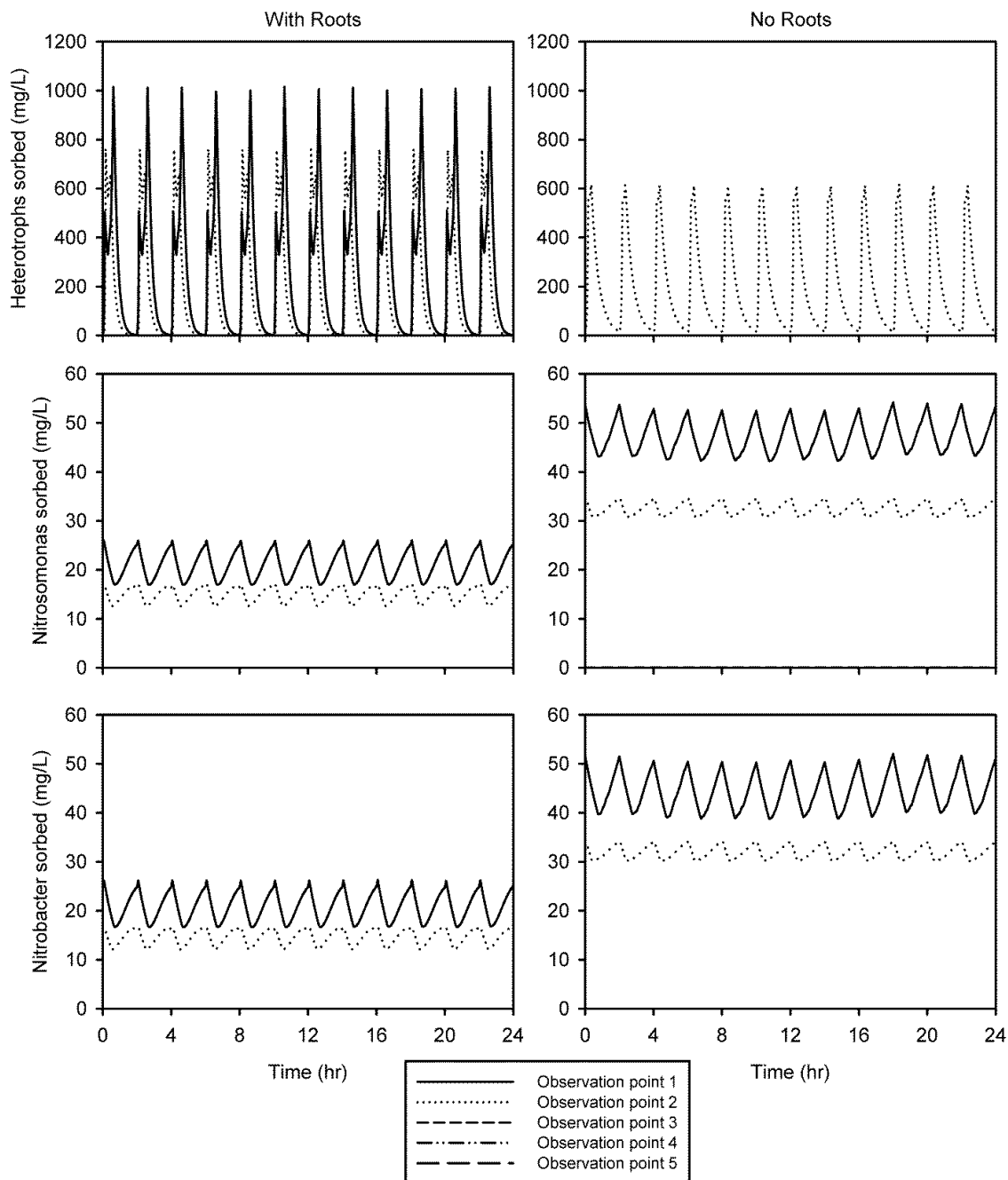


Figure 51: Simulated bacterial concentration data (final 24 hours shown) for total heterotrophs (top panels), *Nitrosomonas spp.* (middle panels), and *Nitrobacter spp.* (bottom panels) at five observation points for the with-root and no-root Hydrus scenarios

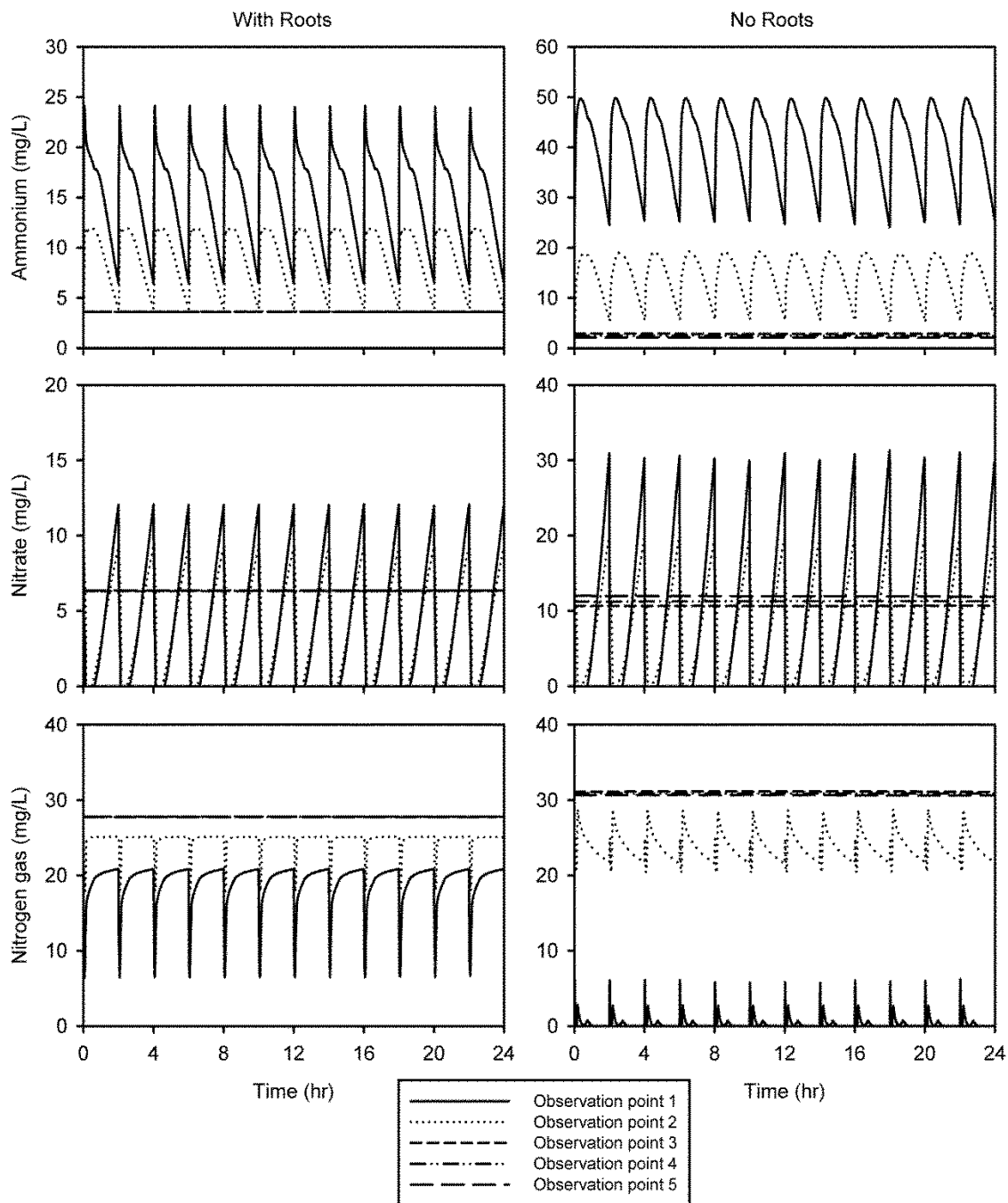


Figure 52: Simulated nitrogen concentration data (final 24 hours shown) for ammonium (top panels), nitrate (middle panels), and nitrogen gas (bottom panels) at five observation points for the with-root and no-root Hydrus scenarios. Note the differing y-axis scales

Table 6: Optimized values for fitted soil hydraulic and solute transport parameters and associated goodness of fit measures

	Hydraulic values			Transport values			Goodness of fit			
	$\alpha$	$n$	$K_s$	Disp.L.	Disp.T.	ThIMob.	$R^2$	$ME^*$	$MAE^*$	$RMSE^*$
No roots	0.34	2.10	49.7	0.13	0.6	0.043	0.94	0.0038	0.024	0.052
With roots	0.83	1.74	34.0	3.78	5.0	0.020	0.95	-0.0015	0.030	0.044

\*ME = mean weighted error

\*MEA = mean weighted absolute error

\*RMSE = root mean square weighted error



Table 7: Hydrus CW2D wetland module parameterization values

	Description [unit]	Value
<b>Hydrolysis</b>		
$K_h$	hydrolysis rate constant [1/d]	0.0002
$K_x$	saturation/inhibition coefficient for hydrolysis [g COD <sub>cs</sub> /g COD <sub>bm</sub> ]	0.22
<b>Heterotrophic bacteria (aerobic growth)</b>		
$\mu_H$	maximum aerobic growth rate on CR [1/d]	3
$b_H$	rate constant for lysis [1/d]	0.2
$K_{het,O_2}$	saturation/inhibition coefficient for S <sub>O</sub> [mg O <sub>2</sub> /L]	0.2
$K_{het,CR}$	saturation/inhibition coefficient for substrate [mg COD <sub>CR</sub> /L]	2
$K_{het,NH_4N}$	saturation/inhibition coefficient for NH <sub>4</sub> (nutrient) [mg N/L]	0.05
$K_{het,IP}$	saturation/inhibition coefficient for P [mg P/L]	0.01
<b>Heterotrophic bacteria (denitrification)</b>		
$\mu_{DN}$	maximum aerobic growth rate on CR [1/d]	2.4
$K_{het,O_2}$	saturation/inhibition coefficient for S <sub>O</sub> [mg O <sub>2</sub> /L]	0.2
$K_{het,NO_3N}$	saturation/inhibition coefficient for NO <sub>3</sub> [mg N/L]	0.5
$K_{het,NO_2N}$	saturation/inhibition coefficient for NO <sub>2</sub> [mg N/L]	0.5
$K_{het,CR}$	saturation/inhibition coefficient for substrate [mg COD <sub>CR</sub> /L]	4
$K_{het,NH_4N}$	saturation/inhibition coefficient for NH <sub>4</sub> (nutrient) [mg N/L]	0.05
$K_{het,IP}$	saturation/inhibition coefficient for P [mg P/L]	0.01
<b>Ammonia oxidizing bacteria (<i>Nitrosomonas</i> spp.)</b>		
$\mu_{Ans}$	maximum aerobic growth rate on S <sub>NH</sub> [1/d]	0.3
$b_{Ans}$	rate constant for lysis [1/d]	0.05
$K_{Ans,O_2}$	saturation/inhibition coefficient for S <sub>O</sub> [mg O <sub>2</sub> /L]	1
$K_{Ans,NH_4N}$	saturation/inhibition coefficient for NH <sub>4</sub> [mg N/L]	0.5
$K_{Ans,IP}$	saturation/inhibition coefficient for P [mg P/L]	0.01
<b>Nitrite oxidizing bacteria (<i>Nitrobacter</i> spp.)</b>		
$\mu_{ANb}$	maximum aerobic growth rate on S <sub>NH</sub> [1/d]	0.35
$b_{ANb}$	rate constant for lysis [1/d]	0.05
$K_{ANb,O_2}$	saturation/inhibition coefficient for S <sub>O</sub> [mg O <sub>2</sub> /L]	0.1
$K_{ANb,NO_2N}$	saturation/inhibition coefficient for NO <sub>2</sub> [mg N/L]	0.1
$K_{ANb,NH_4N}$	saturation/inhibition coefficient for NH <sub>4</sub> (nutrient) [mg N/L]	0.05
$K_{ANb,IP}$	saturation/inhibition coefficient for P [mg P/L]	0.01
<b>Temperature dependence</b>		
Tdep_het	activation energy for processes caused by XH [J/mol]	47,800
Tdep_aut	activation energy for processes caused by XA [J/mol]	69,000
Tdep_Kh	activation energy for hydrolysis [J/mol]	28,000
Tdep_KX	activation energy factor KX for hydrolysis [J/mol]	-53,000
Tdep_KNHA	activation energy factor KNHA for nitrification [J/mol]	-160,000
<b>Stoichiometric parameters</b>		
$f_{Hyd,Cl}$	production of Cl in hydrolysis	0
$f_{BM,CR}$	fraction of CR generated in biomass lysis	0.1
$f_{BM,Cl}$	fraction of Cl generated in biomass lysis	0.02
$Y_{Het}$	yield coefficient for XH	0.63
$Y_{Ans}$	yield coefficient for XANs	0.24
$Y_{ANb}$	yield coefficient for XANb	0.24
<b>Composition parameters</b>		
$i_{N,CR}$	N content of CR [g N/g COD <sub>CR</sub> ]	0.03
$i_{N,CS}$	N content of CS [g N/g COD <sub>CS</sub> ]	0.04
$i_{N,Cl}$	N content of Cl [g N/g COD <sub>Cl</sub> ]	0.01
$i_{N,BM}$	N content of biomass [g N/g COD <sub>BM</sub> ]	0.07
$i_{P,CR}$	P content of CR [g P/g COD <sub>CR</sub> ]	0.01
$i_{P,CS}$	P content of CS [g P/g COD <sub>CS</sub> ]	0.01
$i_{P,Cl}$	P content of Cl [g P/g COD <sub>Cl</sub> ]	0.01
$i_{P,BM}$	P content of biomass [g P/g COD <sub>BM</sub> ]	0.02
<b>Oxygen</b>		
cO2_sat_4.5	saturation concentration of oxygen at 4.5°C [g/m <sup>3</sup> ]	12.5
Tdep_cO2_sat	activation energy for saturation concentration of oxygen [J/mol]	-15,000
Rate_O2	Re-aeration rate [1/d]	2

### 3.5 Conclusions

#### 3.5.1 Summary of Findings

A deterministic mass balance model was developed to better understand the effects of sandy soil rooted vadose zones on nitrogen dynamics in a contained test cell system. The model was developed using HYDRUS modeling software and was calibrated with literature values and highly time resolved data and grab samples obtained from laboratory experiments. The model simulated tracer study breakthrough curves, ammonium, nitrate, pressure heads and water content, fast- and slow-degrading organic matter, bacterial concentrations for total heterotrophs, and nitrogen gas concentrations as with-root and no-root treatment systems. The model correlated well with the experimental tracer study measurements and predicted that effluent slowly degrading organics (organic-N) is larger in with-root systems than no-root systems, indicating more filtration effect occurring in the rooted system. The model also predicted that roots increased the dwell time of water in the vadose zone, increasing the reaction time for microorganisms, which in turn decreased the effluent concentrations of ammonium and nitrate.

#### 3.5.2 Implications for Port of Morrow

The Port of Morrow is currently in the process of installing 60 acres of hybrid poplar and there has been interest to investigate a larger, field-scale installation. Hydrolysis and denitrification rate coefficients estimated from this study and potential future results studies could be applied to the Port of Morrow to assist irrigation application strategies of the food-processing wastewater. Once calibrated with additional research, the Hydrus model could be applied to the larger-scale field site and used as a guide for year-round hybrid poplar nitrogen-rich wastewater treatment capabilities. The Hydrus model would simulate year round nutrient application while incorporating root uptake, evapotranspiration rates, and varying climatic conditions.

### *3.5.3 Future Research*

The results obtained from this study provide opportunities for several future research areas. This model could be used to simulate the effects of rooted poplar systems on nitrogen dynamics for various scenarios. For example, the model could be calibrated with a larger scale system with a deeper root zone and more representative of a realistic irrigation schedule. This model focused on an irrigation regime that occurred every 2 hours for a brief period of time. However, field site water application is typically more flexible, usually involving a long dosing period (several hours) less often (once or twice per week), depending on the season. Additional model scenarios could simulate year round nutrient application with the incorporation of root uptake, evapotranspiration rates, and varying climatic conditions.

## APPENDIX A: WATER CHEMISTRY DATA

### Peak Integration Report

Sample Name:	HT_N_1_2.17.14	Inj. Vol.:	100.00
Injection Type:	Unknown	Dilution Factor:	1.0000
Program:	Test	Operator:	IonSplitter
Inj. Date / Time:	18-Feb-2014 / 14:24	Run Time:	20.00

No.	Time min	Peak Name	Peak Type	Area $\mu\text{S}\cdot\text{min}$	Height $\mu\text{S}$	Amount mg-N/L
1	7.29	Nitrate	BMB*^	0.081	0.169	0.0455
TOTAL:				0.08	0.17	0.05

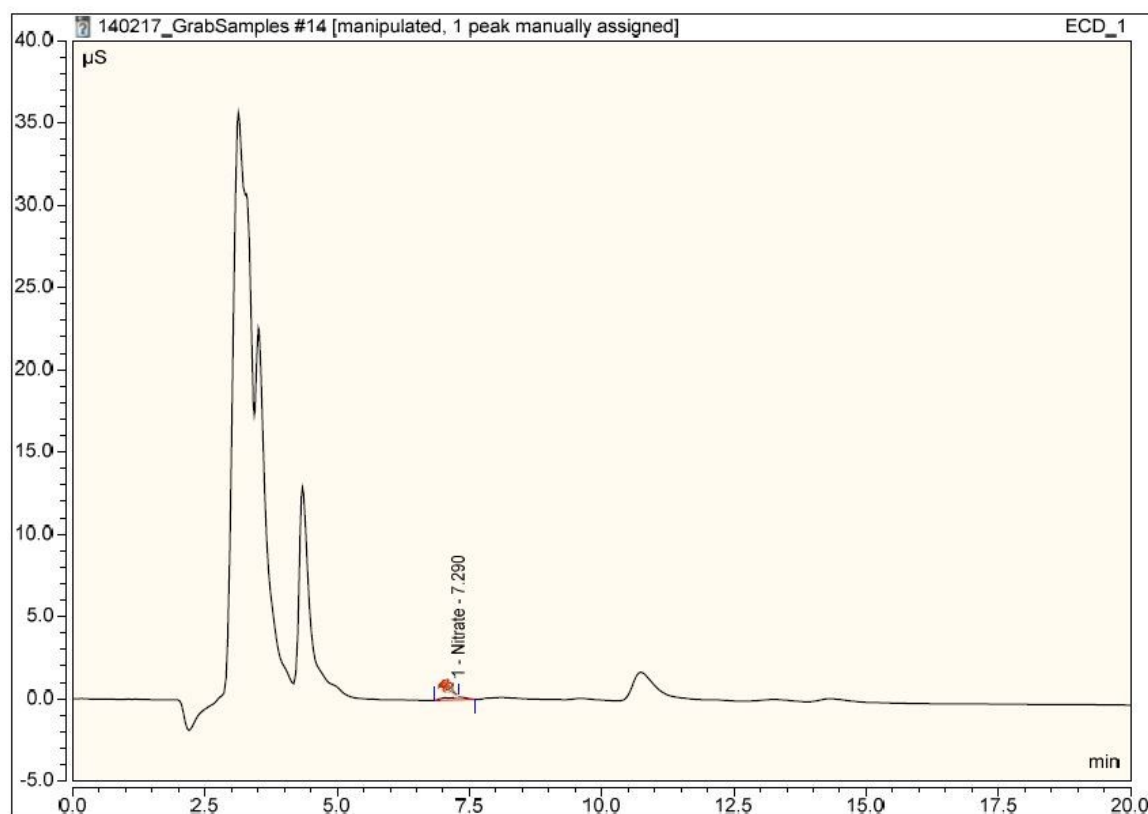


Figure A 1: Typical anion ion chromatography results for the north head tank

## Peak Integration Report

Sample Name:	CP_WT_N_1_2.17.14	Inj. Vol.:	100.00
Injection Type:	Unknown	Dilution Factor:	1.0000
Program:	Test	Operator:	IonSplitter
Inj. Date / Time:	18-Feb-2014 / 11:54	Run Time:	20.00

No.	Time min	Peak Name	Peak Type	Area $\mu\text{S} \cdot \text{min}$	Height $\mu\text{S}$	Amount mg-N/L
1	7.73	Nitrate	BMB^A	0.173	0.220	0.0980
TOTAL:				0.17	0.22	0.10

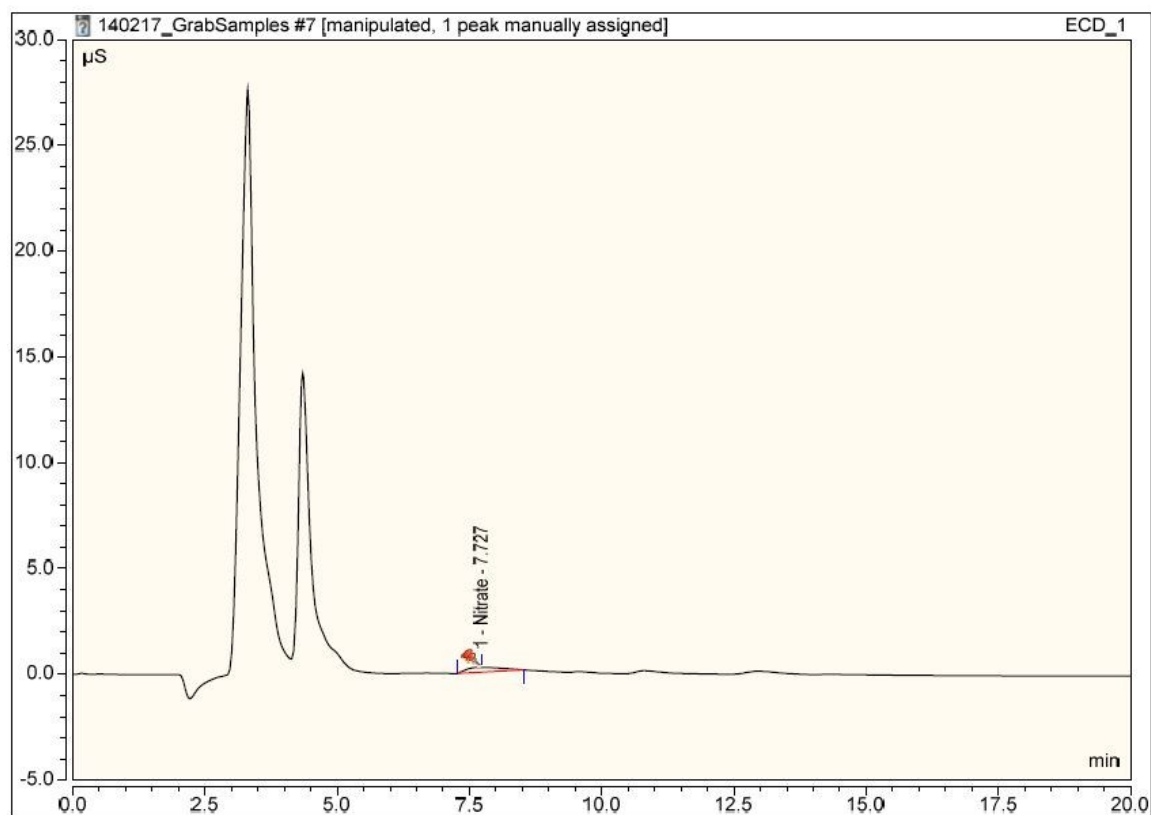


Figure A 2: Typical anion ion chromatography results for the north Cal PAM with tree test cell

## Peak Integration Report

Sample Name:	CP_WT_S_1_2.17.14	Inj. Vol.:	100.00
Injection Type:	Unknown	Dilution Factor:	1.0000
Program:	Test	Operator:	IonSplitter
Inj. Date / Time:	18-Feb-2014 / 11:32	Run Time:	20.00

No.	Time min	Peak Name	Peak Type	Area $\mu\text{S}\cdot\text{min}$	Height $\mu\text{S}$	Amount mg-N/L
1	5.19	Nitrite	BMB*	0.461	1.942	0.3315
2	7.19	Nitrate	BMB**	31.202	38.278	17.6325
TOTAL:				31.66	40.22	17.96

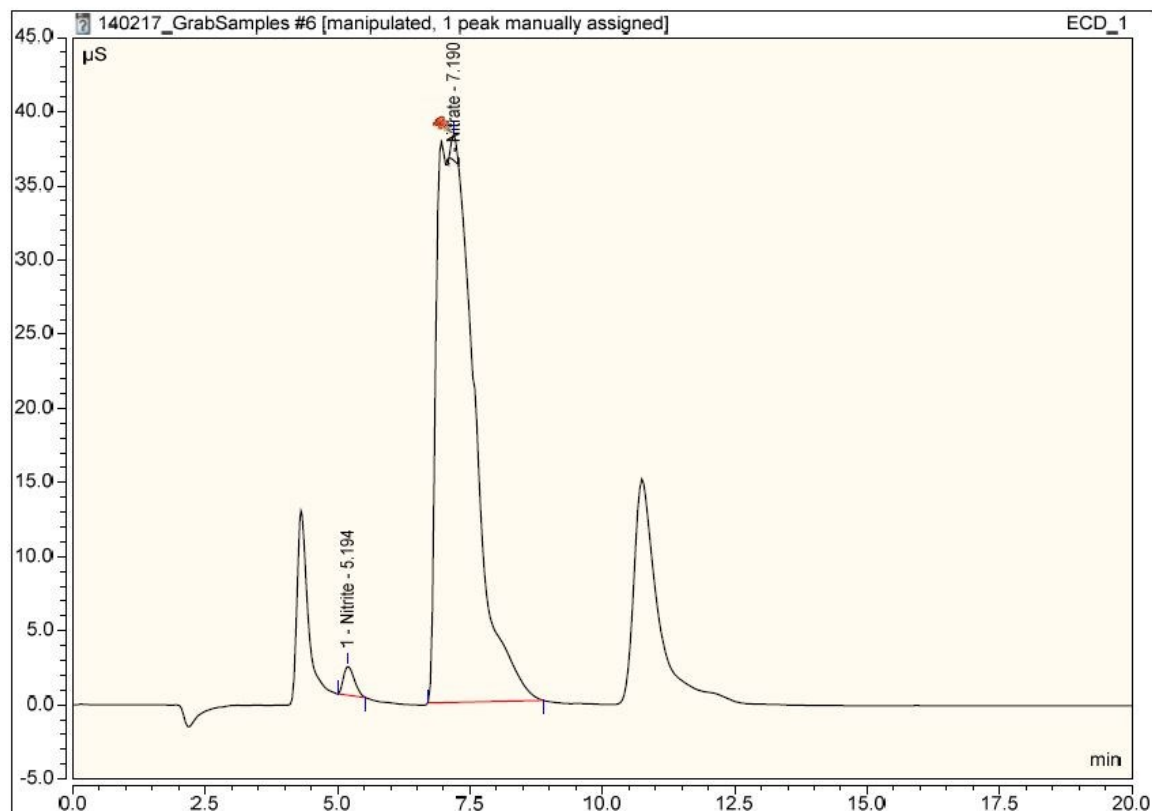


Figure A 3: Typical anion ion chromatography results for the south Cal PAM with tree test cell

## APPENDIX B:

## SOIL CHEMISTRY ANALYSIS

MVTTL		MINNESOTA VALLEY TESTING LABORATORIES, INC.					MEMBER ACIL	
SUBMITTED BY: 007430		DATE RECEIVED: Aug 9 2013			SUBMITTED FOR:			
JON DURST		DATE REPORTED: Aug 15 2013			AUGUST 2013			
UNIVERSITY OF IOWA		WORK ORDER NO: 201391-00194						
103 S. CAPITOL ST								
4105 SEAMANS CENTER								
IOWA CITY IA 52242								
SAMPLE ID PREV CROP LAB NUMBER		POM FROM BOX 13-M9321						
		V-LOW	LOW	OPT	HIGH	V-HIGH		
ORGANIC MATTER	0.5	■						
NITROGEN	17.9							
NO3-N ppm	17.9							
PHOSPHORUS								
P2O5-P Meh 3	63	■						
ppm								
POTASSIUM (K) Meh 3 ppm	128.	■						
ZINC (ppm)	0.6	■						
SULFUR ppm SO4-S	5.	■						
ACIDITY pH	7.1	B ppm	Fe ppm	Mn ppm	Cu ppm	Na ppm		
BUFFER INDEX	7.4	0.1 L	12.3 S	2.5 S	0.6 S	16		
CCE %		SALTS mmhos/cm 0.1		Cl lbs/A				
		% BASE SATURATION						
CALCIUM ppm	939	CEC	Ca	Mg	K	Na		H
MAGNESIUM ppm	201	6.7	69.7	24.4	4.9	1.0		0.0
		SAND % 92.5		SILT % 2.5	CLAY % 5.0			
		TEXTURE Sand						
ALL GUIDELINES ARE ON A BROADCAST BASIS								
CROP FERTILIZER GUIDELINES								
CROP AND YIELD GOAL	CORN/BEANS 180/60 BU							
NITROGEN (lbs/A)	216							
P2O5 (lbs/A) ISU	0							
K2O (lbs/A) ISU	152							
ZINC (lbs/A)	5							
SULFUR (lbs/A)	30							
LIME NEEDS AS	to pH 6.5 No lime required.							
100% ENP (lbs/A)	to pH 6.9 No lime required.							

Figure B 1: Soil analysis results with sample taken from the Port of Morrow test cell



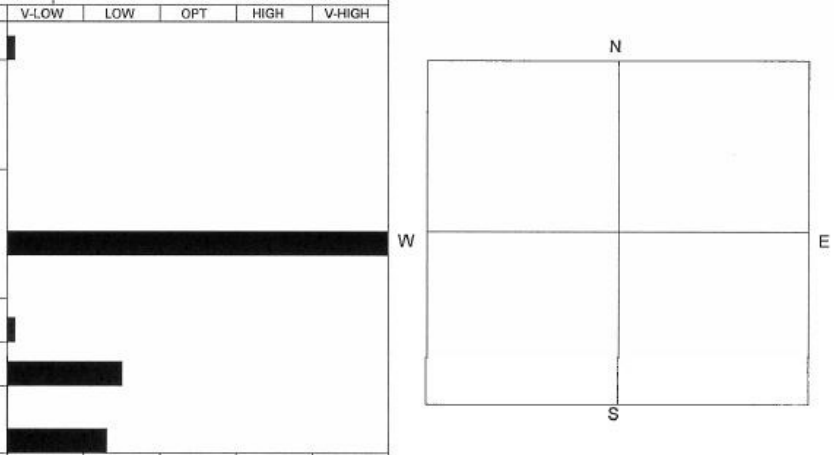
 <b>MINNESOTA VALLEY TESTING LABORATORIES, INC.</b> 1126 North Front St. ~ New Ulm, MN 56073 ~ 800-782-3557 ~ Fax 507-359-2890 2616 East Broadway Ave. ~ Bismarck, ND 58501 ~ 800-279-6885 ~ Fax 701-258-9724 1201 Lincoln Hwy. ~ Nevada, IA 50201 ~ 800-362-0855 ~ Fax 515-382-3885 www.mvtl.com					
<b>SUBMITTED BY:</b> 007430 JON DURST UNIVERSITY OF IOWA 103 S. CAPITOL ST 4105 SEAMANS CENTER IOWA CITY IA 52242		<b>DATE RECEIVED:</b> Aug 2 2013 <b>DATE REPORTED:</b> Aug 8 2013 <b>WORK ORDER NO:</b> 201391-00188		<b>SUBMITTED FOR:</b> CALAMUS SOIL	
<b>SAMPLE ID</b> <b>PREV CROP</b> <b>LAB NUMBER</b>		JULY 2013 13-M9302			
<b>ORGANIC MATTER</b> 0.3		V-LOW LOW OPT HIGH V-HIGH			
<b>NITROGEN</b> 0.5					
<b>NO3-N</b> ppm 0.5					
<b>PHOSPHORUS</b>					
<b>P2O5-P</b> Meh 3 59 ppm					
<b>POTASSIUM (K)</b> Meh 3 ppm 18.					
<b>ZINC (ppm)</b> 0.4					
<b>SULFUR</b> ppm SO4-S 5.					
<b>ACIDITY</b> pH 6.8		B ppm Fe ppm Mn ppm Cu ppm Na ppm			
<b>BUFFER INDEX</b> 7.4		0.0 L 9.1 S 1.3 S 0.3 S 7			
<b>CCE %</b>		SALTS mmhos/cm 0.1 Cl lbs/A			
<b>CALCIUM</b> ppm 248		CEC % BASE SATURATION			
<b>MAGNESIUM</b> ppm 65		Ca Mg K Na H			
		1.8 67.0 28.8 2.5 1.6 0.0			
		SAND % 97.5 SILT % 0.0 CLAY % 2.5			
		TEXTURE Sand			
<small>ALL GUIDELINES ARE ON A BROADCAST BASIS</small>		<b>CROP FERTILIZER GUIDELINES</b>			
<b>CROP AND YIELD GOAL</b>					
<b>NITROGEN (lbs/A)</b>					
<b>P2O5 (lbs/A) ISU</b>					
<b>K2O (lbs/A) ISU</b>					
<b>ZINC (lbs/A)</b>					
<b>SULFUR (lbs/A)</b>					
<b>LIME NEEDS AS</b>		to pH 6.5 No lime required.			
<b>100% ENP (lbs/A)</b>		to pH 6.9 No lime required.			

Figure B 2: Soil analysis results taken from the Calamus field site. This soil was used for all “Cal” test cells.



## APPENDIX C: ORGANIC NITROGEN ANALYSIS

Day	TOTAL MASS NITROGEN APPLIED (mg)									
	HT POM no tree	HT POM with tree	HT CWTN	HT CWTS	HT CPWTN	HT CPWTS	HT CPNTN	HT CPNTS	HT CNTN	HT CNTS
1	128.64	99.48	92.21	115.30	107.68	96.36	111.11	135.91	101.38	98.03
2	257.28	198.96	184.43	230.60	215.35	192.72	222.23	271.82	202.75	196.06
3	385.92	298.44	276.64	345.90	323.03	289.08	333.34	407.72	304.13	294.10
4	514.56	397.92	368.85	461.20	430.71	385.44	444.45	543.63	405.51	392.13
5	643.20	497.40	461.06	576.50	538.39	481.81	555.57	679.54	506.88	490.16
6	771.84	596.88	553.28	691.79	646.06	578.17	666.68	815.45	608.26	588.19
7	900.48	696.36	645.49	807.09	753.74	674.53	777.79	951.36	709.64	686.22
8	1029.12	795.84	737.70	922.39	861.42	770.89	888.91	1087.26	811.01	784.26
9	1157.76	895.32	829.91	1037.69	969.09	867.25	1000.02	1223.17	912.39	882.29
10	1286.40	994.80	922.13	1152.99	1076.77	963.61	1111.14	1359.08	1013.77	980.32
11	1415.04	1094.28	1014.34	1268.29	1184.45	1059.97	1222.25	1494.99	1115.14	1078.35
12	1543.68	1193.76	1106.55	1383.59	1292.12	1156.33	1333.36	1630.90	1216.52	1176.38
13	1672.32	1293.24	1198.77	1498.89	1399.80	1252.69	1444.48	1766.80	1317.90	1274.42
14	1800.96	1392.72	1290.98	1614.19	1507.48	1349.05	1555.59	1902.71	1419.27	1372.45
15	1929.59	1492.20	1383.19	1729.49	1615.16	1445.42	1666.70	2038.62	1520.65	1470.48
16	2058.23	1591.68	1475.40	1844.78	1722.83	1541.78	1777.82	2174.53	1622.03	1568.51
17	2186.87	1691.16	1567.62	1960.08	1830.51	1638.14	1888.93	2310.44	1723.40	1666.54
18	2315.51	1790.64	1659.83	2075.38	1938.19	1734.50	2000.04	2446.34	1824.78	1764.58
19	2444.15	1890.12	1752.04	2190.68	2045.86	1830.86	2111.16	2582.25	1926.16	1862.61
20	2572.79	1989.60	1844.26	2305.98	2153.54	1927.22	2222.27	2718.16	2027.54	1960.64
21	2701.43	2089.08	1936.47	2421.28	2261.22	2023.58	2333.38	2854.07	2128.91	2058.67
22	2830.07	2188.56	2028.68	2536.58	2368.89	2119.94	2444.50	2989.98	2230.29	2156.70
23	2958.71	2288.04	2120.89	2651.88	2476.57	2216.30	2555.61	3125.88	2331.67	2254.74
24	3087.35	2387.52	2213.11	2767.18	2584.25	2312.66	2666.72	3261.79	2433.04	2352.77
25	3215.99	2487.01	2305.32	2882.48	2691.93	2409.03	2777.84	3397.70	2534.42	2450.80
26	3344.63	2586.49	2397.53	2997.77	2799.60	2505.39	2888.95	3533.61	2635.80	2548.83
27	3473.27	2685.97	2489.74	3113.07	2907.28	2601.75	3000.06	3669.52	2737.17	2646.86
28	3601.91	2785.45	2581.96	3228.37	3014.96	2698.11	3111.18	3805.42	2838.55	2744.90
29	3730.55	2884.93	2674.17	3343.67	3122.63	2794.47	3222.29	3941.33	2939.93	2842.93
30	3859.19	2984.41	2766.38	3458.97	3230.31	2890.83	3333.41	4077.24	3041.30	2940.96
31	3987.83	3083.89	2858.60	3574.27	3337.99	2987.19	3444.52	4213.15	3142.68	3038.99
32	4116.47	3183.37	2950.81	3689.57	3445.66	3083.55	3555.63	4349.06	3244.06	3137.02
33	4245.11	3282.85	3043.02	3804.87	3553.34	3179.91	3666.75	4484.96	3345.43	3235.06
34	4373.75	3382.33	3135.23	3920.17	3661.02	3276.27	3777.86	4620.87	3446.81	3333.09
35	4502.39	3481.81	3227.45	4035.47	3768.70	3372.64	3888.97	4756.78	3548.19	3431.12
36	4631.03	3581.29	3319.66	4150.76	3876.37	3469.00	4000.09	4892.69	3649.56	3529.15
37	4759.67	3680.77	3411.87	4266.06	3984.05	3565.36	4111.20	5028.60	3750.94	3627.18
38	4888.31	3780.25	3504.08	4381.36	4091.73	3661.72	4222.31	5164.50	3852.32	3725.22
39	5016.95	3879.73	3596.30	4496.66	4199.40	3758.08	4333.43	5300.41	3953.69	3823.25
40	5145.59	3979.21	3688.51	4611.96	4307.08	3854.44	4444.54	5436.32	4055.07	3921.28
41	5274.23	4078.69	3780.72	4727.26	4414.76	3950.80	4555.65	5572.23	4156.45	4019.31
42	5402.87	4178.17	3872.94	4842.56	4522.43	4047.16	4666.77	5708.14	4257.82	4117.34
43	5531.50	4277.65	3965.15	4957.86	4630.11	4143.52	4777.88	5844.04	4359.20	4215.38
44	5660.14	4377.13	4057.36	5073.16	4737.79	4239.88	4888.99	5979.95	4460.58	4313.41
45	5788.78	4476.61	4149.57	5188.46	4845.47	4336.25	5000.11	6115.86	4561.95	4411.44
46	5917.42	4576.09	4241.79	5303.75	4953.14	4432.61	5111.22	6251.77	4663.33	4509.47
47	6046.06	4675.57	4334.00	5419.05	5060.82	4528.97	5222.33	6387.68	4764.71	4607.50
48	6174.70	4775.05	4426.21	5534.35	5168.50	4625.33	5333.45	6523.58	4866.08	4705.54
49	6303.34	4874.53	4518.42	5649.65	5276.17	4721.69	5444.56	6659.49	4967.46	4803.57
50	6431.98	4974.01	4610.64	5764.95	5383.85	4818.05	5555.68	6795.40	5068.84	4901.60
51	6560.62	5073.49	4702.85	5880.25	5491.53	4914.41	5666.79	6931.31	5170.21	4999.63
52	6689.26	5172.97	4795.06	5995.55	5599.20	5010.77	5777.90	7067.22	5271.59	5097.66
53	6817.90	5272.45	4887.28	6110.85	5706.88	5107.13	5889.02	7203.12	5372.97	5195.70
54	6946.54	5371.93	4979.49	6226.15	5814.56	5203.49	6000.13	7339.03	5474.34	5293.73
55	7075.18	5471.41	5071.70	6341.45	5922.24	5299.86	6111.24	7474.94	5575.72	5391.76
56	7203.82	5570.89	5163.91	6456.74	6029.91	5396.22	6222.36	7610.85	5677.10	5489.79
57	7332.46	5670.37	5256.13	6572.04	6137.59	5492.58	6333.47	7746.76	5778.47	5587.82
58	7461.10	5769.85	5348.34	6687.34	6245.27	5588.94	6444.58	7882.66	5879.85	5685.86
59	7589.74	5869.33	5440.55	6802.64	6352.94	5685.30	6555.70	8018.57	5981.23	5783.89
60	7718.38	5968.81	5532.77	6917.94	6460.62	5781.66	6666.81	8154.48	6082.61	5881.92
61	7847.02	6068.29	5624.98	7033.24	6568.30	5878.02	6777.92	8290.39	6183.98	5979.95
62	7975.66	6167.77	5717.19	7148.54	6675.97	5974.38	6889.04	8426.30	6285.36	6077.98
63	8104.30	6267.25	5809.40	7263.84	6783.65	6070.74	7000.15	8562.20	6386.74	6176.02
64	8232.94	6366.73	5901.62	7379.14	6891.33	6167.10	7111.26	8698.11	6488.11	6274.05
65	8361.58	6466.21	5993.83	7494.44	6999.00	6263.47	7222.38	8834.02	6589.49	6372.08
66	8490.22	6565.69	6086.04	7609.73	7106.68	6359.83	7333.49	8969.93	6690.87	6470.11
67	8618.86	6665.17	6178.25	7725.03	7214.36	6456.19	7444.60	9105.84	6792.24	6568.14
68	8747.50	6764.65	6270.47	7840.33	7322.04	6552.55	7555.72	9241.74	6893.62	6666.18
69	8876.14	6864.13	6362.68	7955.63	7429.71	6648.91	7666.83	9377.65	6995.00	6764.21
70	9004.78	6963.61	6454.89	8070.93	7537.39	6745.27	7777.95	9513.56	7096.37	6862.24
71	9133.42	7063.09	6547.11	8186.23	7645.07	6841.63	7889.06	9649.47	7197.75	6960.27
72	9262.05	7162.57	6639.32	8301.53	7752.74	6937.99	8000.17	9785.38	7299.13	7058.30
73	9390.69	7262.05	6731.53	8416.83	7860.42	7034.35	8111.29	9921.28	7400.50	7156.34
74	9519.33	7361.53	6823.74	8532.13	7968.10	7130.71	8222.40	10057.19	7501.88	7254.37
75	9647.97	7461.02	6915.96	8647.43	8075.77	7227.07	8333.51	10193.10	7603.26	7352.40
76	9776.61	7560.50	7008.17	8762.72	8183.45	7323.44	8444.63	10329.01	7704.63	7450.43
77	9905.25	7659.98	7100.38	8878.02	8291.13	7419.80	8555.74	10464.92	7806.01	7548.46
78	10033.89	7759.46	7192.59	8993.32	8398.81	7516.16	8666.85	10600.82	7907.39	7646.50

Figure C 1: Cumulative mass of nitrogen applied per day of experimentation

Day	TOTAL MASS ORGANIC NITROGEN APPLIED (grams)									
	POM no tree	POM with tree	Cal w/ tree north	Cal w/ tree south	Cal PAM w/ tree north	Cal PAM w/ tree south	Cal PAM no tree north	Cal PAM no tree south	Cal no tree north	Cal no tree south
1	0.07	0.05	0.05	0.06	0.06	0.05	0.06	0.07	0.06	0.05
2	0.14	0.11	0.10	0.13	0.12	0.11	0.12	0.15	0.11	0.11
3	0.21	0.16	0.15	0.19	0.18	0.16	0.18	0.22	0.17	0.16
4	0.28	0.22	0.20	0.25	0.23	0.21	0.24	0.30	0.22	0.22
5	0.35	0.27	0.25	0.32	0.29	0.26	0.30	0.37	0.28	0.27
6	0.42	0.33	0.30	0.38	0.35	0.32	0.36	0.45	0.33	0.32
7	0.49	0.38	0.35	0.44	0.41	0.37	0.42	0.52	0.39	0.38
8	0.56	0.44	0.40	0.51	0.47	0.42	0.48	0.60	0.44	0.43
9	0.63	0.49	0.45	0.57	0.53	0.48	0.54	0.67	0.50	0.48
10	0.70	0.55	0.50	0.63	0.59	0.53	0.60	0.75	0.55	0.54
11	0.77	0.60	0.55	0.70	0.64	0.58	0.66	0.82	0.61	0.59
12	0.84	0.65	0.60	0.76	0.70	0.63	0.73	0.89	0.66	0.65
13	0.91	0.71	0.65	0.82	0.76	0.69	0.79	0.97	0.72	0.70
14	0.98	0.76	0.70	0.89	0.82	0.74	0.85	1.04	0.77	0.75
15	1.05	0.82	0.75	0.95	0.88	0.79	0.91	1.12	0.83	0.81
16	1.12	0.87	0.80	1.01	0.94	0.85	0.97	1.19	0.88	0.86
17	1.19	0.93	0.85	1.08	1.00	0.90	1.03	1.27	0.94	0.91
18	1.26	0.98	0.90	1.14	1.05	0.95	1.09	1.34	0.99	0.97
19	1.33	1.04	0.95	1.20	1.11	1.00	1.15	1.42	1.05	1.02
20	1.40	1.09	1.00	1.27	1.17	1.06	1.21	1.49	1.10	1.08
21	1.47	1.15	1.05	1.33	1.23	1.11	1.27	1.57	1.16	1.13
22	1.54	1.20	1.10	1.39	1.29	1.16	1.33	1.64	1.21	1.18
23	1.61	1.26	1.15	1.45	1.35	1.22	1.39	1.71	1.27	1.24
24	1.68	1.31	1.20	1.52	1.41	1.27	1.45	1.79	1.32	1.29
25	1.75	1.36	1.25	1.58	1.46	1.32	1.51	1.86	1.38	1.34
26	1.82	1.42	1.30	1.64	1.52	1.37	1.57	1.94	1.43	1.40
27	1.89	1.47	1.35	1.71	1.58	1.43	1.63	2.01	1.49	1.45
28	1.96	1.53	1.40	1.77	1.64	1.48	1.69	2.09	1.54	1.51
29	2.03	1.58	1.45	1.83	1.70	1.53	1.75	2.16	1.60	1.56
30	2.10	1.64	1.50	1.90	1.76	1.59	1.81	2.24	1.65	1.61
31	2.17	1.69	1.55	1.96	1.82	1.64	1.87	2.31	1.71	1.67
32	2.24	1.75	1.60	2.02	1.87	1.69	1.93	2.39	1.76	1.72
33	2.31	1.80	1.65	2.09	1.93	1.74	1.99	2.46	1.82	1.77
34	2.38	1.86	1.70	2.15	1.99	1.80	2.05	2.53	1.87	1.83
35	2.45	1.91	1.75	2.21	2.05	1.85	2.11	2.61	1.93	1.88
36	2.52	1.96	1.81	2.28	2.11	1.90	2.18	2.68	1.98	1.94
37	2.59	2.02	1.86	2.34	2.17	1.96	2.24	2.76	2.04	1.99
38	2.66	2.07	1.91	2.40	2.22	2.01	2.30	2.83	2.09	2.04
39	2.73	2.13	1.96	2.47	2.28	2.06	2.36	2.91	2.15	2.10
40	2.80	2.18	2.01	2.53	2.34	2.11	2.42	2.98	2.20	2.15
41	2.87	2.24	2.06	2.59	2.40	2.17	2.48	3.06	2.26	2.20
42	2.94	2.29	2.11	2.66	2.46	2.22	2.54	3.13	2.32	2.26
43	3.01	2.35	2.16	2.72	2.52	2.27	2.60	3.21	2.37	2.31
44	3.08	2.40	2.21	2.78	2.58	2.33	2.66	3.28	2.43	2.37
45	3.15	2.46	2.26	2.85	2.63	2.38	2.72	3.36	2.48	2.42
46	3.22	2.51	2.31	2.91	2.69	2.43	2.78	3.43	2.54	2.47
47	3.29	2.56	2.36	2.97	2.75	2.48	2.84	3.50	2.59	2.53
48	3.36	2.62	2.41	3.04	2.81	2.54	2.90	3.58	2.65	2.58
49	3.43	2.67	2.46	3.10	2.87	2.59	2.96	3.65	2.70	2.64
50	3.50	2.73	2.51	3.16	2.93	2.64	3.02	3.73	2.76	2.69
51	3.57	2.78	2.56	3.23	2.99	2.70	3.08	3.80	2.81	2.74
52	3.64	2.84	2.61	3.29	3.04	2.75	3.14	3.88	2.87	2.80
53	3.71	2.89	2.66	3.35	3.10	2.80	3.20	3.95	2.92	2.85
54	3.78	2.95	2.71	3.42	3.16	2.85	3.26	4.03	2.98	2.90
55	3.85	3.00	2.76	3.48	3.22	2.91	3.32	4.10	3.03	2.96
56	3.92	3.06	2.81	3.54	3.28	2.96	3.38	4.18	3.09	3.01
57	3.99	3.11	2.86	3.61	3.34	3.01	3.44	4.25	3.14	3.07
58	4.06	3.17	2.91	3.67	3.40	3.07	3.50	4.32	3.20	3.12
59	4.13	3.22	2.96	3.73	3.45	3.12	3.56	4.40	3.25	3.17
60	4.20	3.27	3.01	3.80	3.51	3.17	3.63	4.47	3.31	3.23
61	4.27	3.33	3.06	3.86	3.57	3.22	3.69	4.55	3.36	3.28
62	4.34	3.38	3.11	3.92	3.63	3.28	3.75	4.62	3.42	3.33
63	4.41	3.44	3.16	3.98	3.69	3.33	3.81	4.70	3.47	3.39
64	4.48	3.49	3.21	4.05	3.75	3.38	3.87	4.77	3.53	3.44
65	4.55	3.55	3.26	4.11	3.81	3.44	3.93	4.85	3.58	3.50
66	4.62	3.60	3.31	4.17	3.86	3.49	3.99	4.92	3.64	3.55
67	4.69	3.66	3.36	4.24	3.92	3.54	4.05	5.00	3.69	3.60
68	4.76	3.71	3.41	4.30	3.98	3.59	4.11	5.07	3.75	3.66
69	4.83	3.77	3.46	4.36	4.04	3.65	4.17	5.14	3.80	3.71
70	4.90	3.82	3.51	4.43	4.10	3.70	4.23	5.22	3.86	3.76
71	4.97	3.87	3.56	4.49	4.16	3.75	4.29	5.29	3.91	3.82
72	5.04	3.93	3.61	4.55	4.22	3.81	4.35	5.37	3.97	3.87
73	5.11	3.98	3.66	4.62	4.27	3.86	4.41	5.44	4.02	3.93
74	5.18	4.04	3.71	4.68	4.33	3.91	4.47	5.52	4.08	3.98
75	5.25	4.09	3.76	4.74	4.39	3.96	4.53	5.59	4.13	4.03
76	5.32	4.15	3.81	4.81	4.45	4.02	4.59	5.67	4.19	4.09
77	5.39	4.20	3.86	4.87	4.51	4.07	4.65	5.74	4.24	4.14
78	5.46	4.26	3.91	4.93	4.57	4.12	4.71	5.82	4.30	4.19

Figure C 2: Cumulative mass of organic-nitrogen applied per day of experimentation

	Day	TOTAL MASS NITROGEN IN EFFLUENT (mg)									
		POM no tree	POM with tree	CWTN	CWTS	CPWT N	CPWTS	CPNT N	CPNT S	CNT N	CNT S
Dosed synthetic WW onto test cells for 60 days prior to any grab sample analysis, which began on Feb 4. Results here are inferred from slope of TN trendline	1	0.00	0.00	0.00	0.00	0.00	0.00	0.00	0.00	0.00	0.00
	2	0.00	0.00	0.00	0.00	0.00	0.00	0.00	0.00	0.00	0.00
	3	0.00	0.00	0.00	0.00	0.00	0.00	0.00	0.00	0.00	0.00
	4	0.00	0.00	0.00	0.00	0.00	0.00	0.00	0.00	0.00	0.00
	5	0.00	0.00	0.00	0.00	0.00	0.00	0.00	0.00	0.00	0.00
	6	0.00	0.00	0.00	0.00	0.00	0.00	0.00	0.00	0.00	0.00
	7	0.00	0.00	0.00	0.00	0.00	0.00	0.00	0.00	0.00	0.00
	8	2.38	1.31	2.31	2.81	1.36	0.13	2.61	2.75	2.84	0.73
	9	4.77	2.61	4.61	5.63	2.71	0.27	5.22	5.51	5.68	1.46
	10	7.15	3.92	6.92	8.44	4.07	0.40	7.82	8.26	8.53	2.19
	11	9.54	5.22	9.23	11.26	5.42	0.53	10.43	11.02	11.37	2.92
	12	11.92	6.53	11.53	14.07	6.78	0.67	13.04	13.77	14.21	3.66
	13	14.31	7.83	13.84	16.89	8.13	0.80	15.65	16.53	17.05	4.39
	14	16.69	9.14	16.15	19.70	9.49	0.94	18.25	19.28	19.90	5.12
	15	19.07	10.44	18.45	22.52	10.85	1.07	20.86	22.04	22.74	5.85
	16	21.46	11.75	20.76	25.33	12.20	1.20	23.47	24.79	25.58	6.58
	17	23.84	13.05	23.07	28.14	13.56	1.34	26.08	27.54	28.42	7.31
	18	26.23	14.36	25.37	30.96	14.91	1.47	28.69	30.30	31.26	8.04
	19	28.61	15.66	27.68	33.77	16.27	1.60	31.29	33.05	34.11	8.77
	20	30.99	16.97	29.99	36.59	17.63	1.74	33.90	35.81	36.95	9.50
	21	33.38	18.27	32.29	39.40	18.98	1.87	36.51	38.56	39.79	10.24
	22	35.76	19.58	34.60	42.22	20.34	2.01	39.12	41.32	42.63	10.97
	23	38.15	20.88	36.91	45.03	21.69	2.14	41.72	44.07	45.48	11.70
	24	40.53	22.19	39.21	47.84	23.05	2.27	44.33	46.82	48.32	12.43
	25	42.92	23.49	41.52	50.66	24.40	2.41	46.94	49.58	51.16	13.16
	26	45.30	24.80	43.83	53.47	25.76	2.54	49.55	52.33	54.00	13.89
	27	47.68	26.10	46.13	56.29	27.12	2.67	52.16	55.09	56.84	14.62
	28	50.07	27.41	48.44	59.10	28.47	2.81	54.76	57.84	59.69	15.35
	29	52.45	28.71	50.75	61.92	29.83	2.94	57.37	60.60	62.53	16.08
	30	54.84	30.02	53.05	64.73	31.18	3.08	59.98	63.35	65.37	16.81
	31	57.22	31.32	55.36	67.55	32.54	3.21	62.59	66.11	68.21	17.55
	32	59.61	32.63	57.67	70.36	33.89	3.34	65.20	68.86	71.06	18.28
	33	61.99	33.93	59.97	73.17	35.25	3.48	67.80	71.61	73.90	19.01
	34	64.37	35.24	62.28	75.99	36.61	3.61	70.41	74.37	76.74	19.74
	35	66.76	36.54	64.59	78.80	37.96	3.74	73.02	77.12	79.58	20.47
	36	69.14	37.85	66.89	81.62	39.32	3.88	75.63	79.88	82.42	21.20
	37	71.53	39.15	69.20	84.43	40.67	4.01	78.23	82.63	85.27	21.93
	38	73.91	40.46	71.51	87.25	42.03	4.15	80.84	85.39	88.11	22.66
	39	76.29	41.76	73.81	90.06	43.38	4.28	83.45	88.14	90.95	23.39
	40	78.68	43.07	76.12	92.88	44.74	4.41	86.06	90.89	93.79	24.13
	41	81.06	44.38	78.43	95.69	46.10	4.55	88.67	93.65	96.64	24.86
	42	83.45	45.68	80.73	98.50	47.45	4.68	91.27	96.40	99.48	25.59
	43	85.83	46.99	83.04	101.32	48.81	4.81	93.88	99.16	102.32	26.32
	44	88.22	48.29	85.35	104.13	50.16	4.95	96.49	101.91	105.16	27.05
	45	90.60	49.60	87.65	106.95	51.52	5.08	99.10	104.67	108.00	27.78
	46	92.98	50.90	89.96	109.76	52.88	5.22	101.70	107.42	110.85	28.51
	47	95.37	52.21	92.27	112.58	54.23	5.35	104.31	110.18	113.69	29.24
	48	97.75	53.51	94.57	115.39	55.59	5.48	106.92	112.93	116.53	29.97
	49	100.14	54.82	96.88	118.20	56.94	5.62	109.53	115.68	119.37	30.71
	50	102.52	56.12	99.19	121.02	58.30	5.75	112.14	118.44	122.22	31.44
	51	104.91	57.43	101.49	123.83	59.65	5.88	114.74	121.19	125.06	32.17
	52	107.29	58.73	103.80	126.65	61.01	6.02	117.35	123.95	127.90	32.90
	53	109.67	60.04	106.11	129.46	62.37	6.15	119.96	126.70	130.74	33.63
	54	112.06	61.34	108.41	132.28	63.72	6.29	122.57	129.46	133.58	34.36
	55	114.44	62.65	110.72	135.09	65.08	6.42	125.17	132.21	136.43	35.09
	56	116.83	63.95	113.03	137.91	66.43	6.55	127.78	134.96	139.27	35.82
	57	119.21	65.26	115.33	140.72	67.79	6.69	130.39	137.72	142.11	36.55
	58	121.59	66.56	117.64	143.53	69.14	6.82	133.00	140.47	144.95	37.28
	59	123.98	67.87	119.95	146.35	70.50	6.95	135.61	143.23	147.80	38.02
	60	126.36	69.17	122.25	149.16	71.86	7.09	138.21	145.98	150.64	38.75
These cells account for the mass of TN applied per day during grab sample analysis	61	123.98	67.87	119.95	146.35	70.50	6.95	135.61	143.23	147.80	38.02
	62	128.25	64.56	91.53	144.28	78.30	8.77	135.02	143.72	144.43	40.66
	63	132.18	74.65	93.86	146.97	82.25	10.97	130.08	147.25	144.17	48.75
	64	127.12	78.76	93.86	145.73	81.78	12.85	126.68	145.42	137.53	49.46
	65	130.16	80.43	102.58	149.63	81.47	15.89	128.23	153.15	145.08	53.74
	66	133.19	82.10	111.30	153.53	81.15	18.93	129.79	160.88	152.63	58.02
	67	136.22	83.76	120.03	157.42	80.84	21.97	131.34	168.60	160.19	62.30
	68	131.62	86.53	121.64	158.36	79.62	23.87	129.40	165.92	159.92	64.77
	69	133.64	86.62	126.87	161.46	79.52	25.60	132.31	172.02	161.78	66.35
	70	144.42	95.91	133.95	172.43	84.98	32.70	133.28	182.02	160.89	74.98
	71	143.70	95.84	136.21	171.52	83.92	36.81	130.45	181.63	161.39	80.29
	72	142.98	95.77	138.46	170.61	82.87	40.93	127.61	181.24	161.88	85.61
	73	142.26	95.69	140.71	169.70	81.82	45.05	124.78	180.85	162.38	90.92
	74	141.54	95.62	142.97	168.79	80.76	49.17	121.95	180.46	162.88	96.24
	75	140.82	95.55	145.22	167.88	79.71	53.28	119.12	180.07	163.37	101.55
	76	132.21	99.00	137.06	170.43	79.09	57.96	115.69	173.81	159.60	103.90
	77	123.60	102.46	128.91	172.98	78.46	58.30	112.26	167.55	155.82	106.25
	78	115.00	105.91	120.75	175.54	77.83	58.65	108.83	161.28	152.04	108.59
SUM		5814.70	3454.71	5506.66	6931.00	3384.98	770.05	6004.19	6930.65	6860.97	2376.56

Figure C 3: Cumulative mass of effluent nitrogen for each test cell

## BIBLIOGRAPHY

1. Allen, Simon J., Robin L. Hall, and Paul T. Rosier. 1999. "Transpiration by Two Poplar Varieties Grown as Coppice for Biomass Production." *Tree Physiology* 19: 493-501.
2. Almasri, Mohammad N. 2007. "Nitrate Contamination of Groundwater: A Conceptual Management Framework." *Environmental Impact Assessment Review* 27 (3): 220-242.
3. Aranibar, J. N., L. Otter, S. A. Mako, C. J. W. Feral, H. E. Epstein, P. R. Dowty, F. Echardt, H. H. Shugart, and R. J. Swap. 2004. "Nitrogen Cycling in the Soil-Plant System Along a Precipitation Gradient in the Kalahari Sands." *Global Change Biology* 10: 359-373.
4. Aronsson, P. G. and L. F. Bergström. 2001. "Nitrate Leaching from Lysimeter-Grown Short-Rotation Willow Coppice in Relation to N-Application, Irrigation and Soil Type." *Biomass and Bioenergy* 21 (3): 155-164.
5. Attard, E., S. Recous, A. Chabbi, C. De Berranger, N. Guillaumaud, J. Labreuche, L. Philippot, B. Schmid, and X. Le Roux. 2011. "Soil Environmental Conditions rather than Denitrifier Abundance and Diversity Drive Potential Denitrification After Changes in Land Uses." *Global Change Biology* 17: 1975-1989.
6. Bachand, Philip A. M. and Alexander J. Horne. 1999. "Denitrification in Constructed Free-Water Surface Wetlands: II. Effects of Vegetation and Temperature." *Ecological Engineering* 14 (1-2): 17-32.
7. Bedard-Haughn, A., K. W. Tate, and C van Kessel. 2005. "Quantifying the Impact of Regular Cutting on Vegetative Buffer Efficacy for Nitrogen-15 Sequestration." *Journal of Environmental Quality* 34 (5): 1651-64.
8. Braker, Gesche, Julia Schwarz, and Ralf Conrad. 2010. "Influence of Temperature on the Composition and Activity of Denitrifying Soil Communities." *Federation of European Microbiological Societies* 73: 134-148.
9. Bundy, L. G., T. W. Andraski, and W. L. Bland. 1997. "Nitrogen Cycling in Crop Residues and Cover Crops." *Proceedings of Wisconsin Annual Potato Meetings* 10: 53-61.
10. CFR (Code of Federal Regulations). 2012. "Title 40 - Protection of Environment, Parts 136-149. US Government Printing Office, Washington, DC." .
11. Chávez, A., K. Rodas, B. Prado, R. Thompson, and B. Jiménez. 2012. "An Evaluation of the Effects of Changing Wastewater Irrigation Regime for the Production of Alfalfa (*Medicago Sativa*)." *Agricultural Water Management* 113 (0): 76-84.

12. Chen, Peizhen, Ji Li, Qing X. Li, Yingchun Wang, Shaopeng Li, Tianzhi Ren, and Ligang Wang. 2012. "Simultaneous Heterotrophic Nitrification and Aerobic Denitrification by Bacterium *Rhodococcus* Sp. CPZ24." *Bioresource Technology* 116: 266-270.
13. Chen, Shufeng, Wenliang Wu, Kelin Hu, and Wei Li. 2010. "The Effects of Land use Change and Irrigation Water Resource on Nitrate Contamination in Shallow Groundwater at County Scale." *Ecological Complexity* 7 (2): 131-138.
14. Connolly, Roseanne, Yaqian Zhao, Guangzhi Sun, and Stephen Allen. 2004. "Removal of Ammoniacal-Nitrogen from an Artificial Landfill Leachate in Downflow Reed Beds." *Process Biochemistry* 39 (12): 1971-1976.
15. Cooke, Janice E. K. and Martin Weih. 2005. "Nitrogen Storage and Seasonal Nitrogen Cycling in *Populus*: Bridging Molecular Physiology and Ecophysiology." *New Phytologist* 167 (1): 19-30.
16. Darwish, T., T. Atallah, R. Francis, C. Saab, I. Jomaa, A. Shaaban, H. Sakka, and P. Zdruli. 2011. "Observations on Soil and Groundwater Contamination with Nitrate: A Case Study from Lebanon-East Mediterranean." *Agricultural Water Management* 99 (1): 74-84.
17. de Klein, C. M. and R. P. van Logtestijn. 1996. "Denitrification in Grassland Soils in the Netherlands in Relation to Irrigation, N-Application Rate, Soil Water Content and Soil Temperature." *Soil Biology and Biochemistry* 28: 231-237.
18. Dimitriou, I. and P. Aronsson. 2011. "Wastewater and Sewage Sludge Application to Willows and Poplars Grown in lysimeters—Plant Response and Treatment Efficiency." *Biomass and Bioenergy* 35 (1): 161-170.
19. Du, Lian-feng, Tong-ke Zhao, Cheng-jun Zhang, Zhi-zhuang An, Qiong Wu, Bao-cun Liu, Peng Li, and Mao-ting Ma. 2011. "Investigations on Nitrate Pollution of Soil, Groundwater and Vegetable from Three Typical Farmlands in Beijing Region, China." *Agricultural Sciences in China* 10 (3): 423-430.
20. Elmi, Abdirashid A., Chandra Madramootoo, Chantal Hamel, and Aiguo Liu. 2003. "Denitrification and Nitrous Oxide to Nitrous Oxide Plus Dinitrogen Ratios in the Soil Profile Under Three Tillage Systems." *Biology and Fertility of Soils* 38: 340-348.
21. Fan, Jinlin, Wengang Wang, Bo Zhang, Yeye Guo, Huu Hao Ngo, Wenshan Guo, Jian Zhang, and Haiming Wu. 2013. "Nitrogen Removal in Intermittently Aerated Vertical Flow Constructed Wetlands: Impact of Influent COD/N Ratios." *Bioresource Technology* 143 (0): 461-466.

22. Focht, D. D., R. A. Bowman, and H. A. Joseph. 1972. "Denitrification Rates in Vitro and in Situ. Presented at Western Regional Research Project W-111, Salt Lake City, Utah." .
23. Fortier, Julien, Daniel Gagnon, Benoit Truax, and France Lambert. 2010. "Nutrient Accumulation and Carbon Sequestration in 6-Year-Old Hybrid Poplars in Multiclonal Agricultural Riparian Buffer Strips." *Agriculture, Ecosystems & Environment* 137 (3–4): 276-287.
24. Friend, Alexander L., Guisepe Scarascia-Mugnozza, J. G. Isebrands, and Paul E. Heilman. 1991. "Quantification of Two-Year-Old Hybrid Poplar Root Systems: Morphology, Biomass, and  $^{14}C$  Distribution." *Tree Physiology* 8: 109-119.
25. Galloway, James N., John D. Aber, Jan Willem Erisman, Sybil P. Seitzinger, Robert W. Howarth, Ellis B. Cowling, and B. Jack Cosby. 2003. "The Nitrogen Cascade." *BioScience* 53 (4): 341-356.
26. Gemal, Khaled M. Said. 2012. "Monitoring of Wastewater Percolation in Unsaturated Sandy Soil using Geoelectrical Measurements at Gabal El Asfar Farm, Northeast Cairo, Egypt." *Environmental Earth Sciences* 66 (3): 749-761.
27. Goodlass, G., M. Green, B. Hilton, and S. McDonough. 2007. "Nitrate Leaching From Short-Rotation Coppice." *Soil use and Management* 23: 178-184.
28. Hajhamad, Lubna and Mohammad N. Almasri. 2009. "Assessment of Nitrate Contamination of Groundwater using Lumped-Parameter Models." *Environmental Modelling & Software* 24 (9): 1073-1087.
29. Hansen, Edward A. 1993. "Soil Carbon Sequestration Beneath Hybrid Poplar Plantations in the North Central United States." *Biomass and Bioenergy* 5 (6): 431-436.
30. Haycock, N. E. and G. Pinay. 1993. "Groundwater Nitrate Dynamics in Grass and Poplar Vegetated Riparian Buffer Strips during the Winter." *Journal of Environmental Quality* 22: 273-278.
31. Hecnar, S. J. 1995. "Acute and Chronic Toxicity of Ammonium Nitrate Fertilizer to Amphibians from Southern Ontario." *Environmental Toxicology and Chemistry* 14: 2131-2137.
32. Holm, Bert and Katrin Heinsoo. 2013. "Municipal Wastewater Application to Short Rotation Coppice of Willows – Treatment Efficiency and Clone Response in Estonian Case Study." *Biomass and Bioenergy* 57 (0): 126-135.

33. Isosaari, P., S. W. Hermanowicz, and Y. Rubin. 2010. "Sustainable Natural Systems for Treatment and Disposal of Food Processing Wastewater." *Critical Reviews in Environmental Science and Technology* 40 (7): 662-697.
34. Jackson, L. E., F. J. Calderon, K. L. Steenwerth, K. M. Scow, and D. E. Rolston. 2003. "Responses of Soil Microbial Processes and Community Structure to Tillage Events and Implications for Soil Quality." *Geoderma* 114 (3-4): 305-317.
35. Jansson, Stefan and Carl J. Douglas. 2007. "*Populus*: A Model System for Plant Biology." *Annual Review of Plant Biology* 58: 435-458.
36. Jassal, Rachhpal S., T. Andrew Black, Carmela Arevalo, Hughie Jones, Jagtar S. Bhatti, and Derek Sidders. 2013. "Carbon Sequestration and Water use of a Young Hybrid Poplar Plantation in North-Central Alberta." *Biomass and Bioenergy* 56 (0): 323-333.
37. Jimenez, B. and A. Chávez. 2004. "Quality Assessment of an Aquifer Recharged with Wastewater for its Potential use as Drinking Source: "El Mezquital Valley" Case." *Water Science and Technology* 50 (2): 269-276.
38. Jordahl, James L., Lesley Foster, Jerald L. Schnoor, and Pedro J. J. Alvarez. 1997. "Effect of Hybrid Poplar Trees on Microbial Populations Important to Hazardous Waste Bioremediation." *Environmental Toxicology and Chemistry* 16 (6): 1318-1321.
39. Kavdir, Y., H. J. Hellebrand, and J. Kern. 2008. "Seasonal Variations of Nitrous Oxide Emission in Relation to Nitrogen Fertilization and Energy Crop Types in Sandy Soil." *Soil and Tillage Research* 98 (2): 175-186.
40. Kelly, J. M., J. L. Kovar, and R. Sokolowsky. 2007. "Phosphorus Uptake during Four Years by Different Vegetative Cover Types in a Riparian Buffer." *Nutrient Cycling in Agroecosystems* 78: 239-251.
41. Kennedy/Jenks Consultants. 2007. *Port of Morrow Water Management and Conservation Plan*. Portland, OR 97201: Kennedy/Jenks Consultants.
42. Kincheloe, J. W., G. A. Wedemeyer, and D. L. Koch. 1979. "Tolerance of Developing Salmonid Eggs and Fry to Nitrate Exposure." *Environmental Contamination and Toxicology* 23: 575-578.
43. Kraft, George J. and Will Stites. 2003. "Nitrate Impacts on Groundwater from Irrigated-Vegetable Systems in a Humid North-Central US Sand Plain." *Agriculture, Ecosystems & Environment* 100 (1): 63-74.
44. Kumon, Yasuyuki, Yasuyuki Sasaki, Isao Kato, Naoki Takaya, Hirofumi Shoun, and Teruhiko Beppu. 2002. "Codennitrification and Denitrification are Dual Metabolic

- Pathways through which Dinitrogen Evolves from Nitrate in *Streptomyces Antibioticus*." *Journal of Bacteriology* 184 (11): 2963-2968.
45. Labrecque, Michel and Traian I. Teodorescu. 2003. "High Biomass Yield Achieved by Salix Clones in SRIC Following Two 3-Year Coppice Rotations on Abandoned Farmland in Southern Quebec, Canada." *Biomass and Bioenergy* 25 (2): 135-146.
  46. Langergraber, Günter. 2007. "Simulation of the Treatment Performance of Outdoor Subsurface Flow Constructed Wetlands in Temperate Climates." *Science of the Total Environment* 380 (1-3): 210-219.
  47. Langergraber, Günter and J. Šimůnek. 2005. "Modeling Variably Saturated Water Flow and Multicomponent Reactive Transport in Constructed Wetlands." *Vadose Zone Journal* 4 (4): 924-938.
  48. Langergraber, Günter, David Giraldo, Javier Mena, Daniel Meyer, Miguel Peña, Attilio Toscano, Alessandro Brovelli, and E. Asuman Korkusuz. 2009. "Recent Developments in Numerical Modelling of Subsurface Flow Constructed Wetlands." *Science of the Total Environment* 407 (13): 3931-3943.
  49. Licht, Louis A. 2012. *Final Draft Port of Morrow. RE: POM Effluent Treatability Study - Phase 1, Demonstrating Phyto Processes to Manage Nitrate-Nitrogen*. North Liberty, IA: Ecolotree, Inc.
  50. Lin, Chin-Ching, A. B. Arun, P. D. Rekha, and Chiu-Chung Young. 2008. "Application of Wastewater from Paper and Food Seasoning Industries with Green Manure to Increase Soil Organic Carbon: A Laboratory Study." *Bioresource Technology* 99 (14): 6190-6197.
  51. Lin, Ying-Feng, Shuh-Ren Jing, Tze-Wen Wang, and Der-Yuan Lee. 2002. "Effects of Macrophytes and External Carbon Sources on Nitrate Removal from Groundwater in Constructed Wetlands." *Environmental Pollution* 119 (3): 413-420.
  52. Long, Lauren M., Louis A. Schipper, and Denise A. Bruesewitz. 2011. "Long-Term Nitrate Removal in a Denitrification Wall." *Agriculture, Ecosystems & Environment* 140 (3-4): 514-520.
  53. Lu, Songliu, Hongying Hu, Yingxue Sun, and Jia Yang. 2009. "Effect of Carbon Source on the Denitrification in Constructed Wetlands." *Journal of Environmental Sciences* 21 (8): 1036-1043.
  54. Luo, J., R. W. Tillman, and P. R. Ball. 2000. "Nitrogen Loss through Denitrification in a Soil Under Pasture in New Zealand." *Soil Biology and Biochemistry* 32: 497-509.



55. Maître, Véronique, Anne-Claude Cosandey, Eric Desagher, and Aurèle Parriaux. 2003. "Effectiveness of Groundwater Nitrate Removal in a River Riparian Area: The Importance of Hydrogeological Conditions." *Journal of Hydrology* 278 (1–4): 76-93.
56. Marco, A., C. Quilchano, and A. R. Blaustein. 1999. "Sensitivity to Nitrate and Nitrite in Pond-Breeding Amphibians from the Pacific Northwest, USA." *Environmental Toxicology and Chemistry* 18: 2836-2839.
57. McKeon, C. A., F. L. Jordan, E. P. Glenn, W. J. Waugh, and S. G. Nelson. 2005. "Rapid Nitrate Loss from a Contaminated Desert Soil." *Journal of Arid Environments* 61 (1): 119-136.
58. Miyahara, Morio, Sang-Wan Kim, Shinya Fushinobu, Koki Takaki, Takeshi Yamada, Akira Watanabe, Keisuke Miyauchi, Ginro Endo, Takayoshi Wakagi, and Hirofumi Shoun. 2010. "Potential of Aerobic Denitrification by *Pseudomonas Stutzeri* TR2 to Reduce Nitrous Oxide Emissions from Wastewater Treatment Plants." *Applied and Environmental Microbiology* 76 (14): 4619-4625.
59. Mkhabela, M. S., A. Madani, R. Gordon, D. Burton, D. Cudmore, A. Elmi, and W. Hart. 2008. "Gaseous and Leaching Nitrogen Losses from no-Tillage and Conventional Tillage Systems Following Surface Application of Cattle Manure." *Soil and Tillage Research* 98 (2): 187-199.
60. Nadav, Itamar, Gilboa Arye, Jorge Tarchitzky, and Yona Chen. 2012. "Enhanced Infiltration Regime for Treated-Wastewater Purification in Soil Aquifer Treatment (SAT)." *Journal of Hydrology* 420–421 (0): 275-283.
61. Nadav, Itamar, Jorge Tarchitzky, and Yona Chen. 2012. "Soil Cultivation for Enhanced Wastewater Infiltration in Soil Aquifer Treatment (SAT)." *Journal of Hydrology* 470–471 (0): 75-81.
62. Ndour, N. Y. B., E. Baudoin, A. Guisse, M. Seck, M. Kouma, and A. Brauman. 2008. "Impact of Irrigation Water Quality on Soil Nitrifying and Total Bacterial Communities." *Biology and Fertility of Soils* 44 (5): 797-803.
63. Nelson, W. M., A. J. Gold, and P. M. Groffman. 1995. "Spatial and Temporal Variation in Groundwater Nitrate Removal in a Riparian Forest." *Journal of Environmental Quality* 24: 691-699.
64. Oregon Department of Environmental Quality. 2012. "Analysis of Groundwater Nitrate Concentrations in the Lower Umatilla Basin Groundwater Management Area. DEQ Water Quality Division. Accessed on December 28th, 2013 at [Http://www.Deq.State.Or.Us/Wq/Groundwater/Docs/Lubgwma/Nitrate/NitrateReport.Pdf](http://www.Deq.State.Or.Us/Wq/Groundwater/Docs/Lubgwma/Nitrate/NitrateReport.Pdf) .

65. Parnaudeau, Virginie, Bernard Nicolardot, Philippe Robert, Gonzague Alavoine, Jérôme Pagès, and Francis Duchiron. 2006. "Organic Matter Characteristics of Food Processing Industry Wastewaters Affecting their C and N Mineralization in Soil Incubation." *Bioresource Technology* 97 (11): 1284-1295.
66. Paterson, Kurtis G. and Jerald L. Schnoor. 1993. "Vegetative Alteration of Nitrate Fate in Unsaturated Zone." *Journal of Environmental Engineering* 119 (5): 986-993.
67. Patureau, D., E. Helloin, E. Rustrian, T. Bouchez, J. P. Delgenes, and R. Moletta. 2001. "Combined Phosphate and Nitrogen Removal in a Sequencing Batch Reactor using the Aerobic Denitrifier, *Microvirgula Aerodenitrificans*." *Water Research* 35 (1): 189-197.
68. Pistocchi, Chiara, Werther Guidi, Emiliano Piccioni, and Enrico Bonari. 2009. "Water Requirements of Poplar and Willow Vegetation Filters Grown in Lysimeter Under Mediterranean Conditions: Results of the Second Rotation." *Desalination* 246 (1-3): 137-146.
69. Port of Morrow. "POM.", accessed January/24, 2014, <http://www.portofmorrow.com>.
70. Premrov, Alina, Catherine E. Coxon, Richard Hackett, Laura Kirwan, and Karl G. Richards. 2012. "Effects of Over-Winter Green Cover on Groundwater Nitrate and Dissolved Organic Carbon Concentrations Beneath Tillage Land." *Science of the Total Environment* 438 (0): 144-153.
71. Prunty, Lyle and Richard Greenland. 1997. "Nitrate Leaching using Two Potato-Corn N-Fertilizer Plans on Sandy Soil." *Agriculture, Ecosystems & Environment* 65 (1): 1-13.
72. Rennenberg, H., H. Wildhagen, and B. Ehling. 2010. "Nitrogen Nutrition of Poplar Trees." *Plant Biology* 12: 275-291.
73. Richerson, Phil. 2011. *Third Trend Analysis of Food Processor Land Application Sites in the Lower Umatilla Basin Groundwater Management Area*. Eastern Region Office, Pendleton, OR: DEQ Water Quality Division.
74. Rittmann, Bruce E. and Perry L. McCarty. 2001. "Environmental Biotechnology: Principles and Applications." *McGraw-Hill Series in Water Resources and Environmental Engineering*.
75. Robertson, L. A., R. Cornelisse, P. De Vos, R. Hadjoetomo, and J. G. Kuenen. 1989. "Aerobic Denitrification in various Heterotrophic Nitrifiers." *Antonie Van Leeuwenhoek* 56 (4): 289-299.

76. Röver, Manuela, Otto Heinemeyer, and Ernst-August Kaiser. 1998. "Microbial Induced Nitrous Oxide Emissions from an Arable Soil during Winter." *Soil Biology and Biochemistry* 30 (14): 1859-1865.
77. Ruijter, F. J., L. J. M. Boumans, A. L. Smit, and M. van der Berg. 2007. "Nitrate in Upper Groundwater on Farms Under Tillage as Affected by Fertilizer use, Soil Type and Groundwater Table." *Nutrient Cycling in Agroecosystems* 77: 155-167.
78. Saeed, Tanveer and Guangzhi Sun. 2011a. "A Comparative Study on the Removal of Nutrients and Organic Matter in Wetland Reactors Employing Organic Media." *Chemical Engineering Journal* 171 (2): 439-447.
79. Saeed, Tanveer and Guangzhi Sun. 2011b. "The Removal of Nitrogen and Organics in Vertical Flow Wetland Reactors: Predictive Models." *Bioresource Technology* 102 (2): 1205-1213.
80. Saeed, Tanveer and Guangzhi Sun. 2013. "A Lab-Scale Study of Constructed Wetlands with Sugarcane Bagasse and Sand Media for the Treatment of Textile Wastewater." *Bioresource Technology* 128 (0): 438-447.
81. Saffigna, P. G. and D. R. Keeney. 1977. "Nitrogen and Chloride Uptake by Irrigated Russet Burbank Potatoes." *Agronomy Journal* 69: 258-264.
82. Schipper, Louis A. and Maja Vojvodić-Vuković. 2001. "Five Years of Nitrate Removal, Denitrification and Carbon Dynamics in a Denitrification Wall." *Water Research* 35 (14): 3473-3477.
83. Simek, Miloslav, Linda Jisova, and David W. Hopkins. 2002. "What is the so-Called Optimum pH for Denitrification in Soil?" *Soil Biology and Biochemistry* 34: 1227-1234.
84. Simmons, R. C., A. J. Gold, and P. M. Groffman. 1992. "Nitrate Dynamics in Riparian Forests: Groundwater Studies." *Journal of Environmental Quality* 21: 659-665.
85. Šimůnek, Jiří, M. Sejna, and M. T. van Genuchten. 1999. "The Hydrus-2D Software Package for Simulating Two-Dimensional Movement of Water, Heat, and Multiple Solutes in Variably Saturated Media. Version 2.0." *IGWMC - TPS - 53, International Ground Water Modeling Center: Colorado School of Mines, Golden, Colorado.*
86. Skjemstad, J. O., L. J. Janik, and J. A. Taylor. 1998. "Non-Living Soil Organic Matter: What do we Know about it?" *Australian Journal of Experimental Agriculture* 38 (7): 667-680.

87. Sklarz, Menachem Y., Amit Gross, M. Ines M. Soares, and Alexander Yakirevich. 2010. "Mathematical Model for Analysis of Recirculating Vertical Flow Constructed Wetlands." *Water Research* 44 (6): 2010-2020.
88. Smith, M. Scott and James M. Tiedje. 1979. "Phases of Denitrification Following Oxygen Depletion in Soil." *Soil Biology and Biochemistry* 11 (3): 261-267.
89. State Hygienic Laboratory. 2013. *The University of Iowa*. January ed. Iowa City, IA:.
90. Sun, Guangzhi, Yafei Zhu, Tanveer Saeed, Guangxin Zhang, and Xianguo Lu. 2012. "Nitrogen Removal and Microbial Community Profiles in Six Wetland Columns Receiving High Ammonia Load." *Chemical Engineering Journal* 203 (0): 326-332.
91. Suthar, Surindra, Preeti Bishnoi, Sushma Singh, Pravin K. Mutiyar, Arvind K. Nema, and Nagraj S. Patil. 2009. "Nitrate Contamination in Groundwater of some Rural Areas of Rajasthan, India." *Journal of Hazardous Materials* 171 (1-3): 189-199.
92. Takaya, Naoki, Maria Antonina B. Catalan-Sakairi, Yasushi Sakaguchi, Isao Kato, Zhemin Zhou, and Hirofumi Shoun. 2003. "Aerobic Denitrifying Bacteria that Produce Low Levels of Nitrous Oxide." *Applied and Environmental Microbiology* 69 (6): 3152-3157.
93. Toscano, Attilio, Günter Langergraber, Simona Consoli, and Giuseppe L. Cirelli. 2009. "Modelling Pollutant Removal in a Pilot-Scale Two-Stage Subsurface Flow Constructed Wetlands." *Ecological Engineering* 35 (2): 281-289.
94. Trudell, M. R., R. W. Gillham, and J. A. Cherry. 1986. "An in-Situ Study of the Occurrence and Rate of Denitrification in a Shallow Unconfined Sand Aquifer." *Journal of Hydrology* 83: 251-268.
95. Tusseau-Vuillemin, Marie-Hélène. 2001. "Do Food Processing Industries Contribute to the Eutrophication of Aquatic Systems?" *Ecotoxicology and Environmental Safety* 50 (2): 143-152.
96. Ulrich, Kristina, Andreas Ulrich, and Dietrich Ewald. 2008. "Diversity of Endophytic Bacterial Communities in Poplar Grown Under Field Conditions." *Federation of European Microbiological Societies* 63: 169-180.
97. Virto, I., P. Bescansa, M. J. Imaz, and A. Enrique. 2006. "Soil Quality Under Food-Processing Wastewater Irrigation in Semi-Arid Land, Northern Spain; Aggregation and Organic Matter Fractions." *Journal of Soil and Water Conservation* 61 (6): 398-407.
98. Vymazal, Jan. 2007. "Removal of Nutrients in various Types of Constructed Wetlands." *Science of the Total Environment* 380 (1-3): 48-65.

99. WHO (World Health Organization). 1998. "Guidelines for Drinking Water Quality, World Health Organization, Geneva." .
100. Williams, Haydn G., Andrzej Białowiec, Fred Slater, and Peter F. Randerson. 2010. "Diurnal Cycling of Dissolved Gas Concentrations in a Willow Vegetation Filter Treating Landfill Leachate." *Ecological Engineering* 36 (12): 1680-1685.
101. Zhang, Jibin, Pengxia Wu, Bo Hao, and Ziniu Yu. 2011. "Heterotrophic Nitrification and Aerobic Denitrification by the Bacterium *Pseudomonas Stutzeri* YZN-001." *Bioresource Technology* 102 (21): 9866-9869.